

A Study on the Role of Rhizospheric Bacteria in Promoting Plant Growth and Alleviating Biotic Stress in its Host

A Thesis

Submitted to the

Assam Agricultural University

In partial fulfillment of the requirements for the degree of

DOCTOR OF PHILOSOPHY (Agriculture)

IN

AGRICULTURAL BIOTECHNOLOGY



BY

ALOKESH GHOSH

Registration No. 251 of 2018

[Roll No. 2018-ADJ-01]

**DEPARTMENT OF AGRICULTURAL BIOTECHNOLOGY
COLLEGE OF AGRICULTURE
ASSAM AGRICULTURAL UNIVERSITY
JORHAT-785 013 (ASSAM)
AUGUST, 2023**

Dedicated

to my

Beloved Grand

Parents, Maa,

Papa, Buda, and

Family... 

ASSAM AGRICULTURAL UNIVERSITY

Faculty of Agriculture

CERTIFICATE – I

This is to certify that the thesis entitled “**A Study on the Role of Rhizospheric Bacteria in Promoting Plant Growth and Alleviating Biotic Stress in its Host**” submitted to the Faculty of Agriculture, Assam Agricultural University in partial fulfillment for the degree of **Doctor of Philosophy (Agriculture) in Agricultural Biotechnology** is a record of research work carried out by **Alokesh Ghosh** under my personal supervision and guidance.

All help received by him have been duly acknowledged.

No part of this thesis has been reproduced elsewhere for any degree.

Dated, Jorhat

The....., 2023

(Robin Chandra Boro)

Major Adviser

Department of Agricultural Biotechnology

Faculty of Agriculture

Assam Agricultural University

Jorhat 785 013

CERTIFICATE – II

This is to certify that the thesis entitled “**A Study on the Role of Rhizospheric Bacteria in Promoting Plant Growth and Alleviating Biotic Stress in its Host**” submitted by **Alokesh Ghosh, Roll No. 2018-ADJ-01** to the Assam Agricultural University in partial fulfillment of the requirements for the degree of **Doctor of Philosophy (Agriculture)** in the discipline of **Agricultural Biotechnology** has been examined and approved by the student’s Advisory Committee and the External Examiner, after viva-voice.

(R.C. Boro)
Major Adviser

External Examiner

Members of the Advisory Committee:

1. _____
(M. Barooah)

2. _____
(M. K. Modi)

3. _____
(B. C. Nath)

4. _____
(S. Rathi)

(M. K. Modi)
Professor and Head
Department of Agricultural Biotechnology
Assam Agricultural University
Jorhat- 785 013

(A. K. Das)
Director
Post-Graduate Studies
Assam Agricultural University
Jorhat- 785 013

ACKNOWLEDGEMENT

The author extends his heartfelt gratitude and appreciation to his major advisor, Dr. Robin Chandra Boro, Assistant Professor, Department of Agricultural Biotechnology, Assam Agricultural University, Jorhat for his invaluable guidance, unwavering support, and insightful suggestions that have played a crucial role in planning, designing, and executing the research work culminating in this manuscript.

Special thanks are conveyed to the members of the Advisory Committee: Dr. Mahendra Kumar Modi, Professor and HoD, Department of Agricultural Biotechnology; Dr. Madhumita Barooah, Professor, Department of Agricultural Biotechnology for her constant support and trust; Dr. Bharat Chandra Nath, Asst. Professor, Department of Plant Pathology; and Dr. Sunayana Rathi, Asst. Professor, Department of Biochemistry and Agricultural Chemistry. Their intellectual mentorship, valuable advice, and prompt assistance have been instrumental throughout the research process.

The author expresses sincere gratitude to Dr. Anup Kr. Das, DPGS for funding the research work. The author also expresses gratitude to Dr. B.K. Sarmah, Director of the North-East Centre for Agricultural Biotechnology for facilitating necessary resources, PhD scholarship, valuable support, and encouragement in carrying out the research.

Heartfelt thanks are extended to Dr. Priyabrata Sen, Dr. Salvinder Singh, Dr. Akhil R. Baruah, Dr. Tankeshwar Nath, Dr. Priyadarshini Bhorali and all other esteemed professors of the Department of Agricultural Biotechnology, AAU, Jorhat for their generous guidance and selfless contributions during his Ph.D. journey. Special thanks to Dr. Rajen Baruah, Professor, Department of Soil Science for his valuable support and guidance.

The author is thankful to the SAIF, CDRI Lucknow and SAIF, CSIR- NEIST, Jorhat for providing LC-MS and SEM facilities.

The author expresses sincere thanks to all his seniors – Dibyo da, Gunojit da, Sudipto da, Romen da, Trishna di, Merilin Ba, Samimba, Namishaba, Rajib da, Lipikaba Vipinbhaiya, and Arindom da for their constant guidance and support throughout his Ph.D. journey.

The author also expresses his gratitude to all the members of the Microbial Biotechnology Lab, RNA Lab, Transformation Lab, Marker Lab and Endophyte Lab for their constant support. Special thanks to Manoj da, Malobikaba, Dwipen da, and all other non-teaching staff and office staff of the Department of Agricultural Biotechnology & DBT-NECAB.

The author expresses his deep love and gratitude to all his batch mates Dipen, Richita, Subhrota, Gracia, Atsie, Manav sir, Debjyoti, and Jyotsna Di for their continuous support, motivation, and help throughout the Ph.D. journey. The author immensely expresses his gratitude to his roommate Dr. Kuntal for his constant guidance and help.

The author also expresses special thanks to his juniors – Sanjyukta, Pratim, Tanushree, Madhurjya, Rahul, Darshana, Swarup, Ratna, Rohit, Dipankar, Shubham, and all his hostel mates.

The author is forever grateful to his Maa, Papa, Buda, and his extended family for their unwavering love, guidance, support, and motivation throughout the PhD journey. The author also acknowledges the support of his brothers and sisters for their love and constant support.

The author also extends acknowledgment to all who have contributed directly or indirectly to the completion of this research work. Lastly, the author expresses gratitude to the Almighty for providing invisible guidance and support at every step of life's journey.

Dated, Jorhat

The..... August, 2023

The Author

ABSTRACT

Cabbage is susceptible to various fungal pathogens such as *Xanthomonas campestris*, *Alternaria brassica*, *Rhizoctonia solani*, etc. Various fungicides have been recommended such as chlorothalonil and tebuconazole, which are highly toxic to both soil and aquatic ecosystem and may induce tumors in mammalian cells. Bio-inputs can be the most sustainable and eco-friendly approach to mitigate plant diseases. In the present study, two rhizospheric bacterial isolates *Bacillus amyloliquefaciens* AG1B and *B. subtilis* AG2B showed antagonistic activity against *Alternaria brassicicola* AG1F. Previously reported endophytic bacteria, *B. subtilis* Scb-1 also showed similar antagonistic activity against the same pathogenic fungi. The cell-free supernatant of the bacterial isolates showed a significant reduction in fungal growth. Microscopic studies revealed deformed hyphae and conidia with bubble formation when co-cultured with the antagonist bacterial isolates. Lipopeptides are bioactive compounds that pose substantial challenges to the structural integrity of fungal cell walls and are regarded as antifungal in nature. LC-MS analysis showed that co-cultivation of *B. amyloliquefaciens* AG1B with *A. brassicicola* AG1F results in the secretion of several lipopeptide and polyketide compounds such as surfactin, iturin, etc. Similar results were also obtained when *B. subtilis* AG2B and *B. subtilis* Scb-1 were co-cultured with *A. brassicicola* AG1F, respectively. The complete genome of the potential bacterial isolate; *B. amyloliquefaciens* AG1B with a percentage inhibition of 76.47 % against *A. brassicicola* AG1F was reconstructed through *de novo* assembly, revealing a genome size of 3.89 Mbp. This genome encompasses genes associated with plant growth promotion, lipopeptides and polyketides synthesis, and genes that confirm its affiliation with rhizobacterial interactions. Differential expression analysis of key genes such *srfAB*, *ItuA*, *fenF* etc., involved in the synthesis of lipopeptides and polyketides during the dual culture condition showed significant transcriptional up-regulation, validating the results of metabolite profiling. Moreover, the bio-primed seeds of cabbage with the potential bacterial isolates, *B. amyloliquefaciens* AG1B, *B. subtilis* AG2B and *B. subtilis* Scb-1 respectively, showed better germination percentage, increase in root, and shoot length. Foliar application of the potential bacterial isolates *B. amyloliquefaciens* AG1B, *B. subtilis* AG2B and *B. subtilis* Scb-1 efficiently resulted in a reduction of disease severity up to 80%. Thus, multifaceted bio-inputs like *B. amyloliquefaciens* AG1B, *B. subtilis* AG2B and *B. subtilis* Scb-1 can be used for making bio-formulation for sustainable management of fungal diseases.

CONTENTS

CHAPTER NO.	TITLE	PAGE NO.
I.	INTRODUCTION	1-4
II.	REVIEW OF LITERATURE	5-27
III.	MATERIALS AND METHODS	28-58
IV.	RESULTS AND DISCUSSIONS	59-111
V.	SUMMARY AND CONCLUSION	112-116
	BIBLIOGRAPHY	117-132
	APPENDIX	i-ii

LIST OF TABLES

Table No.	Title	Page No.
2.1	List of bacterial strains reported as bio-control agents	8
3.1	Components of PCR reaction for the amplification of ITS region of Fungi	30
3.2	List of reference sequences used in the phylogenetic analysis of the pathogenic fungal isolate.	32
3.3	Reading Table for biochemical tests	37-39
3.4	Components of PCR reaction for the amplification of 16s RNA region of the bacterial DNA.	41
3.5	List of reference sequences used in the phylogenetic analysis of the rhizo-bacterial isolates.	42
3.6	Primers used in the expression analysis of the fungal genes	47
3.7	Chromatographic conditions for metabolite profiling using gradient elution	49
3.8	Primers used for the expression analysis of the bacterial genes	54
4.1	Morphological characteristics of the bacterial isolates	80
4.2	Results of biochemical characterization of the bacterial isolates	82-83
4.3	List of bacterial secondary metabolites having antifungal property detected in this study by using LC-ESI-MS	94
4.4	List of important genes conferring to plant growth promoting and antifungal compound production.	95
4.5	Outcome of the foliar application of the bio-inoculums on disease management	106

LIST OF FIGURES

Figure No.	Title	Page No.
2.1	Bacterial-Fungal Interactions and its potential applications	6
2.2	Internal transcribed spacer (ITS) region of fungal genome	13
2.3	Secondary metabolites and their associated gene clusters produced by <i>Bacillus amyloliquefaciens</i> for plant growth promotion.	17
2.4	Nutrient solubilization and its role in plant growth promotion by <i>Bacillus amyloliquefaciens</i> (BA).	17
2.5	Mechanism of biotic stress management of <i>Bacillus subtilis</i> .	19
2.6	Functional role of <i>Bacillus</i> lipopeptides in disease suppression	20
2.7	Superoxide dismutase activity	25
3.1	A schematic diagram showing the dual bacterial- fungal culture	34
3.2	Workflow demonstrating the use of NEBNext Ultra II FS DNA Library Prep Lit Illumina	51
3.3	Workflow of the downstream analysis of the raw data to achieve the <i>de novo</i> bacterial genome with functional annotation.	53
4.1	Pathogenic fungi, AG1F isolated from an infected cabbage leaf	61
4.2	Detached leaf assay showed similar black spot symptoms upon inoculated with the spore suspension of AG1F	61
4.3	Macroscopic and microscopic characteristics of the pathogenic fungal isolate, AG1F	62
4.4	PCR amplification of target ITS gene of the fungal isolate detected on agarose gel and the phylogenetic tree.	64
4.5	Antagonistic activity exerted by the rhizospheric bacterial isolates AG1B and AG2B against the pathogenic fungi, AG1F in dual culture condition	66
4.6	Endo-fungal bacterial isolate, <i>Serratia marcescens</i> D1 (SM) and endophyte bacterial isolate, <i>Bacillus subtilis</i> Scb-1 shows significant growth reduction of the pathogenic fungi, AG1F in dual culture experiment.	67

Figure No.	Title	Page No.
4.7	The growth of the pathogenic fungal isolate, <i>Alternaria brassicicola</i> AG1F gets retardated upon co-culture with the bacterial isolates with each of the four bacterial isolates, AG1B, AG2B, <i>Serratia marcescens</i> D1 (SM) and <i>Bacillus subtilis</i> Scb-1 (BsScb1)	68
4.8	The growth of the different pathogenic fungal isolates gets retardated upon co-culture with each of the four bacterial isolates, AG1B, AG2B, <i>Serratia marcescens</i> D1 (SM) and <i>Bacillus subtilis</i> Scb-1. (BsScb1)	69-70
4.9	Colony morphology of the pathogenic fungal isolate, AG1F when co-cultured with antagonistic bacterial isolates after 20 dpi	72
4.10	Percentage Inhibition (PI) Assay.	73
4.11	Effect of the cell free supernatant of the bacterial isolates against the fungi, AG1F. (A -C) represents the well diffusion inhibitory effects of the bacterial supernatant. (D-E) results of the poisoned food assay.	74
4.12	Effect of Bacterial Volatiles on the linear growth of the pathogenic fungal isolate, AG1F	76
4.13	Light microscopic study of the antagonistic effects of the bacterial isolates <i>B. subtilis</i> Scb-1, AG1B and AG2B on <i>Alternaria brassicicola</i> AG1F	77
4.14	SEM study of the antagonistic effects of the bacterial isolates <i>B. subtilis</i> Scb-1, AG1B and AG2B on <i>Alternaria brassicicola</i> AG1F	78
4.15	SEM study of the antagonistic effects of the bacterial isolates <i>B. subtilis</i> Scb-1, AG1B and AG2B on the conidia of <i>Alternaria brassicicola</i> AG1F.	79
4.16	Morphological characteristics of the bacterial isolates AG1B and AG2B.	81
4.17	PCR amplification of target 16s rRNA gene of the bacterial isolates detected on agarose gel and the phylogenetic tree.	85
4.18	Plant growth promoting traits of the bacterial isolates	88
4.19	Comparative profile of the Superoxide Dismutase Activity.	90

Figure No.	Title	Page No.
4.20	Differential expression of key fungal genes during the interaction between each of (A) <i>Bacillus subtilis</i> Scb-1, (B) <i>B. amyloliquefaciens</i> AG1B and (C) <i>B. subtilis</i> AG2B with <i>A. brassicicola</i> AG1F in different time intervals.	92
4.21	TLC confirmation of the bacterial lipopeptide.	94
4.22	Circular map of the <i>de novo</i> assembled whole genome of AG1B	96
4.23	Gene ontology study of the genome of AG1B	97
4.24	Genes associated with the pathway using KEGG	98
4.25	Pan Genome phylogeny showing the Average Nucleotide Identity	99
4.26	Differential expression of key genes involved in the biosynthesis of bacterial secondary metabolites during the interaction between each of (A) <i>Bacillus subtilis</i> Scb-1, (B) <i>B. amyloliquefaciens</i> AG1B and (C) <i>B. subtilis</i> AG2B with <i>Alternaria brassicicola</i> AG1F in different time intervals	101
4.27	Bio-priming increased the germination percentage, root and shoot length of cabbage and rapeseed	103
4.28	Bacterial Priming enhances the growth of cabbage	105
4.29	Bacterial priming enhances the root length (A- Representative Image of the increased root length), shoot length (B), leaf count (C) and leaf area index (D).	105
4.30	Phenotypic observation of the effect of foliar application of bio-inoculums on disease management	107
4.31	Trypan blue staining of the leaf showing the level of necrosis	108
4.32	Physiological and biochemical changes during biotic stress alleviation	111
5.1	Overall Summary of the research work	116

ABBREVIATIONS AND SYMBOLS USED

%	: Per cent
(M+H ⁺) ⁺	: Hydrogen adduct ion of a molecule
≤	: Less than or equal to
®	: Registered
°C	: Degree Centigrade
µg	: Microgram(s)
µg/ml	: Microgram(s) per milliliter
µl	: Microlitre(s)
µM	: Micromolar
ACN	: Acetonitrile
ATCC	: American Type Culture Collection
BLAST	: Basic Local Alignment Search Tool
Bp	: Base pair
CBS	: Central Bureau of Fungal Culture
cDNA	: Complementary Deoxyribonucleic acid
CFU	: Colony Forming Units
cm	: Centimetre(s)
CO ₂	: Carbon dioxide
Da	: Dalton
DEGs	: Differentially Expressed Genes
DEPC	: Diethyl Pyrocarbonate
DMSO	: Dimethyl Sulfoxide
DNA	: Deoxyribonucleic Acid
e.g.	: Exempli gratis (for example)
EDTA	: Ethylene diamine tetra acetic acid
ESI	: Electrospray Ionization
<i>et al.</i>	: Et alia
EtBr	: Ethidium Bromide
FAO	: Food and Agriculture Organisation
FeCl ₃	: Ferric Chloride
Fig.	: Figure
g	: Gram(s)

g/l	: Gram(s) per litre
GC-MS	: Gas Chromatography-Mass Spectrometry
Gel-Doc	: Gel Documentation System
H ₂ O	: Water
H ₂ S	: Hydrogen sulphide
HCl	: Hydrochloric acid
HClO ₄	: Perchloric Acid
HPLC	: High-Performance Liquid Chromatography
hrs	: Hour(s)
i.e.	: Id est (That is)
IAA	: Indole_3_Acetic Acid
IDT	: Integrated DNA Technologies
IPCC	: International Panel for Climate Change
ITS	: Internal Transcribed Spacer
Kb	: Kilobase pair(s)
KH ₂ PO ₄	: Potassium dihydrogen phosphate
L	: Litre
LC- MS	: Liquid chromatography-mass spectrometry
LC-ESI-MS	: Liquid chromatography-electrospray ionization mass spectrometry
M	: Molar
m/z	: Mass/charge
MAP	: Mitogen Activated Protein
MAPKs	: Mitogen Activated Protein Kinases
Mbp	: Megabase pairs
MEGA X	: Molecular Evolutionary Genetics Analysis
mg	: Milligram(s)
mg/ml	: Milligram(s) per milliliter
min	: Minute(s)
ML	: Maximum Likelihood
ml	: Millilitre(s)
mm	: Millimetre(s)
mM	: Millimolar
MOPS	: 3-(<i>N-morpholino</i>) propane sulphonic
MP	: Maximum Parsimony

MS	: Mass Spectrometry
MS/MS	: Mass Spectrometry/ Mass Spectrometry
NA	: Nutrient Agar
NaCl	: Sodium Chloride
NaOH	: Sodium Hydroxide
NB	: Nutrient Broth
NCBI	: National Centre for Biotechnology Information
ng	: Nanogram(s)
ng/μl	: Nanogram(s) per microliter
NJ	: Neighbor joining
nm	: Nanometer
NMR	: Nuclear Magnetic Resonance
No. (or) no.	: Number(s)
O ₃	: Ozone
OD	: Optical Density
OD ₆₀₀	: Optical Density at 600nm
PCR	: Polymerase Chain Reaction
PDA	: Potato Dextrose Agar
PGPB	: Plant Growth Promoting Bacteria
PGPR	: Plant Growth Promoting Rhizobacteria
pH	: Negative logarithm of Hydrogen ion concentration
PVK	: Pikovskaya
QC	: Quality Check
qRT-PCR	: Quantitative Real-Time Polymerase Chain Reaction
rDNA	: Ribosomal Deoxyribonucleic Acid
<i>R_f</i>	: Retention factor
rpm	: Revolution per minute
rRNA	: Ribosomal Ribonucleic Acid
RT	: Room Temperature
sec	: Second(s)
SEM	: Scanning Electron Microscope
SOD	: Superoxide dismutase
sp.	: Species
spp.	: Species pluralis

TAE	: Tris Acetic acid EDTA
TE	: Tris EDTA buffer
TLC	: Thin Layer Chromatography
Tris-HCl	: Tris hydrochloride
TSA	: Tryptic Soya Agar
UN	: United Nations
UV	: Ultra Violet
UV-Vis	: Ultra Violet-Visible
V	: Volt
v/v	: Volume/Volume
W/V	: Weight/ Volume
λ_{\max}	: Absorption maximum

CHAPTER I

INTRODUCTION

The world population is expected to reach 9.8 billion by 2050 and 11.2 billion by 2100 (Department of Economic and Social Affairs, UN). Food and Agriculture Organisation (FAO) declared that by 2050, we need to produce 60% more food to fulfil the need of 9.8 billion global populations. Moreover, due to climate change and global warming huge fluctuations of temperature, heavy precipitations have promoted and proliferated disease incidences in crop plants. International Panel for Climate Change (IPCC) clearly stated that increase in temperature and carbon-dioxide (CO₂) concentration will directly influence the growth and spread of phytopathogens. Khan *et al.* (2021) reported that the global crop yield reductions ranging from 8% to 40% are attributed to fungal pathogens. Thus, the compounding effects of these outcomes impart additional stress upon farmers, compelling them to enhance productivity within a constant land area, given that agricultural expenses remain static despite the expansion of the global population.

As a result, to feed this rapidly growing population, farmers mostly depend on chemical fertilizers and pesticides to increase plant fitness and manage diseases. This excessive use of chemically synthesized inorganic fertilizers and pesticides has affected soil health and contaminates both the surface water and groundwater as a result of leaching and de-nitrification which is disastrous for plants, animals and humans. The persistence of chemically synthesized fertilizers and pesticides in the soil for longer period engenders a consequential impact on soil micro-flora and thereby disrupting soil ecosystem integrity. Kenarova and Boteva, (2023) reported that soil hydrogenase enzyme is highly sensitive to most of the widely used fungicides in the agricultural fields. Fungicides such as chlorothalonil, tebuconazole are highly toxic to soil health. Scoy and Tjeerdema, (2014) reported that chlorothalonil exhibits pronounced toxicity towards aquatic organisms. In terms of mammalian toxicity, particularly in rats and mice, it manifests at a moderate level, inducing adverse physiological responses such as the formation of tumors, ocular irritation, and muscular debilitation. Therefore, using multifaceted bio-inputs like beneficial microbes can be the most sustainable and eco-friendly approach to increase plant fitness, better nutrient uptake and manage plant diseases.

1.1 Microbial Interactions

In a natural habitat, several microbial communities co-exist and interact with plants. These co-existence and interactions occur in many ways and on many dimensions. Interestingly, all parts of plants have been found interacting with microorganisms at certain periods of their life cycle. Microbes interact with their host plant for food and space. The plant-microbe interaction can range from mutualism, commensalism to parasitism. Mutualism and commensalism represent the balanced interaction in which both the microbe and the host are being benefited. Whereas parasitism represents the unbalanced interaction in which only the microbe will be benefited (Rai and Agarkar, 2016). Endophytes and rhizospheric PGPBs are examples of mutualistic microorganisms having symbiotic relationship with the plants, where the plant provides its photosynthetic carbon assimilates to the microbes and the microbes, in turn, promote plant growth, enhance tolerance to various abiotic and biotic stresses, improve nutrient or mineral acquisition by plants and induce hormone production. The parasitic microorganism includes pathogens such as *Phytophthora*, Tobacco mosaic virus, *Xanthomonas*, *Botrytis*, *Alternaria*, *Fusarium*, etc. causes serious damage to plants and results in reduction of crop yields. Pathogens are very specific to their host and can change their lifestyle to become endophytes and *vice versa* (Rai and Agarkar, 2016). During the course of evolution, pathogens have developed several molecular mechanisms to cause disease susceptibility in their host and plants have also adapted several strategies to cope with the invading pathogens (Andersen *et al.*, 2018). Thus, the evolutionary arms race is going hand-in-hand.

1.2 Plant growth-promoting rhizobacterial (PGPR)

PGPR are the soil bacteria inhabiting around/on the root surface or are living inside the plants as endophytes and are directly or indirectly involved in promoting plant growth and development *via* the production and secretion of various regulatory chemicals (Grover *et al.*, 2011). PGPR help in plant growth by assisting in nutrient uptake or by modulating plant hormone levels and plays a key role in plant immunity against phytopathogens (Hayat *et al.*, 2010). Different PGPRs have been shown to increase plant health and productivity in both normal and stressed conditions, thereby decreasing the dependence on hazardous agrochemicals. Endophytic bacteria are those bacteria that live inside the plant, colonizing the internal root or shoot tissue, providing beneficial effects to the plants without any degree of pathogenesis. Numerous gram-positive and gram-negative bacteria have been reported to colonize nearly all plants, ranging from the woody plants (e.g.

Oak, Pear, etc.) to the herbaceous plants including crops (rice, maize, sugar beet, etc.). Inoculations of the crop plants with certain strains of the PGPR during the early stage of development enhance biomass production through direct induction of roots and shoot growth in plants. PGPR, when inoculated in ornamental plants, essential forest trees, crops and vegetables shows multiple effects on early-season plant growth through enhancement of seed germination, plant vigor, plant height, root and shoot weight, net chlorophyll content, etc. PGPR employs multiple mechanisms for increasing the growth of plants (Lodewyckx *et al.*, 2002). They induce nitrogen fixation in legumes, help in the promotion of other free-living nitrogen-fixing bacteria, increase the supply of other minerals and nutrients, such as phosphorus, iron, sulfur and copper, produce plant hormones essential for plant growth, provide resistance from pathogenic bacteria and fungus and help in controlling insect pests. The micro-ecosystem in plants is exploited by several genera of bacteria such as *Agrobacterium*, *Agromonas*, *Azorhizobium*, *Azotobacter*, *Azospirillum*, *Bacillus*, *Burkholderia*, *Photobacterium*, *Pseudoalteromonas*, *Pseudomonas*, *Rhizobacter*, *Rhizobium*, *Rhizomonas*, *Serratia*, *Streptomyces*, *Xanthomonas*, etc. (Lodewyckx *et al.*, 2002). Several studies have suggested the use of rhizospheric bacteria either through bio-priming or foliar/soil application or in combination reduces the disease susceptibility of the host plant and increases plant growth parameters.

1.3 Antagonistic Bacterial- Fungal Interactions

Bacillus species and other PGPR holds a great significance in the realm of biopesticides. This is attributed to their capacity to synthesize a diverse array of antimicrobial compounds, such as lipopeptides, antibiotics, and enzymes. These bioactive agents facilitate plant growth and concurrently impede the proliferation of pathogenic microorganisms. *Bacillus* species are prevalently found in soil ecosystems and are adept at generating metabolites endowed with antibiotic properties, which exhibit the potential to diminish or suppress the growth of coexisting microorganisms (Khan *et al.*, 2021). Furthermore, *Bacillus* species also release volatile compounds that contribute to augmenting the host plant's defense mechanisms. The biocontrol attributes of *Bacillus* species have proven antagonistic activity against bacterial and fungal phytopathogens, signifying their substantial role in safeguarding plants against disease. Among the antimicrobial substances synthesized by *Bacillus* species are subtilin, bacilysin, bacillomycin, iturin, fengycin and surfactin. These compounds collectively exhibit both antifungal and antibacterial activities. Given their proficiency in producing a diverse range of antimicrobial agents and their environmentally benign nature,

Bacillus species emerge as compelling contenders for deployment as bio-control agents (Khan *et al.*, 2021).

Brassica oleracea L. var. *capitata* commonly known as cabbage and *Brassica juncea* L. commonly known as rapeseed- mustard are the most cultivated leafy vegetable and oilseed crops worldwide (Morebet *al.*, 2022). Both crops are severely affected by several pathogens like *Albugo candida*, *Erysiphecruciferarum*, *Peronosporaparasitica* and *Alternaria* spp. Among the significant plant pathogens, cabbage black spot disease caused by various *Alternaria* sp. stands out as a pivotal concern due to its potential to inflict both qualitative and quantitative losses on plants, consequently reducing their shelf-life. Kolte, (2002) reported that the impact of *Alternaria* blight disease on oilseed Brassicas can lead to yield losses of up to 60%. The causal agents, *A. brassicicola*, *A. brassicae* and *A. japonica* collectively contribute to the development of black spot disease in cruciferous plants (Peruch *et al.*, 2006; Reis and Boiteux, 2010). India is the second largest producer of cabbage and Assam ranks 5th among the states. To cope up with fungal pathogens, farmers apply fungicides and treat the plantlets with chemical fungicide solutions that are toxic to soil and aquatic life and have an indirect effect on human life.

Objectives of the Investigation

Considering the aforementioned details, the following objectives was devised to explore the rhizospheric bacterial population of healthy cabbage plants and elucidate its potential role as bio-control agents against the devastating fungal pathogen for eco-friendly management practices:

1. Screening and identification of the culturable rhizospheric bacteria from cabbage having antagonistic activity against its pathogenic fungi, *Alternaria* spp.
2. Deciphering the metabolic changes during the antagonist bacterial and pathogenic fungal interaction.
3. Evaluation of the plant growth promoting ability of the potential bacterial isolates and its efficiency in disease suppression in cabbage.

CHAPTER II

REVIEW OF LITERATURE

The literature review is structured into the subsequent subsections, based on the research objectives undertaken for this study.

2.1 Bacterial-Fungal Interactions

Bacteria and fungi are the most dominant group of microbes found in any ecosystem where they live and interact with all its biotic and abiotic components. These interactions have a potential role in their surrounding habitat. When any two microbial species interact, their association may be classified into three main different types *viz.*, mutualism, commensalism and parasitism. Symbiotic interactions between eukaryotes and prokaryotes enable both organisms to survive extremes of the environment. In the evolution of the eukaryotic cell, the acquisitions of mitochondria and plastids were important events, which act as compartmentalized bio-energetic and biosynthetic factories in eukaryotic cell (Dyall, 2004). Bacterial and fungal interaction plays a vital role in the proper functioning and maintenance of an ecosystem. They are keystone communities maintaining the biogeochemical cycles and have direct impact on the soil health, plant and animal fitness and diseases respectively (Fig.1.). Moreover, bacterial and fungal interactions have been exploited by humans over centuries for their role in food, pharmacology and antibiotic industries (Deveau *et al.*, 2018). The by-products of the interactions have been used for ages in the field of agriculture, horticulture, forestry and environment protection and several other biotechnological applications.

2.2 Biological control of plant diseases

Over decades, the scenario of world agriculture experienced high increase in crop yield which was achieved through high use of inorganic fertilizers and pesticides, and mechanization driven by non-renewable fossil fuel. This has led to serious environmental threats such as deterioration of soil quality and health, ground water and ocean pollution and rising of resistant pathogen strains. This brings a big challenge to feed the rising world population on decreasing agricultural lands without causing harm to the environment. One of the efficient ways to decrease the negative impact of the continuous use of chemical fertilizers, herbicides and pesticides on the environment is by using beneficial endophytes

and plant growth-promoting rhizobacteria (PGPR) as biological a control (Kloepper *et al.*, 2004).



Fig. 2.1. Bacterial-Fungal Interactions and its potential applications
(Deveau *et al.*, 2018)

The term ‘biological control’ can be comprehensively defined as the mitigation of detrimental activities carried out by one or more organisms, commonly referred to as natural antagonists. However, within the context of plant pathology, the conceptualization of biological control pertains to the intentional deployment of introduced or indigenous biotic entities, apart from disease-resistant host plants, with the aim of diminishing the activities and populations of one or more plant pathogens (Pal and Gardener, 2006). The growing interest in the selection of advantageous microorganisms to raise the development of biological control agents (BCAs) has been encouraged by the crucial role of microbial biopesticides within the framework of Integrated Pest Management (IPM) (Matyjaszczyk *et al.*, 2015). While strains of microorganisms (including bacteria, fungi and

viruses) for the management of plant diseases and pests are economically viable (Montesinos and Bonaterra, 2017), the efficacy of these biological products might exhibit variation across experimental trials or experience decline under field conditions due to the interplay of biotic and abiotic factors (Sundin *et al.*, 2009).

2.3 Biological control of soil-borne pathogens

The term PGPR was first defined by Kloepper and Schroth in 1978 to describe the bacteria living in the soil that colonize the rhizosphere of plants, growing in, or around plant tissues that promote plant growth by various mechanisms. PGPR maintains good soil health through several mechanisms such as nutrient recycling, uptake of nutrients, suppression of plant pathogens and induction of resistance in plant host (Kloepper *et al.*, 2004; Haas and Defago, 2005). For more than eight decades, the exploration of using microorganisms for the biological control of soil-borne plant pathogens has been ongoing. Rhizospheric microorganisms stand as ideal candidates for their bio-control activity due to their inherent property, as the rhizospheric microbes confer frontline resistance to root systems against pathogenic incursions (Suprpta *et al.*, 2012). Although synthetic pesticides provide swift disease management, their profound impact on human health and the environment is undeniable. Synthetic pesticides directly influence both flora and fauna while disrupting the populations of beneficial microorganisms crucial for plant growth. Consequently, there is an increase need to seek alternatives to chemical pesticides for effective plant disease management. The biological control of plant diseases involves the suppression of plant pathogen populations through the actions of living organisms (Heimpel and Mills, 2017). Biological control, a multi-faceted phenomenon, hinges upon the rhizospheric adeptness of microbial inoculants, their interactions with the indigenous microbiota, competitive prowess for nutrient acquisition, adaptability to shifts in environmental conditions, and conferring resistance to the host plant against pathogens (Pal and Gardener, 2006). Biological control emerges as a promising alternative for disease management (Table 2.1), offering eco- friendly solutions. This approach not only safeguards the delicate balance of ecosystems but also enhances soil fertility.

Table 2.1. List of bacterial strains reported as bio-control agents (Adapted from Tariq et al., 2020)

Bacterial strains	Test Plant/Disease	Target pathogen	References
<i>Azospirillum brasilense</i>	Strawberry/anthracnose	<i>Colletotrichum acutatum</i>	Tortora et al. (2011)
<i>Azotobacter chroococcum</i>	Cotton and rice	<i>Rhizoctonia solani</i>	Chauhan et al. (2012)
<i>B. subtilis</i> BY-2	Oil seed rape	<i>S. sclerotiorum</i>	Hu et al. (2014)
<i>Bacillus licheniformis</i> BL06	Pepper	<i>Phytophthora capsici</i>	La et al. (2020)
<i>Bacillus megaterium</i>	Curus fruit	Blue mould	Mohammadi et al. (2017)
<i>Bacillus methylotrophicus</i>	Maize/Stalk rot	<i>Fusarium graminearum</i>	Cheng et al. (2019)
<i>Bacillus subtilis</i> 26DCryChS	Wheat	<i>Stagonospora nodorum</i> Berk.	Maksimovet al. (2020)
<i>Bacillus thuringiensis</i>	Sclerotinirose/Brassica campestris L.	<i>Sclerotinia sclerotiorum</i>	Wang et al. (2020)
<i>Brevibacillus brevis</i>	Strawberry/Grey mould	<i>Botrytis cinerea</i>	HaggagWafaa (2008)
<i>Brevibacillus brevis</i>	Tomato	<i>Fusarium oxysporum f.sp. lycopersici</i>	Chandel et al. (2010)
<i>Burkholderia cepacia</i> strain BY	Tomato/Damping-off	<i>Rhizoctonia solani</i>	Szczech and Shoda (2004)
<i>Ochrobactrum anthropi</i> BMO-111	Tea/blister blight	<i>Exobasidium vexans</i>	Sowndhararajan et al. (2013)
<i>P. chlororaphis</i>	Canola plant	<i>S. sclerotiorum</i>	Savchuk and Fernando (2004)
<i>Paenibacillus alvei</i> K- 165	Cotton/black root rot	<i>Thielaviopsis basicola</i>	Schoina et al. (2011)
<i>Paenibacillus polymyxa</i> BRF-1	Soybean/Root rot	<i>Phialophora gregata</i>	Zhou et al. (2008)
<i>Pantoeaag glomerans</i>	Wheat root pathogen	<i>Rhizoctonia solani</i> AG-8	Barnett et al. (2006)
<i>Pantoeaag glomerans</i>	Banana/crown rot	<i>Colletotrichum musae</i> and <i>Lasiodiplodia theobromae</i>	Gunasinghe and Karunaratne (2009)
<i>Pseudomonas and Burkholderia</i>	NA	<i>Phytophthora capsici</i>	Khatun et al. (2018)
<i>Pseudomonas fluorescens</i>	Apple/Mucor rot	<i>Mucor piriformis</i>	Wallace et al. (2018)
<i>Pseudomonas parafulva</i> JBCS1880	Soybean/Bacterial pustule Rice/Panicle blight	<i>Xanthomonas axonopodispv. glycines</i> , <i>Burkholderia glumae</i>	Kakembo and Lee (2019)
<i>Pseudomonas putida</i> BP25	Blast Disease/Rice	<i>Magnaporthe oryzae</i>	Ashajyothia et al. (2020)
<i>Rhizobium japonicum</i>	Soybean/Root rot	<i>Fusarium solani</i> ; <i>Macrophomina phaseolina</i>	Al-Ani et al. (2012)

2.4 Plant pathogenic Fungi

Fungi are the most common causative agents of plant diseases. In their pursuit to colonize plants and induce diseases, pathogenic fungi employ a diverse array of strategies. These interactions encompass a broad spectrum of outcomes, ranging from beneficial associations to disease occurrence in the host plant (Doehlemann *et al.*, 2017). The majority of fungal plant pathogens are found within the phyla Ascomycota (e.g., *Botrytis*, *Magnaporthe*, *Alternaria*, etc.) and Basidiomycota (e.g., Pucciniomycetes and Ustilaginomycotina). Fungal infections elicit a wide array of disease symptoms. Traditionally, plant pathogenic fungi are categorized into two primary groups: biotrophic pathogens, which establish intimate interactions with plants and can subsist within and exploit living tissues (biotrophs) and necrotrophic pathogens, which cause tissue demise to extract nutrients (necrotrophs). In addition to these two categories, a distinct group known as hemibiotrophic pathogens starts their interaction as biotrophs and then transition to necrotrophic behavior. The actions of necrotrophs lead to necrosis and, ultimately, the death of infected plants (Doehlemann *et al.*, 2017). Several methodologies have been used for the isolation of pathogenic fungi from diverse sources. Predominantly, these techniques employ Potato Dextrose Agar (PDA) as a medium for fungal isolation (Singh *et al.*, 2015; Sharma and Pandey, 2010). Nevertheless, alternative common media for fungal isolation encompass Czapek Agar, Malt Extract Agar, Yeast Extract Agar, Sabouraud Dextrose Agar and occasionally synthetic agar media, selected based on the specific characteristics of the fungi to be isolated (Levetin and Dorsey, 2006; Smit *et al.*, 1999; Sharma and Pandey, 2010). In the context of plant samples, fungal pathogens are typically isolated through the inoculation of minute segments of diseased plant tissue, such as leaf segments, stems, affected flower parts, seeds, fruits, etc. Furthermore, fungal spores generated on plant surfaces like leaves or fruits can also serve as viable material for isolation of fungal pathogens (Sharma and Pandey, 2010). Surface sterilization is an important procedure aimed at eliminating surface contaminants, such as spores of fungi and bacterial cells, during the isolation of pathogenic fungi. The conventional methods for surface sterilization encompass the utilization of sodium hypochlorite, mercuric chloride, ethanol, potassium permanganate and other sterilizing agents.

2.5 Plant growth promoting rhizospheric bacteria

Plant growth-promoting rhizobacteria (PGPR) includes the bacteria living on the rhizospheric zone of plant and profoundly influence plant growth and provide stress

resistance through a diverse array of mechanisms (Glick, 2012). PGPR are currently the subject of extensive investigation due to their attributes, which hold significant promise for both conventional and sustainable agricultural practices (Farrar *et al.*, 2014). The multifaceted roles of PGPR encompass plant mineral nutrition *via* nitrogen fixation partnerships (Kuan *et al.*, 2016), catalyzing phosphate mobilization within the soil matrix (Chen *et al.*, 2006, Mehta *et al.*, 2015), generating siderophores (Vansuyt *et al.*, 2007, Zhou *et al.*, 2016), fostering mycorrhizal symbiosis development, and modulating root architecture (Navarro-Rodenas *et al.*, 2016). Additionally, PGPR can elicit plant defense against pathogens (Van de Mortel *et al.*, 2012, Sharifi and Ryu, 2016), hinder pathogen proliferation (Ali *et al.*, 2014, Saraf., 2014, Prasannakumar *et al.*, 2015) and mitigate the inhibitory impacts of abiotic stressors such as drought (Lim and Kim, 2013), salinity (Kim *et al.*, 2014) and heavy metal contamination (Gupta *et al.*, 2002, Zhu *et al.*, 2015). Owing to a rising public apprehension regarding the deleterious impacts of chemical fertilizers and pesticides, there exists a mounting interest in enhancing our comprehension of the intricate molecular mechanisms that underlie the interactions between plants and their microbial community within the rhizosphere (Tsukanova *et al.*, 2017).

2.6 Characterization of bacterial and fungal isolates

2.6.1 Morphological characterization

The foundational tools of classical microbiology play a pivotal role in the comprehensive characterization of bacteria, many of which trace their origins to Leeuwenhoek's invention of the microscope in 1674. Initial profiling of bacterial and fungal isolates entails the exploration of macroscopic and microscopic attributes that facilitate the categorization of these microorganisms into distinct major groups. These defining parameters encompass colony morphology, cellular morphology encompassing shape, size, and arrangement, cell wall properties, growth patterns and various others. As an illustrative instance, the morphological attributes of an endofungal bacterium such as *Burkholderia rhizoxinica* can be delineated as possessing irregular colonies during pure culture, exhibiting cell sizes ranging from 1.2 to 2.0 μm in length and 0.6 to 1.2 μm in width, and presenting short or coccoid rod-shaped cells that occur individually, in pairs, or as irregular clusters. By virtue of its cell wall properties, *Burkholderia rhizoxinica* can be categorized as gram-negative (Partida-Martinez *et al.*, 2007b). Of notable significance, the Gram staining technique stands as a critical parameter for the dichotomous classification of bacteria into two principal classes: Gram-positive and Gram-negative. The former encompasses bacteria

characterized by a robust cell wall comprised of peptidoglycan that exhibits distinct staining characteristics when compared to the latter. Gram-negative bacteria, on the other hand, exhibit a notably thinner layer of peptidoglycan enveloped by an outer lipid membrane (Schleifer and Kandler, 1972).

The morphological analysis of fungi encompasses the examination of various characteristics, including colony morphology (such as color, texture, pattern, and growth behavior), the microscopic architecture of hyphae (encompassing size, septation and branching arrangement), sporangiophores (covering position, shape and size), as well as spores (encompassing size, shape and arrangement). These factors, among others, contribute to the comprehensive understanding of fungal species. The initial phase of fungal identification hinges upon distinguishing between yeast and mold. This differentiation can be achieved through morphological observations. Yeasts manifest as regular colonies on solid substrates and appear as single-celled organisms displaying budding when observed under a microscope. On the other hand, molds, referred to as filamentous fungi, develop elongated structures known as hyphae. The identification of molds relies on a combination of their visible macroscopic attributes, microscopic traits and the structures responsible for asexual reproduction (Byrne, 2014). For the purpose of fungal identification, algorithms have been developed (Merz and Roberts, 2003). These algorithms facilitate the recognition of specific fungal species, enabling identification at least up to the genus level. Isolates of *Alternaria brassicae* exhibited diverse cultural attributes. These attribute encompassed variations in colony color, ranging from white, off-white to light brown. The appearance of colonies displayed a spectrum from cottony to flurry and further to feathery textures. In terms of colony growth rate, a range of slow, medium and fast growth was observed. Additionally, colony margins exhibited diversity, spanning from wavy to smooth and even rough in certain instances. Notably, there was noticeable heterogeneity in colony diameter on the PDA medium (Dixon, 1981; Macioszek *et al.*, 2018).

2.6.2 Biochemical characterization of bacteria

Biochemical characterization is a valuable approach for assessing the metabolic efficiency of bacteria with direct or indirect links to their genetic composition. This involves examining various enzymatic properties that govern the utilization of specific substrates, such as sugars, amino acids and polysaccharides. The outcomes encompass the generation of acids, pigments, gases and other products. Several pivotal biochemical tests include:

Indole Production Test: This assay detects the organism's ability to oxidize tryptophan, resulting in the creation of indole, pyruvic acid and ammonia.

Methyl Red Test: Utilized to detect microorganisms' capacity to oxidize glucose, yielding high levels of acid and related products.

Voges-Proskauer Test: This test distinguishes microorganisms that produce non-acidic or neutral end products, like acetyl methyl carbinol and 2,3-butanediol.

Citrate Utilization Test: It differentiates bacteria based on their capacity to utilize citrate as a sole carbon source. Citrate breakdown relies on the enzyme citrase, leading to oxaloacetic and acetic acids.

Catalase Test: Used to differentiate microorganisms according to their ability to oxidize hydrogen peroxide (H_2O_2), yielding oxygen and water.

Oxidase Test: Identifies cytochrome c oxidase-producing bacteria, crucial for the bacterial electron transport chain. It aids in distinguishing between oxidase-positive Pseudomonadaceae and oxidase-negative Enterobacteriaceae, aiding in speciation.

Nitrate Reduction: This test discriminates Enterobacteriaceae members based on their ability to produce nitrate reductase, which converts nitrate (NO_3^-) to nitrite (NO_2^-). Further conversions to nitrogen oxide, nitrous oxide, or ammonia (NH_3) depend on the organism's enzymatic system and growth atmosphere.

Thus, biochemical characterization is a powerful method for probing the metabolic attributes of microorganisms, unveiling insights into their genetic underpinnings and physiological capabilities.

2.6.3 Molecular characterization

The rapid advancement in molecular biological research has greatly facilitated the development of novel methodologies for characterizing and identifying microorganisms. Molecular techniques have gained prominence as valuable tools for acquiring data to investigate the taxonomic and phylogenetic relationships among microorganisms (Zambino and Szabo, 1993). Integrating molecular methods with morphological approaches for bacterial and fungal species identification enhances the accuracy of taxonomic investigations. Woese and Fox (1977) originally proposed utilizing ribosomal RNA genes for molecular taxonomic inquiries. The process of bacterial identification through molecular means utilizes PCR amplification of the 16S ribosomal RNA gene, followed by sequencing. Sequencing the

16S rRNA gene permits bacterial identification due to a distinct variable sequence unique to each species. Amplifying and sequencing the 16S rRNA gene enables the assignment of bacteria to their respective taxonomic positions (Buszewski *et al.*, 2017). Weisburg *et al.* (1991) introduced a set of universal forward and reverse primers capable of amplifying the 16S rRNA gene across most bacterial species, widely employed for bacterial molecular characterization. Lane (1991) proposed a widely accepted universal primer pair for 16S rRNA gene amplification, a modification of the fD1 and rP2 primers originally outlined by Weisburg *et al.* (1991). These two sets of universal primers have been extensively used for bacterial species identification (Dymock *et al.*, 1996; Rolph *et al.*, 2001).

In fungi, ribosomal RNA genes are found on a single chromosome and exist as repeated subunits within a tandem array of transcribed and non-transcribed DNA segments, known for their high conservation (Wipf *et al.*, 1999). The Internal Transcribed Spacer (ITS) region, a non-functional RNA segment between structural ribosomal RNAs on a common precursor transcript, is a prominent feature in eukaryotes. Comprising two parts, ITS1 and ITS2, it separates the 18S and 5.8S rRNA genes and the 5.8S and 28S rRNA genes, respectively (Fig. 2.2) (Lafontaine and Tollervey, 2001). The ITS region is widely employed in taxonomy and molecular phylogeny due to its amplification ease from small DNA quantities and substantial variation among closely related species. The ITS region is a frequently sequenced DNA segment in fungal molecular ecology (Peay *et al.*, 2008) and is recommended as the universal fungal barcode sequence (Schoch *et al.*, 2012). Beyond the widely used ITS1 and ITS4 primers (White *et al.*, 1990), various taxon-specific primers have been developed to selectively amplify fungal sequences (Gardes and Bruns, 1993; Larena *et al.*, 1999).

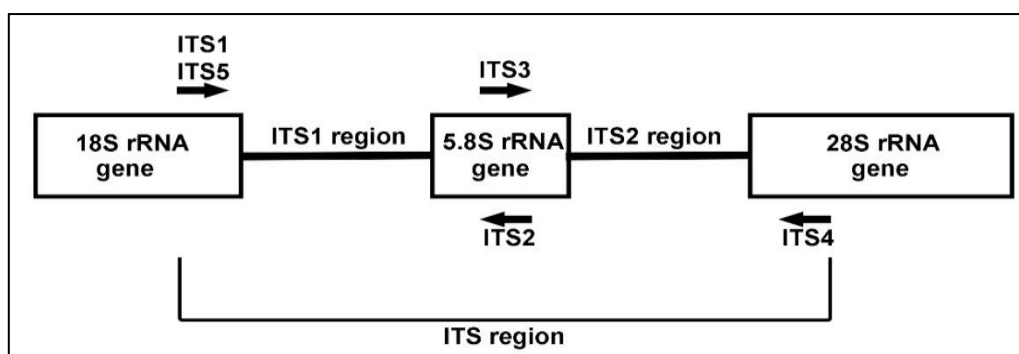


Fig. 2.2. Internal transcribed spacer (ITS) region of fungal genome

2.6.4 Phylogenetic analysis

A phylogenetic tree, also known as an evolutionary tree, is a visual representation resembling a branching diagram. It illustrates the inferred evolutionary connections among diverse biological species or entities based on the similarities and differences in their genetic or physical attributes. The arrangement of taxa within the tree implies their shared ancestry. In this representation, each node signifies the hypothesized most recent common ancestor of its descendants. Some trees may depict edge lengths as time estimates. The nodes, often referred to as taxonomic units, include internal nodes, which are hypothetical and cannot be directly observed. Phylogenetic trees find application in biology fields like bioinformatics, systematics and phylogenetic comparative methods. A rooted phylogenetic tree demonstrates the evolutionary progression of organisms originating from a common source. Unrooted trees only display the relationships among leaf nodes and do not necessitate knowledge or inference of the ancestral root. Constructing phylogenetic trees involving a substantial number of input sequences employs computational phylogenetics methods. Methods for building these trees can be categorized as distance-based or character-based. Distance-based methods gauge the dissimilarity (distance) between aligned sequences to construct trees. If all genetic divergence events were precisely captured in the sequence, a distance method would accurately reconstruct the true tree. Notably, distance-matrix techniques like neighbor-joining (NJ) (Saitou and Nei, 1987) compute genetic distances from multiple sequence alignments. While relatively straightforward, these methods do not incorporate an explicit evolutionary model. More sophisticated methods include maximum parsimony (MP), which estimates phylogenetic trees based on a principle of minimal evolutionary changes (parsimony). Advanced techniques often employ the maximum likelihood (ML) optimality criterion, sometimes within a Bayesian framework, incorporating an explicit model of evolution for accurate tree estimation (Felsenstein, 2004). Several software programs are available to compute phylogenetic relationships, employing algorithms from the aforementioned tree-building methods. MEGA, for instance, integrates various inference techniques (such as NJ and MP) to estimate evolutionary distances from nucleotide and amino acid sequence data (Kumar *et al.*, 1994; Tamura *et al.*, 2013).

2.7 *Bacillus amyloliquefaciens*

Bacillus amyloliquefaciens classified as a Gram-positive bacterium with the ability to form spores, is commonly found in soil environments. This microorganism exhibits the capacity to establish colonization within the rhizosphere of plants and demonstrates

resilience when exposed to adverse conditions. Notably, *B. amyloliquefaciens* is regarded as a biologically safe and environmentally friendly agent with the potential to stimulate plant growth (Chen *et al.*, 2007; Qiao *et al.*, 2014). Functioning as a representative member of plant growth-promoting rhizobacteria (PGPR), *B. amyloliquefaciens* stands out as a promising candidate for the development of biofertilizers and biocontrol agents in the realm of agriculture. Its utility extends to enhancing plant resistance against both biotic and abiotic stressors (Dimopoulou *et al.*, 2021; Gamez *et al.*, 2019; Kazerooni *et al.*, 2021). The versatility of *B. amyloliquefaciens* has led to its widespread application in diverse plant species such as rice, watermelon, cucumber and tobacco (Wu *et al.*, 2019; Saechow *et al.*, 2018; Jiao *et al.*, 2021). Due to its substantial potential as both a biofertilizer and biocontrol agent, *B. amyloliquefaciens* has been the subject of active investigation regarding its mechanisms for promoting plant growth (PGP) and its antimicrobial activities. *B. amyloliquefaciens* strains possess a multitude of genes dedicated to producing various substances, encompassing phytohormones for inducing plant growth, polysaccharides for fostering biofilm formation, siderophores to enhance iron solubilization, lytic enzymes, as well as an array of non-ribosomal synthesized polyketides and lipopeptides (Fig. 2.3) that effectively inhibit pathogens (Qin *et al.*, 2015; Rückert *et al.*, 2011). Extensive research involving *in vitro* and field trials has demonstrated the ability of *B. amyloliquefaciens* to enhance plant growth through diverse mechanisms. These include the production of hormones, volatile organic compounds (VOCs), siderophores, and the augmentation of soil nutrient availability, coupled with the suppression of soil-borne pathogens (Sheteiwy *et al.*, 2021; Shahid *et al.*, 2021). Additionally, *B. amyloliquefaciens* exhibits the capacity to positively modulate the expression of stress-responsive genes in plants subjected to abiotic stressors (Chen *et al.*, 2017; Tiwari *et al.*, 2017).

2.7.1 Effect of *Bacillus amyloliquefaciens* on plant growth

Recent research efforts have predominantly centered on the application of *Bacillus amyloliquefaciens* in various fields, particularly in agriculture. These investigations have revealed that numerous strains of *B. amyloliquefaciens* exhibit the ability to enhance plant growth through a diverse array of mechanisms. For example, strains like B1, B5 and B21 have been demonstrated to exert strong inhibitory effects on fungal phytopathogens, concurrently eliciting significant positive impacts on *Arabidopsis* total plant fresh weight, with an increase of 21.27%, 51.16% and 35.92%, respectively (Lu *et al.*, 2021). The inoculation of tomatoes with the *B. amyloliquefaciens* strain MBI600 resulted in a 75%

reduction in disease severity and disease index. This treatment also led to substantial enhancements in fresh shoot weight (15.32%), height (13.63%) and root length (20.91%) compared to untreated control plants (Samaras *et al.*, 2016). Another *B. amyloliquefaciens* strain, SB-1, exhibited remarkable broad-spectrum antifungal activity attributed to the production of antifungal metabolites including surfactins, iturins and fengycins. This strain also synthesized indole acetic acid (IAA) linked to plant growth promotion, significantly augmenting the total dry weight (29.76%), root dry weight (96.63%) and shoot dry weight (66.17%) of wheat (Shahid *et al.*, 2021). Additionally, the application of *B. amyloliquefaciens* as biofertilizer (strain A3) demonstrated substantial enhancements in the yield and quality of tea plants (Bai *et al.*, 2014). Research indicated that *B. amyloliquefaciens* can foster plant growth and suppress phytopathogens by emitting volatile organic compounds (VOCs) (Chen *et al.*, 2007; Yu *et al.*, 2012; Ji *et al.*, 2021).

A significant impediment to plant growth is the scarcity of soil nutrients. Addressing this challenge, *B. amyloliquefaciens* stands out as a potent biofertilizer, offering attributes that enhance soil nutrient availability. *B. amyloliquefaciens* effectively ameliorates soil nutrient status through various mechanisms (Xue *et al.*, 2021). These encompass the enhancement of nitrogen (N) supply, the solubilization of phosphates, the facilitation of potassium (K) solubilization and the production of siderophores (Fig. 2.4).

Substances#	Strains	Genes and gene cluster	Function
IAA	FZB42, SQR9, Ba13, UCMB5113	<i>dhaS, patB, yclB, yclC, yhcX</i> and <i>ysnE</i>	Plant growth promotion
Phytase	FZB45, SQR9, Ba13	<i>phyC</i>	Improve phytate phosphorus available
Siderophores	FZB42, B9601-Y2, Ba13, UCMB5113, DSM7T	<i>dhbACDEBF</i>	Chelate Fe ³⁺
LP: Fengycin	FZB42, B9601-Y2, PG12, 32a, UCMB5113, DSM7T	<i>fenABCDE</i>	Antifungal, Antibacterial
LP: Surfactins	FZB42, Ba13, 32a, UCMB5113, DSM7T	<i>surfABCD</i>	Antifungal, Antibacterial, Antiviral, Biofilm formation, ISR
LP: Bacillomycin D	FZB42, B9601-Y2, Ba13, PG12, 32a, UCMB5113	<i>bmyCBAD</i>	Antifungal, Antibacterial
LP: Ituin A	FZB42, PG12, 32a	<i>ituD</i>	Antifungal, Antibacterial
Polyketides: Bacillaene	FZB42, B9601-Y2, Ba13, 32a, UCMB5113, DSM7T	<i>bacABCDE, acpK, bacGHIJLMNRS</i>	Antibacterial
Polyketides: Difficidin	FZB42, B9601-Y2, 32a	<i>dfnA-YXBCDEFGHIJKLM</i>	Antibacterial
Polyketides: Macrolactin	FZB42, CHO104, B9601-Y2, 32a, UCMB5113	<i>mlnABCDEFGHI</i>	Antibacterial
Dipeptide: Bacilysin	FZB42, Ba13, B9601-Y2, 32a, UCMB5113, DSM7T	<i>bmyD, pks2, pks3, nrs, bacABCDEFGH</i>	Antibacterial
Peptide: Plantazolicin	FZB42	<i>RBAM_007470</i>	Antinematodes, Antibacterial
VOC: 2,3-butanediol	FZB42, B9601-Y2, Ba13, UCMB5113	<i>bdhA</i>	Against pathogens, ISR, Plant growth promotion, Antifungal
VOC: Acetoin	SQR9, UCMB5113	<i>alsDRS</i>	Against pathogens, ISR, Plant growth promotion, Antifungal

Fig. 2.3. Secondary metabolites and their associated gene clusters produced by *Bacillus amyloliquefaciens* for plant growth promotion. (#) IAA: indole acetic acids; VOC: volatile organic compounds LP: cyclic lipopeptides (Adapted from Luo *et al.*, 2022).

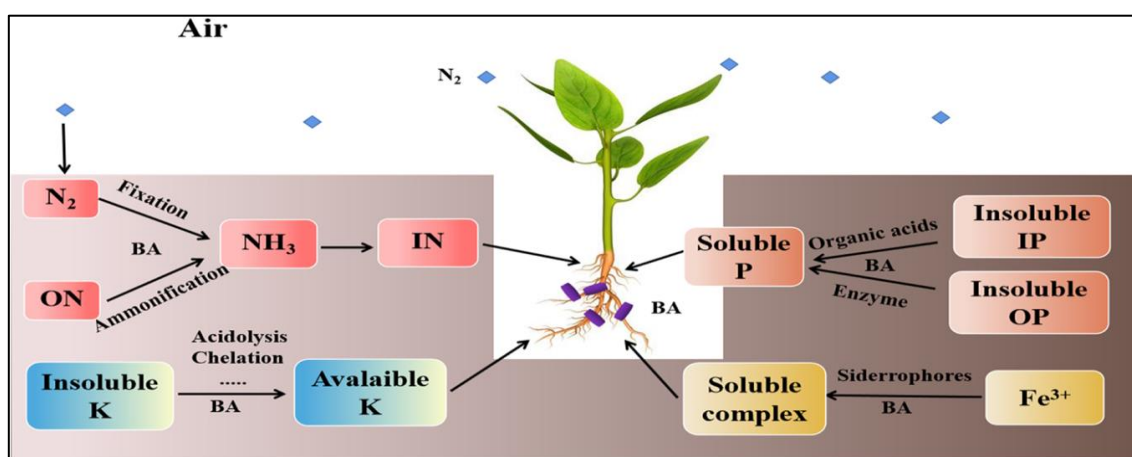


Fig. 2.4. Nutrient solubilization and its role in plant growth promotion by *Bacillus amyloliquefaciens* (BA). Organic nitrogen (ON), organic phosphorus (OP), inorganic nitrogen (IN), ammonia (NH₃), inorganic phosphorus (IP), potassium (K), phosphorus (P) and iron (Fe³⁺) and atmospheric nitrogen (N₂) (Adapted; Luo *et al.*, 2022)

A comparative genome analysis of *Bacillus amyloliquefaciens* and phylogenetic analysis reveals that *B. amyloliquefaciens* forms two clades. The clustering analysis revealed that the predominant *B. amyloliquefaciens* strains associated with plants were grouped within clade 2. Whereas, the clade-1, *B. amyloliquefaciens* are associated with a food-related environment. Employing genome mining techniques, an investigation into the prevalence of antimicrobial resistance and virulence genes across all strains was conducted, that showed specific genetic elements in clade 2. Genes such as *tmrB* and *yuaB*, encoding the tunicamycin resistance protein and hydrophobic coat forming protein, respectively, were exclusively present in clade 2. In contrast, clade 1 harbored the *clpP* gene, encoding serine proteases. This genetic divergence between the two clades reflects their adaptation to distinct ecological niches (Liu *et al.*, 2021).

2.8 *Bacillus subtilis*

Bacillus subtilis, a gram - positive bacterium usually found associated with the rhizosphere of plants and capable of producing spores that endure extended periods in soil, even amidst adverse environmental conditions. *B. subtilis* assumes a pivotal role in enhancing biotic stress tolerance as well (Fig. 2.5). This enhancement of disease resistance involves the orchestrated expression of specific genes and hormones, including 1-aminocyclopropane-1-carboxylate deaminase (ACC). Ethylene, while instrumental in plant homeostasis, also constrains root and shoot growth. Bacterial ACC acts by degrading the ethylene precursor (ACC), thereby alleviating plant stress and fostering normal growth even in challenging conditions (Glick *et al.*, 2007). *B. subtilis* strains are recognized for their ability to synthesize antibiotic lipopeptides, such as surfactin, fengycin and iturin. These lipopeptides are characterized by their amphiphilic properties and relatively small molecular weight. The demand for surfactants and antimicrobial compounds secreted by *B. subtilis* has been on the rise (Fig. 2.6). The presence of lipopeptide genes is widespread across various species and strains of bio-control agents, whereas certain strains produce antibiotics particularly in countering fungal roots pathogens. These strains have even been commercialized, showcasing their practical utility (Joshi and McSpadden Gardener, 2006). Research conducted by Romero *et al.* (2007) reveals the protective attributes of lipopeptides for plants, extending to both pre- and post-harvest scenarios. Their effects encompass direct suppression of pathogenic fungi as well as the induction of systemic resistance within host plants. *B. subtilis* strains like PCL1608 and PCL1612 exhibit high iturinA production. This compound assumes a pivotal

role in effectively controlling *Fusarium oxysporum* and *Rosellinia necatrix* (Cazorla *et al.*, 2007).

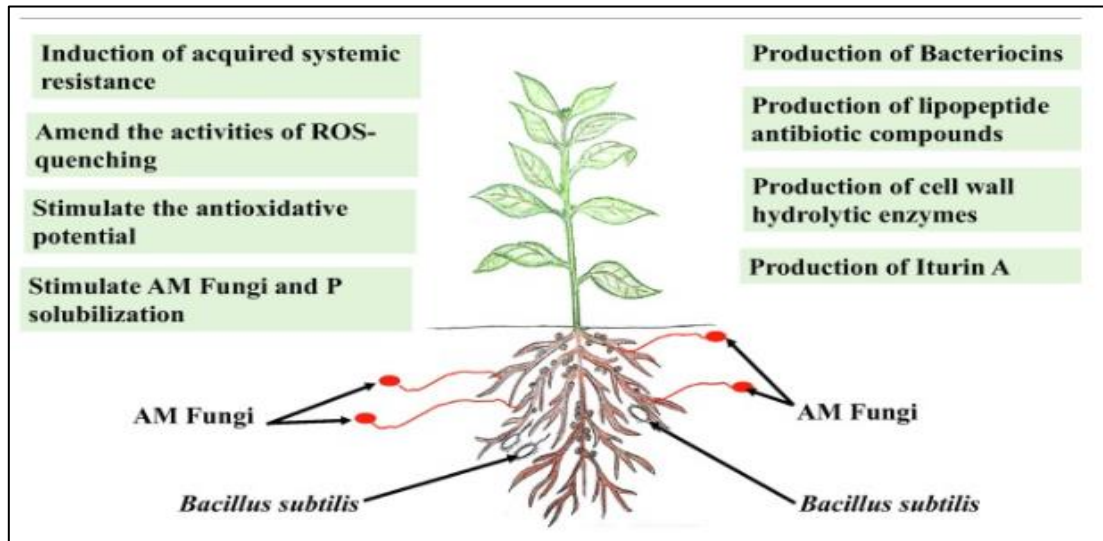


Fig. 2.5. Mechanism of biotic stress management of *Bacillus subtilis*. *AM- Arbuscular mycorrhiza (Adapted from Hashem *et al.*, 2019)

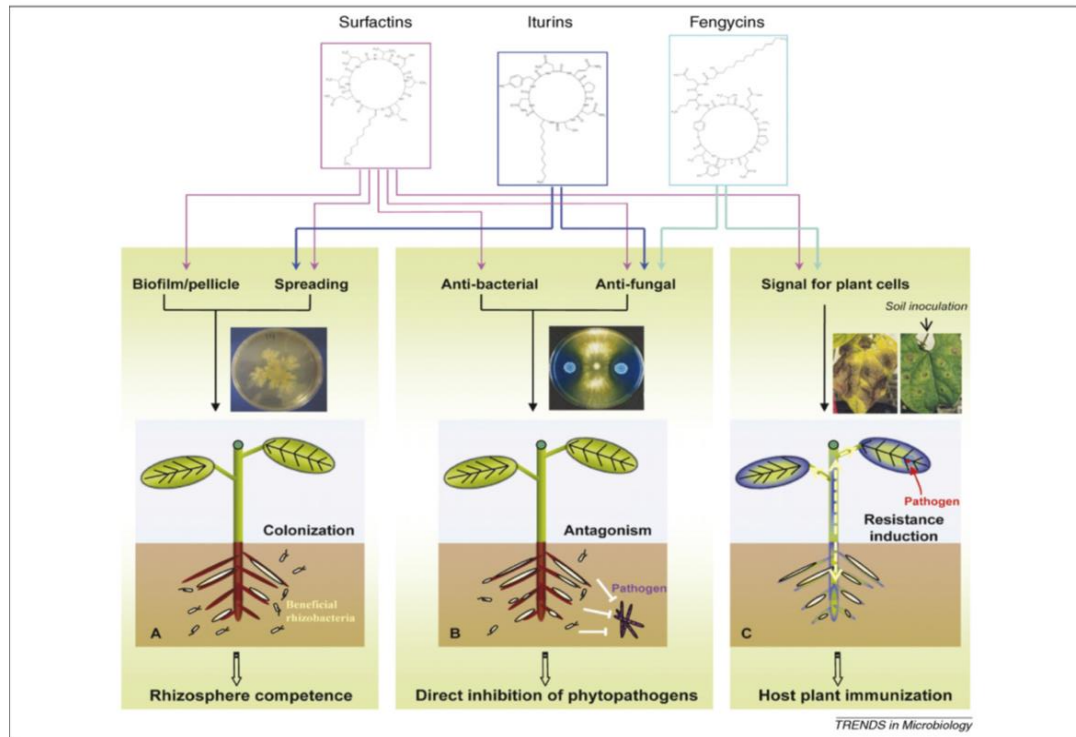


Fig. 2.6 Functional role of *Bacillus* lipopeptides in disease suppression (Adapted from Ongena and Jacques 2008)

2.9 *Alternaria brassicicola*

Alternaria brassicicola, a highly destructive parasitic plant pathogen, inflicts substantial harm across a diverse spectrum of host plants. It is responsible for black spot disease in nearly all members of the Brassicaceae family (Cho *et al.*, 2015). This encompassing range of host crops includes species like *Brassica oleracea* (vegetables), *Brassica rapa* (vegetables, oilseeds, and forages), *Brassica juncea* (vegetables and seed mustard) and *Brassica napus* (oilseeds) (Warwick and Fransis, 1994). The economic implications of this disease are felt globally leading to yield reductions in the range of 20% to 50% for crops such as canola and rape. Functioning as a necrotrophic plant pathogen, *A. brassicicola* thrives by both absorbing nutrients from dead tissue as well as from the nearby tissue of its host plants. This mechanism stands in contrast to that of biotrophic plant pathogens, which feed solely on living host tissues. The pathogenesis strategy of necrotrophic fungi is conceptually summarized in a two-step process. First, it involves the elimination of host cells or the initiation of programmed cell death through the release of toxins (Cho *et al.*, 2015). Subsequently, necrotrophic fungi degrade the deceased tissues using various carbohydrate-active enzymes, commonly referred to as cell wall-degrading enzymes (CWDEs) (Lebada *et al.*, 2001; Vidhyasekaran, 2008). Numerous physiological and morphological traits exhibited by different pathogenic fungi have been identified or postulated to play roles in necrotrophic pathogenesis. These attributes encompass specialized morphology (Howard and Ferrari, 1989), the secretion of secondary metabolites and toxins (Osborn, 2001), the synthesis of lipases (Voigt *et al.*, 2005), CWDEs (Lebada *et al.*, 2001; Vidhyasekaran, 2008), and proteases (Ball, 1991), along with unobstructed mycelial growth. The effectiveness of pathogenesis mechanisms is also influenced by a pathogen's capacity to withstand diverse environmental stresses, such as reactive oxygen species, pH fluctuations and host defense molecules. Additionally, deficiencies in development or metabolic processes within the organism can impact its pathogenic potential.

2.9.1 Genes associated with pathogenesis of *Alternaria brassicicola*

Alternaria brassicicola exhibits pathogenicity towards *Arabidopsis thaliana*, and the interaction between *A. brassicicola* and *A. thaliana* serves as an occasional model for investigating host-pathogen dynamics (Thomma *et al.*, 1999; Oh *et al.*, 2005). Essential components of pathogenesis include a conserved mitogen-activated protein kinase encoded by Amk1, along with its downstream transcription factor encoded by AbSte12 (Cho *et al.*, 2007, 2009). Amk1 governs the expression of genes that encode hydrolytic enzymes in *A.*

brassicicola. Cho *et al.* (2013) has reported that AbPf2, a transcription factor encoding gene is a key regulator of pathogenesis. The transcripts of the AbPf2 gene undergo exponential up-regulation immediately upon contact of wild-type conidia of *A. brassicicola* with their host plants, revealing its crucial role in the initial phase of the interaction process. Amk2, a MAPK encoding gene is responsible for maintaining the cell wall integrity of the fungi. Camalexin and brassinin are phytoalexin secreted by *A. thaliana* and can suppress the growth of *A. brassicicola*. AbHog1 and AbSlt2 MAP kinases are important in detoxifying the effect of the phytoalexin in *A. brassicicola* respectively. AbHog1 is involved in the high-osmolarity glycerol pathway maintaining cell wall integrity. However, mutation in AbHog1 and AbSlt2 reduces the pathogenicity and virulence of *A. brassicicola* (Joubertet *al.*, 2010).

2.10 Extraction and characterization of metabolites

2.10.1 Extraction techniques

Various methodologies have been documented for the extraction of secondary metabolites from a wide range of sources including fungi, bacteria, plants, fungi, and other organisms. These methods commonly rely on utilizing appropriate solvents, often coupled with heat and agitation, to extract bioactive compounds from biomass. Among the established classical techniques, three prominent approaches for obtaining bioactive compounds are Soxhlet extraction, maceration and hydrodistillation.

Soxhlet Extraction: This method involves the placement of dry biomass within a thimble, which is then subjected to extraction in a specialized apparatus called a Soxhlet apparatus, utilizing a suitable solvent. The process employs controlled heating and cooling to facilitate the circulation of the solvent throughout the biomass, aiding in efficient compound extraction (Azmir *et al.*, 2013).

Maceration: Widely employed in extracting bioactive compounds from bacteria, fungi, and medicinal plants, maceration is achieved by soaking either fresh or dried biomass in a container containing one or more solvents. The mixture is allowed to stand at room temperature with periodic agitation for an extended duration. Variations of this technique frequently incorporate enhancements such as heating, microwave assistance, ultrasound, or other methods to expedite the breakdown of biomass tissue/cells for more effective extraction (Azwanida, 2015).

Hydrodistillation: This conventional approach targets the extraction of essential oils and bioactive compounds from plant and fungal biomass. Three variations of hydrodistillation

exist: water distillation, water and steam distillation and direct steam distillation. Biomass is enclosed within a distillation apparatus and exposed to either boiling water or direct steam injection. The heat facilitates the release of essential oils and volatiles from the biomass, which then vaporizes and condenses alongside water vapor. The subsequent separation yields essential oils and bioactive compounds. Nonetheless, elevated temperatures can lead to the loss of volatile components and the degradation of thermo-labile compounds, a notable drawback (Azmir *et al.*, 2013).

Liquid-Liquid Extraction (LLE): The effectiveness of conventional extraction methods is heavily reliant on the selection of solvents. Solvent choice hinges on the polarity of the targeted compound and the molecular interaction between the solvent and solute. Liquid-liquid extraction exploits the differing solubility of bioactive compounds in aqueous and immiscible organic phases. This technique selectively extracts compounds into one solvent while leaving other matrix components in the alternative solvent. Solvents like hexane, cyclohexane and petroleum ether are employed to eliminate non-polar impurities, such as lipids and cholesterol. LLE proves valuable for toxins and small-scale preparations (Bauer and Gareis, 1987; Turner *et al.*, 2009).

2.10.2 Characterization techniques

The characterization and identification of secondary metabolites synthesized by bacteria or fungi can be achieved using several techniques, with several key properties being considered for the identification of specific metabolites. Fundamental properties, such as polarity, solubility, light absorption patterns, molecular mass and side chain information, play pivotal roles. To scrutinize the structural and functional attributes of extracted metabolites, a purification process is undertaken.

Thin Layer Chromatography: Among the chromatographic techniques employed for the purification and characterization of bioactive metabolites, TLC holds significance due to its simplicity and efficacy. In TLC, a stationary phase, like silica gel, is coated onto a glass plate or an aluminum sheet and the crude extract is applied as a spot or a line. A mobile phase composed of solvent combinations with varying polarities is employed. This differential polarity prompts the migration of compounds within the crude extract, leading to their distinct separation. The Retardation factor (R_f value) is specific to a particular compound, solvent system and stationary phase, and serves as a defining characteristic for the separated compounds (Sherma and Fried, 2003).

Gas Chromatography: Gas chromatography (GC) is a characterization method capable of separating compound mixtures while simultaneously detecting and quantifying their constituents. Primarily, volatile compounds with molecular masses below 1200 Daltons are amenable to gas chromatography. This technique employs a gaseous mobile phase for separation. The selected carrier gas remains inert to the sample mixture, facilitating the movement of sample molecules within the GC apparatus. The procedure commences with the introduction of a sample, possessing a known crude extract concentration, into the system through an inlet using a syringe or an autosampler. The inlet connects to an analytical column housing a stationary phase like polyethylene glycol or polydimethylsiloxane. Positioned within a detector, the column discerns signals emanating from distinct compounds. These signals manifest as peaks in a chromatogram, with each peak indicative of a particular compound. Following data acquisition *via* dedicated software, the chromatogram showcases these peaks at distinct time intervals (Zuo *et al.*, 2013).

Liquid Chromatography: Liquid chromatography (LC) is a characterization technique that employs a liquid as the mobile phase. Different types of LC exist based on the selection of stationary and mobile phases, with each type further distinguished by its performance level. Low-pressure liquid chromatography (LPLC) pertains to methods utilizing non-rigid materials with a particle size exceeding 40 μm in diameter. Utilizing low pressure in LPLC yields suboptimal system efficiencies and heightened plate heights. Consequently, peak broadening, reduced detection limits, elongated separation times, and diminished operating pressures and flow rates arise. In contrast, high-performance liquid chromatography (HPLC) is a superior LC methodology employing small, uniform and rigid materials. A column positioned between the stationary and mobile phases facilitates compound separation. The stationary phase comprises granular substances with minutely porous particles within a separation column. Conversely, the mobile phase incorporates a solvent or solvent mixture propelled through the separation column under high pressure. Diverse compounds within a sample traverse the column at varying rates. Upon exiting the column, compounds are detected through a suitable detector, generating a chromatogram presenting peaks at distinct retention times. These compounds are subsequently identified and quantified using methodologies like standards or reference databases (Kupiec, 2004; Nikolin *et al.*, 2004).

Mass Spectrometry: Mass spectrometry is a valuable analytical technique used for quantifying known compounds, identifying unknown compounds and elucidating the structure and chemical properties of various substances. It is often coupled with liquid

chromatography or gas chromatography for compound analysis. This technique involves an ion source, an analyzer and a detector. Various ionization methods such as electrospray ionization (ESI) generate multiple ions without fragmenting compounds that could break down at high temperatures, while atmospheric pressure chemical ionization (APCI) produces a single ion. This process converts compounds into gaseous ions, leading to fragment production, identifiable by their mass-to-charge (m/z) ratios on the x-axis and relative intensity on the y-axis. The resulting spectra can be used to identify compounds by matching them against a reference library or database (Awad *et al.*, 2015; Cooks and Yan, 2018).

2.11 Superoxide dismutase activity during bacterial fungal interaction

Superoxide dismutase (SOD; EC 1.15.1.1) are metalloenzymes present in both eukaryotic and certain prokaryotic organisms. They are localized within the cytosolic compartment, inner membrane, extracellular space and mitochondrial matrix. The initial insights into superoxide dismutase were provided by Joe McCord and Irwin Fridovich, described their critical role in the organism's defense mechanisms (Landis and Tower, 2005). The primary function of superoxide dismutase (SOD) involves catalyzing the conversion of the free radical superoxide ($O_2^{\cdot-}$) into hydrogen peroxide (H_2O_2), accompanied by the liberation of oxygen (Fig. 2.7). Subsequently, hydrogen peroxide undergoes reduction to water (H_2O) through reactions involving catalase, glutathione peroxidase, and the enzyme thioredoxin-dependent peroxidoredoxin. In certain cases, hydrogen peroxide may also generate hydroxide ions, a reactive oxygen species, facilitated by the presence of a ferrous ion.

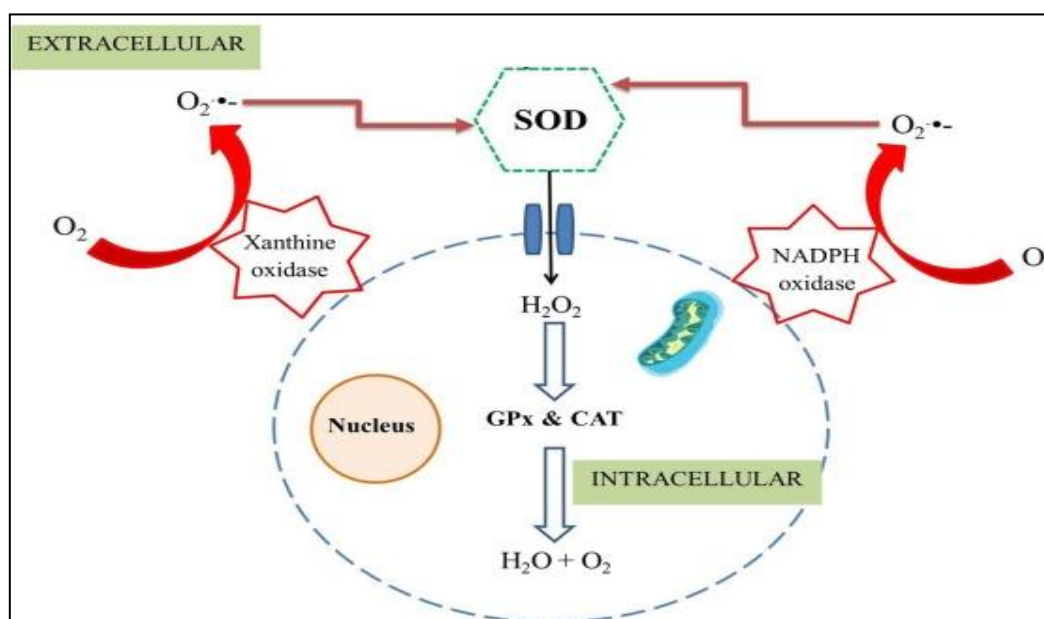


Fig. 2.7. Superoxide dismutase activity (Adapted from Stephenie *et al.*, 2020)

2.12 Analysis of gene expression

2.12.1 RNA isolation

For gene expression analysis, the initial step involves the isolation of RNA from the targeted sample species. RNA extraction methodologies are generally similar across various species and typically involve a combination of techniques. These techniques include mechanical cell disruption, use of chaotropic salts to deactivate RNases, degradation of macromolecules and separation of RNA from nucleotide complexes containing undesirable biomolecules such as DNA. The extracted RNA was then obtained through precipitation from solution or retrieval from a solid matrix (Chomczynski and Sacchi, 1987; Chomczynski and Sacchi, 2006). To ensure the removal of any residual DNA, the isolated RNA should be treated with DNase (Grillo and Margolis, 1990). In contemporary practice, RNA isolation is often streamlined by utilizing specialized kits, which expedite and simplify the isolation process.

2.12.2 Assessment of RNA

The quality and concentration of RNA within samples can be assessed using tools such as a UV/Vis spectrophotometer or a nano-drop system. The absorption at 260 nm provides a specific measurement of nucleic acid concentration, whereas absorbance at 280 nm and 230 nm offers insights into protein content and background absorption, respectively, indicating potential contaminants. Typically, a pure RNA sample exhibits an A₂₆₀/A₂₈₀ ratio ranging from 1.8 to 2.1, with a ratio greater than 2 indicating high-quality RNA. A pure RNA sample also demonstrates an A₂₆₀/A₂₃₀ ratio around 2 or slightly higher (Fleige and Pfaffl, 2006; Cicinnatiet *al.*, 2008; Ahlfen and Schlumpberger, 2010).

2.12.3 cDNA library preparation

Following RNA isolation, the process of reverse transcription is employed to synthesize complementary DNA (cDNA) using the isolated RNA as a template. This procedure involves utilizing the isolated RNA as a template along with oligo-dT primers for eukaryotes and random primers for prokaryotes, which promote the proper formation of the initial strand of cDNA. The resulting cDNA is subsequently utilized in quantitative polymerase chain reaction (qPCR) reactions. Various types of reverse transcriptases are employed for cDNA synthesis, each offering distinct advantages. Therefore, there is no universally established method applicable to all experiments. Instead, tailored protocols must be developed for specific experiments to achieve optimal outcomes (Nolan *et al.*, 2006).

2.12.4. qRT-PCR analysis

For qRT-PCR analysis, the precise design of primers specific to the synthesized cDNA from a given sample is of utmost importance. To ascertain the specificity of the designed primers for cDNA, a qPCR assay was conducted. This involves the utilization of the synthesized cDNA along with an RT control and water as templates. The resulting amplicons can subsequently be separated using electrophoresis. If the primers are specifically bound to the cDNA, a single distinct DNA band of a known size should be generated. Additionally, the primer specificity can be assessed through melting curve analysis utilizing dyes like SYBR green during the PCR reaction. These dyes cause the disruption of the DNA double bonds. The qPCR method aids in deciphering the expression patterns of target genes (Gkarmiri *et al.*, 2015). The employment of the qPCR technique offers numerous advantages in comparison to other methodologies. It eliminates the need for post-amplification manipulations and yields quantitative data with a precise dynamic range spanning seven to eight logarithmic orders of magnitude (Morrison *et al.*, 1998). Its accuracy surpasses that of the dot blot technique by a factor of about a thousand (Malinen *et al.*, 2003).

CHAPTER III

MATERIALS AND METHODS

3.1 Collection of the samples

Samples were collected from different locations of Jorhat district, Assam. Rhizospheric soil samples associated with healthy cabbage plant and infected cabbage leaves were collected for isolation of the rhizospheric bacteria and pathogenic fungi respectively. Essential equipment such as sterilized sample collection bags, scissors, forceps and knives were prepared and transported to the designated collection locations. The diseased leaves were subjected to fungal isolation on the same day of their collection. Similarly, the rhizospheric soils were also subjected to serial dilution for the isolation of rhizo-bacterial isolates on the same day.

3.2 Isolation of pathogenic fungi from diseased plant parts

For the isolation of pathogenic fungi, diseased plant leaves showing typical *Alternaria* disease symptoms were subjected to surface sterilization using sterile distilled water. Leaves were then dissected into small fragments keeping the necrotic rings using aseptic surgical blades (Himedia, India). These fragments were subsequently subjected to surface sterilization utilizing a 1% solution of sodium hypochlorite (Himedia, India) for 1 min, followed by a triple sequence of rinsing with sterile distilled water to remove superficial contaminants. Post-surface sterilization, the sterilized samples were inoculated onto potato dextrose agar (PDA; Himedia, India) medium in 9 cm petri-plates (Tarsons, India). The culture plates were then sealed and incubated at a temperature of 28°C for a period ranging from 2 to 7 days for fungal growth (Hazarika *et al.*, 2019, Soliman *et al.*, 2023). Hyphal tips from mixed fungal colonies were sub-cultured for pure culture onto fresh PDA medium. Fungal spores were collected from a full-grown culture plate and 5 µl of spore suspension of concentration 1×10^7 spore per ml (maintained using haemocytometer) was drop inoculated on cabbage leaf for the establishment of the Koch's postulates.

3.2.1 Characterization of the pathogenic fungi

The pathogenic fungus isolated from the diseased leaf of cabbage was characterized based on its morphological and molecular characteristics.

3.2.2 Morphological characterization of the fungal isolate

Preliminary morphological characterization of the fungal isolate was carried out by studying colony morphology (colour, texture, and growth pattern), hyphal morphology (shape, size and septation) and structural organization of the spores and sporangia.

3.2.3 Molecular identification of the pathogenic fungal isolate

The molecular identification of the pathogenic fungal isolate was done by amplifying the ITS region of the fungal genome.

3.2.3.1 Isolation of Genomic DNA of the pathogenic fungal isolate

For the isolation of fungal genomic DNA, the pathogenic fungal isolate was inoculated on PDA plate and allowed to grow for 72 hrs at 28°C. Fungal hyphae (100 mg) were crushed using liq. N₂ in a mortar and pestle. The crushed hyphae were taken in a 2 ml tube and 500 µl of fungal lysis buffer was added to the tube and vortexed for 5 mins. Added 500 µl of phenol: chloroform: isoamyl alcohol (25 : 24 : 1) to the same tube and was again vortexed for 10 mins using Tarson 3020 Spinix Vortex Shaker (Tarsons, India) followed by centrifugation at 12000 rpm for 12 mins. The aqueous phase was transferred to a new 1.5 ml tube, followed by the addition of an equal volume (500 µl) of chloroform:isoamyl alcohol (24:1) mixture. After gentle mixing, the mixture was again subjected to centrifugation at 12000 rpm for 10 mins at a temperature of 4°C. Subsequently, the supernatant was then carefully transferred to a fresh tube. For the precipitation of DNA, 50 µl of 5 M ammonium acetate was added, followed by the addition of double the volume (~1 ml) of ice-cold 100% ethanol. The mixture was centrifuged again at 12000 rpm for 10 mins at 4°C. As a result, DNA molecules underwent precipitation, leading to their separation from the solution. The DNA precipitate was then consolidated by means of centrifugation at the same conditions, and the resultant pellet was subsequently washed utilizing 70% ethanol before another round of centrifugation. To conclude the procedure, the DNA pellet was allowed to air dry and was subsequently reconstituted in 50 µl TE buffer (as detailed in APPENDIX II) and stored at -20°C for future use.

3.2.3.2 Visualization of DNA bands in Agarose Gel

To visualize DNA fragments, an agarose gel with a concentration of 0.8% was prepared. This was prepared by mixing 0.8 gms of agarose (Invitrogen, USA) in 100 ml of 1X TAE buffer (as detailed in APPENDIX II). The mixture was then subjected to

microwave heating until the solution turned completely transparent. The solution was allowed to cool to a temperature of 50°C to which 2.0 µl of ethidium bromide (EtBr) solution with a concentration of 10 mg/ml (Sigma, USA) was added. Subsequently, the molten agarose solution was poured into a gel casting tray equipped with combs and left undisturbed to solidify. Once solidified, the gel tray, along with the formed gel, was moved into a horizontal electrophoresis chamber (Bio-Rad, USA) that was filled with 1X TAE buffer. The combs used for creating wells in the gel were removed, and the buffer level within the chamber was adjusted accordingly.

3.2.3.3. PCR Amplification of the internal transcribed spacer region

The amplification of the ITS region of the fungal genome was carried out employing universal primers: ITS1 (5'-TCCGTAGGTGAACCTGCGG-3') and ITS4 (5'-TCCTCCGCTTATTGATATGC-3') as outlined in the work of White *et al.*, 1990. The recipe of the PCR is detailed in the Table 3.1. The PCR thermal conditions encompassed an initial denaturation step at 94°C for duration of 3 mins, followed by 35 cycles. Each cycle consisted of denaturation at 94°C for 30 sec, annealing at 50°C for 30 sec, and extension at 72°C for 1 min and 30 sec. A concluding extension step was conducted at 72°C for a span of 7 mins. The resulting amplified products were subjected to analysis on a 1.2% agarose gel. To assess the molecular size of these amplified products, a 100 bp DNA ladder (Himedia, India) was utilized. The amplified PCR product was then stored at -20°C for further use.

Table 3.1. Components of PCR reaction for the amplification of ITS region of Fungi

Reagents	Quantity for 50 µl reaction volume
2X Emerald Amp® MAX HS PCR Master Mix	25 µl
Forward primer: ITS 1 (10 µM)	2.0 µl
Reverse primer: ITS 4 (10 µM)	2.0 µl
Template DNA (~100 ng/ µl)	3.0 µl
Deionized water	18.0 µl
Total	50.0 µl

3.2.3.4 Sequencing and computational analysis of sequencing data

The amplified PCR products were subjected to Sanger sequencing *via* Centyle Biotech Private Limited, India. The forward and reverse sequence reads were assembled to construct a consensus sequence using BioEdit (v7.2) software. Using BLASTn programme, the consensus sequence was compared with the ITS rDNA region sequences of fungi available in the GenBank database of NCBI (Bethesda, MD, USA). The assembled partial sequence was then submitted to the NCBI database and GeneBank Accession Number was obtained.

3.2.3.5 Phylogenetic analysis of the pathogenic fungal isolate

The phylogenetic analysis of the pathogenic fungal isolate was executed using the ITS rDNA sequence to establish its taxonomic position with respect to their closest relatives. The reference sequences of the ITS rDNA of different fungal species (Table 3.2) were collected from GenBank database of NCBI and multiple sequence alignment was done using ClustalW algorithm in MEGA X (Tamura *et al.*, 2018). The aligned sequences so obtained were used to construct the phylogenetic tree in MEGA X using Maximum-Likelihood method and Tamura-Nei model (Tamura and Nei, 1993) with 1000 bootstrap replicate value.

Table 3.2. List of reference sequences used in the phylogenetic analysis of the pathogenic fungal isolate

Sl. No.	Reference Sequence Used	GenBank Accession No.
1.	<i>Alternaria brassicicola</i> strain ABA-01 18S ribosomal RNA gene, partial sequence; internal transcribed spacer 1, 5.8S ribosomal RNA gene, and internal transcribed spacer 2, complete sequence; and 28S ribosomal RNA gene, partial sequence.	KR996754.1
2.	<i>Alternaria brassicicola</i> strain BHU-LMMT27 internal transcribed spacer 1, partial sequence; 5.8S ribosomal RNA gene and internal transcribed spacer 2, complete sequence; and 28S ribosomal RNA gene, partial sequence.	KX139160.1
3.	<i>Alternaria brassicicola</i> strain BHU-LMMT26 internal transcribed spacer 1, partial sequence; 5.8S ribosomal RNA gene, complete sequence; and internal transcribed spacer 2, partial sequence.	KX139159.1
4.	<i>Alternaria brassicae</i> strain BHU-LMMT19 internal transcribed spacer 1, partial sequence; 5.8S ribosomal RNA gene and internal transcribed spacer 2, complete sequence; and 28S ribosomal RNA gene, partial sequence.	KX139152.1
5.	<i>Alternaria solani</i> strain BHU-LMMT17 internal transcribed spacer 1, partial sequence; 5.8S ribosomal RNA gene and internal transcribed spacer 2, complete sequence; and 28S ribosomal RNA gene, partial sequence	KX139150.1
6.	<i>Alternaria eichhorniae</i> ATCC 22255 ITS region; from TYPE material	NR_111832.1
7.	<i>Alternaria alstroemeriae</i> CBS 118809 ITS region; from TYPE material	NR_163686.1
8.	<i>Alternaria arborescens</i> CBS 102605 ITS region; from TYPE material	NR_135927.1
9.	<i>Fusarium oxysporum</i> DNA, 28S-18S ribosomal RNA intergenic spacer region, partial sequence, isolate: 08C-MS4	AB733472.1
10.	<i>Mucor irregularis</i> CBS 103.93 ITS region; from TYPE material	NR_172288.1

3.3 Isolation of rhizospheric bacteria from healthy cabbage plant

The rhizospheric soil associated with the healthy cabbage plant was subjected to serial dilution for the isolation of rhizospheric bacteria. Stock was prepared by dissolving 1 gm of soil in 9 ml of saline water (0.85% w/v). Subsequently, serial dilutions were performed up to 10^5 dilutions (Liu *et al.*, 2019). Samples of 50 μ l from each of 10^4 and 10^5 dilutions were spread on nutrient agar (NA; Himedia, India) culture medium (Himedia, India). The petri-plates were then sealed and incubated at $28\pm 2^\circ\text{C}$ for the bacterial growth. Individual colonies were sub-cultured onto fresh NA medium to obtain pure cultures.

3.4 Screening of Rhizospheric bacteria for Antagonistic Interactions

All the bacterial isolates were screened for antagonistic interaction against the pathogenic fungi using *in vitro* dual-culture method in culture medium following the protocol of Hazarika *et al.* (2021).

3.4.1 Impact of antagonist bacteria on radial growth of the pathogenic fungi

A half- strength nutrient agar and potato dextrose agar was prepared and used for the *in vitro* dual culture interaction experiments. The pathogenic fungus was allowed to grow actively on PDA medium for the inoculums. About 5 mm of mycelium from the actively growing hypha was introduced onto the central region of the petri-plate containing half-strength NA-PDA (as detailed in APPENDIX I) and allowed to grow for 5 days, until attaining a diameter of 2.5 cm. A loop full of antagonistic bacterial isolate was then streaked on two opposing peripheries of the fungal growth as shown in the fig. 3.1 below, while maintaining a separation of 1 cm and the radial diameter of the fungi was recorded at an interval of 24, 48, 72, 96 hrs respectively. A mono- culture plate with pathogenic fungus inoculated on the same day was used as a control.

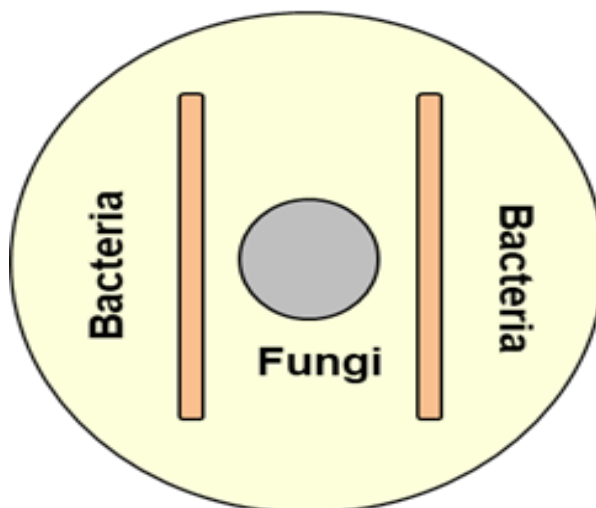


Fig. 3.1. A schematic diagram showing the dual bacterial- fungal culture

3.4.2 Inhibitory effects of bacterial cell free supernatant on fungal radial growth

To evaluate the effect of the bacterial supernatant on the radial growth of pathogenic fungi, agar well diffusion method was used. The bacterial isolates with antagonistic activity were allowed to grow in 100 ml NB medium for 72 hrs at continuous shaking (180 rpm) in a 28°C shaker incubator. Each of the bacterial culture (40 ml) was collected aseptically in a sterile 50 ml falcon tube (Tarsons, India) and centrifuged at 5500 rpm at room temperature. The cell free supernatant was then carefully filter sterilized using a 0.22 μm pore sized PVDF syringe filter (GE healthcare, USA) and collected in another sterile 50 ml falcon tube and stored at 4°C for further use. A part of the filter sterilized supernatant was boiled at 100°C for 15 mins to check the heat stability of the active ingredients.

A 5 mm of fungal inoculum was inoculated onto a petri plate containing PDA medium and incubated at 28°C incubator. The fungus was allowed to attain a radial diameter of 2.5 cm. Wells with 6 mm diameter were made on the same plate 2 cm apart of the fungal hyphae. 50 μl of the each of cell free bacterial supernatant and heat-treated bacterial supernatant was added into two different wells and incubated at 28°C for a duration of 72 hrs and the reduction in fungal radial growth was recorded. Autoclaved distilled H₂O (50 μl) was also added to one well as a control.

A poisoned food assay was also performed where 100 ml of PDA media was poisoned with 1 ml of the bacterial cell free supernatant. The pathogenic fungus was inoculated, and the radial growth was recorded after 10 days. PDA media with 1ml of NB was regarded as control.

3.4.3 Antagonistic activity of Bacterial VOCs on the pathogenic fungi

The bacterial strain with antagonistic activity was grown overnight in NB medium, and subsequently, 100 µl of this culture was spread evenly onto nutrient agar (NA) plates. Parallely, a mycelial plug with a diameter of 5 mm, excised from the edge of actively growing fungal culture was inoculated at the center of a plate containing potato dextrose agar (PDA). The PDA plate, hosting the mycelial plug, was inverted over the NA plate already containing the bacterial cultures. This setup was carefully sealed using Parafilm and subjected to incubation at a temperature of 28°C. The same procedure was conducted using PDA plates inverted over un-inoculated NA plate was used as control. The radial growth of the pathogenic fungi was recorded at 24 hrs interval for 5 days and compared with the control as described by Zhang *et al.*, (2020).

3.5 Microscopic studies of the *in vitro* interaction of the pathosystem

Microscopic examination of the *in vitro* interactions was conducted using a medium consisting of half-strength NA-PDA. The pathogenic fungus was allowed to grow actively on PDA medium for the inoculum. 5 mm from the actively growing hypha was introduced onto the central region of the petri-plate containing half-strength NA-PDA and permitted to grow for duration of 5 days, until attaining a diameter of 2.5 cm. A loop full of antagonistic bacterial isolate was then streaked on two opposing peripheries of the fungal growth as shown in Fig. 3.1, while maintaining a separation of 1 cm and was allowed to grow for 72 hrs. A mono- culture plate with only grown pathogenic fungus was used as a control.

3.5.1 Visualization of the *in vitro* interaction between antagonist bacterial isolates and the pathogenic fungi under light microscope

Hyphal mass from the interaction zone was carefully harvested from the above mentioned (section 3.5) sample plates and washed with saline solution (0.85% w/v) for three times. Hyphal mass was then taken onto a clean grease free glass slides and stained with lactophenol cotton blue (Himedia, India) and incubated for 1 min. A clean cover slip was mounted over the stained sample and the extra stain was removed by using blotting paper and observed under light microscope (Olympus BX51, Olympus Corporation, Japan). Monoculture as control was maintained for every interaction, respectively.

3.5.2 Visualization of the *in vitro* interaction between antagonist bacterial isolates and the pathogenic fungi under Scanning Electron Microscope (SEM)

The mycelial biomass blocks were carefully retrieved from the previously mentioned (3.5) sample dishes for SEM analysis in accordance with the methodology established by Dullah *et al.* (2021). The hyphal structures from both the interaction plates and the monoculture control plate were immersed in a 2.5% glutaraldehyde solution for duration of 4 hrs followed by repeated washing with 0.1 M phosphate buffer having pH 7.8. For enhanced fixation, the samples were subjected to 1% Osmium Tetroxide (OsO₄). A gradual progression through a series of ethanol solutions was then employed to dehydrate the samples and eliminate residual fluids. Following this, the samples were affixed onto carbon-conductive tape and underwent gold coating by a Gold sputter coater. The samples were then visualized under Field Emission Scanning Electron Microscope (Model: ZEISS, SIGMA) at an accelerating voltage of 5.00 kv; generating micrographs at varying levels of magnification.

3.6 Characterization of the rhizospheric bacteria

The rhizo-bacterial isolates exhibiting antagonistic activity were characterized based on their morphological, biochemical and molecular attributes.

3.6.1 Morphological characterization of the bacterial isolate

The initial morphological characterization of the rhizobacterial isolates exhibiting antagonistic property was carried based on the macroscopic and microscopic observations respectively. Macroscopic characters such as shape, color, colony morphology, growth, etc. on nutrient agar plate (Dubey *et al.*, 2021). Cell wall properties were studied using gram staining method under light microscope (Vincent and Sisco, 1970). Ultra-structure of the bacterial isolates was also visualized under FE-SEM. Actively grown bacterial cells (18-24 hrs) were harvested from nutrient broth (NB; Himedia, India) medium through centrifugation in 1.5 ml eppendorf tubes and the similar methodology was applied as described above section 3.5.2.

3.6.2 Biochemical characterization of the bacterial isolate

The rhizospheric bacteria having antagonistic activity was characterized based on their ability to produce acid, utilize carbohydrates and enzyme production using Biochemical Kit: KB001, KB009 Part A, B1 and C (HiMedia, India) as per the protocol provided by the company. Following are the list of tests carried out in the present study:

Table: 3.3 Reading Table for biochemical tests

Test/ Sugar	Reagent to be added	Principle	Original colour	Interpretation	
				+ve Reaction	-ve Reaction
Indole	1-2 Drops of Kovac's reagent	Detects deamination of tryptophan	Colourless	Reddish Pink	Colourless
Methyl Red	1-2 drops of methyl red reagent	Detects acid production	Colourless	Red	Yellow-Orange
Voges-Proskauer's	1-2 drops of Barritt reagent A & B	Detects acetoin production	Colourless	Pinkish red	Colourless
Citrate Utilisation	--	Detects the capability of an organism to utilise citrate as a sole carbon source	Green	Blue	Green
Glucose	--	Carbohydrate Utilization	Pinkish red	Yellow	Red/Pink
Adonitol	--	Carbohydrate Utilization	Pinkish red	Yellow	Red/Pink
Arabinose	--	Carbohydrate Utilization	Pinkish red	Yellow	Red/Pink
Lactose	--	Carbohydrate Utilization	Pinkish red	Yellow	Red/Pink
Sorbitol	--	Carbohydrate Utilization	Pinkish red	Yellow	Red/Pink
Mannitol	--	Carbohydrate Utilization	Pinkish red	Yellow	Red/Pink
Rhamnose	--	Carbohydrate Utilization	Pinkish red	Yellow	Red/Pink
Sucrose	--	Carbohydrate Utilization	Pinkish red	Yellow	Red/Pink
Xylose	--	Carbohydrate Utilization	Pinkish red	Yellow	Red/Pink
Maltose	--	Carbohydrate Utilization	Pinkish red	Yellow	Red/Pink
Fructose	--	Carbohydrate Utilization	Pinkish red	Yellow	Red/Pink
Dextrose	--	Carbohydrate Utilization	Pinkish red	Yellow	Red/Pink

Galactose	--	Carbohydrate Utilization	Pinkish red	Yellow	Red/Pink
Raffinose	--	Carbohydrate Utilization	Pinkish red	Yellow	Red/Pink
Trehalose	--	Carbohydrate Utilization	Pinkish red	Yellow	Red/Pink
Melibiose	--	Carbohydrate Utilization	Pinkish red	Yellow	Red/Pink
Sucrose	--	Carbohydrate Utilization	Pinkish red	Yellow	Red/Pink
L- Arabinose	--	Carbohydrate Utilization	Pinkish red	Yellow	Red/Pink
Mannose	--	Carbohydrate Utilization	Pinkish red	Yellow	Red/Pink
Inulin	--	Carbohydrate Utilization	Pinkish red	Yellow	Red/Pink
Sodium gluconate	--	Carbohydrate Utilization	Pinkish red	Yellow	Red/Pink
Glycerol	--	Carbohydrate Utilization	Pinkish red	Yellow	Red/Pink
Salicin	--	Carbohydrate Utilization	Pinkish red	Yellow	Red/Pink
Dulcitol	--	Carbohydrate Utilization	Pinkish red	Yellow	Red/Pink
Inositol	--	Carbohydrate Utilization	Pinkish red	Yellow	Red/Pink
Sorbitol	--	Carbohydrate Utilization	Pinkish red	Yellow	Red/Pink
Manitol	--	Carbohydrate Utilization	Pinkish red	Yellow	Red/Pink
Arabitol	--	Carbohydrate Utilization	Pinkish red	Yellow	Red/Pink
Erythritol	--	Carbohydrate Utilization	Pinkish red	Yellow	Red/Pink
Alpha-methyl-glucoside	--	Carbohydrate Utilization	Pinkish red	Yellow	Red/Pink
Rhamnose	--	Carbohydrate Utilization	Pinkish red	Yellow	Red/Pink
Cellobiose	--	Carbohydrate Utilization	Pinkish red	Yellow	Red/Pink
Melezitose	--	Carbohydrate Utilization	Pinkish red	Yellow	Red/Pink
Alpha-Methyl-D-Mannoside	--	Carbohydrate Utilization	Pinkish red	Yellow	Red/Pink
Xylitol	--	Carbohydrate Utilization	Pinkish red	Yellow	Red/Pink
ONPG	--	Detects Beta-galactosidase activity	Colourless	Yellow	Colourless
Esculin hydrolysis	--	Detects esculin hydrolysis	Cream	Black	Cream

D Arabinose	--	Carbohydrate Utilization	Pinkish red	Yellow	Red/Pink
Malonate Utilization	--	Detects the capability to utilise Na malonate as a sole carbon source	Light green	Blue	Light green
Sorbose	--	Carbohydrate Utilization	Pinkish red	Yellow	Red/Pink
Lysine Utilization	--	Detects Lysine decarboxylation	Olive green to Light Purple	Purple/Dark Purple	Yellow
Ornithine Utilization	--	Detects Ornithine decarboxylation	Olive green to Light Purple	Purple/Dark Purple	Yellow
Urease	--	Detects Urease activity	Orangish Yellow	Pink	Orangish Yellow
Phenylalanine deamination	2-3 drops of TDA reagent	Detects Phenylalanine deamination activity	Colourless	Green	Colourless
Nitrate Reduction	1-2 drops of sulphanilic acid and 1-2 drops of N,N- Dimethyl-1-Naphthylamine	Detects Nitrate Reduction	Colourless	Pinkish Red	Colourless
H ₂ S production	--	Detects H ₂ S production	Orangish Yellow	Black	Orangish Yellow
Glucose	--	Carbohydrate Utilization	Pinkish red	Yellow	Red/Pink
Adonitol	--	Carbohydrate Utilization	Pinkish red	Yellow	Red/Pink
Lactose	--	Carbohydrate Utilization	Pinkish red	Yellow	Red/Pink
Arabinose	--	Carbohydrate Utilization	Pinkish red	Yellow	Red/Pink
Sorbitol	--	Carbohydrate Utilization	Pinkish red	Yellow	Red/Pink
Catalase	-	Detects catalase activity	Colourless	Rapid bubble formation	No bubble formation

3.6.3 Molecular identification of the antagonist bacterial isolates

The molecular characterization of the bacterial isolates was done by amplifying the 16S rRNA gene.

3.6.3.1 Isolation of Genomic DNA: The bacterial culture was inoculated in Nutrient Broth (NB) and cultivated until reaching an optical density at 600 nm (OD₆₀₀) of 0.6, at a temperature of 28°C. The genomic DNA extraction was performed using the protocol

established by Wilson (2001) with some modifications. For this, a 1.5 ml portion of the bacterial culture was taken within a 2 ml centrifuge tube. Cells were collected through centrifugation at 6000 rpm for 10 mins. The resulting liquid supernatant was discarded, and the cellular pellet was suspended in 600 µl of cell lysis buffer. This mixture was incubated at a temperature of 65°C for 30 mins. Following this step, 100 µl of a 5 M NaCl solution was introduced into the tube, which was then subjected to 10 mins incubation at -20°C. Subsequently, centrifugation was performed at 12000 rpm at 4°C for a duration of 10 mins. The high-viscosity supernatant was transferred into a new tube, and an equal volume of phenol, chloroform, and isoamyl alcohol (in a ratio of 25:24:1) was added with thorough mixing. This mixture was then subjected to centrifugation at 12000 rpm at 4°C for 10 mins. The upper aqueous layer was then transferred into another new tube. A volume twice that of the original sample of ice-cold isopropanol solution was introduced to precipitate the nucleic acids. Agitation was applied by oscillating the tube to facilitate the precipitation process. Centrifugation at 12000 rpm at 4°C for 10 mins was used to collect the DNA content as a pellet. This pellet was cleansed with 70% ethanol, followed by another round of centrifugation. The pellet was subsequently air dried and dissolved in 50 µl of 1X TE buffer.

3.6.3.2 Visualization of DNA bands in Agarose Gel

Same methodology was used as described earlier in the section 3.2.3.2.

3.6.3.3 Amplification of 16S rRNA bacterial gene: The amplification of the bacterial 16S rRNA gene was carried out employing universal primers: 27F (5'-AGAGTTTGATCCTGGCTCAG-3') and 1492R (5'-GGTTACCTTGTTACGACTT-3') as outlined in the work of Lane (1991). The recipe of the PCR is detailed in Table 3.4. The PCR thermal conditions encompassed an initial denaturation step at 94°C for duration of 3 mins, followed by 35 cycles. Each cycle consisted of denaturation at 94°C for 30 sec, annealing at 50°C for 30 sec and extension at 72°C for 1 min and 30 sec. A concluding extension step was conducted at 72°C for a span of 7 mins. The resulting amplified products were subjected to analysis on a 1.2% agarose gel. To assess the molecular size of these amplified products, a 1 kb DNA ladder (Himedia, India) was utilized. The amplified PCR product was then stored at -20°C for further use.

Table 3.4. Components of PCR reaction for the amplification of 16s RNA region of the bacterial DNA

Reagents	Quantity for 50 µl reaction volume
2X Emerald Amp® MAX HS PCR Master Mix	25 µl
Forward primer: 27F (10 µM)	2.0 µl
Reverse primer: 1492R (10 µM)	2.0 µl
Template DNA (~100 ng/ µl)	3.0 µl
Deionized water	18.0 µl
Total	50.0 µl

3.6.3.4 Sequencing and computational analysis of sequencing data

The amplified PCR products were subjected to Sanger sequencing *via* Centyle Biotech Private Limited, India. The forward and reverse sequence reads were assembled to construct a consensus sequence using BioEdit (v7.2) software. Using BLASTn programme, the consensus sequence was compared with the 16s RNA gene sequences of bacteria available in the GenBank database of NCBI (Bethesda, MD, USA). The assembled partial sequence was then submitted to the NCBI database and GeneBank Accession Number was obtained.

3.6.3.5 Phylogenetic analysis of the bacterial isolate

The phylogenetic analysis of the rhizo-bacterial isolates was executed using the 16s RNA gene sequence to establish its taxonomic position with respect to their closest relatives. The reference sequences of the 16s RNA gene sequence of different bacterial species (Table 3.5) were collected from GenBank database of NCBI and multiple sequence alignment was done using ClustalW algorithm in MEGA X (Kumar *et al.*, 2018). The aligned sequences so obtained were used to construct the phylogenetic tree in MEGA X using Maximum-Likelihood method and Tamura-Nei model (Tamura and Nei, 1993) with 1000 bootstrap replicate value.

Table 3.5. List of reference sequences used in the phylogenetic analysis of the rhizobacterial isolates

Sl. No.	Reference Sequence Used	GenBank Accession No.
1.	<i>Bacillus amyloliquefaciens</i> strain ATCC 23350 16S ribosomal RNA gene, partial sequence	NR_118950.1
2.	<i>Bacillus amyloliquefaciens</i> strain NBRC 15535 16S ribosomal RNA, partial sequence	NR_041455.1
3.	<i>Bacillus amyloliquefaciens</i> strain NBRC 15535 16S ribosomal RNA, partial sequence	NR_112685.1
4.	<i>Bacillus subtilissubsp.subtilis</i> strain 168 16S ribosomal RNA, complete sequence	NR_102783.2
5.	<i>Bacillus subtilis</i> strain DSM 10 16S ribosomal RNA, partial sequence	NR_027552.1
6.	<i>Bacillus subtilis</i> strain NBRC 13719 16S ribosomal RNA, partial sequence	NR_112629.1
7.	<i>Bacillus pumilus</i> strain ATCC 7061 16S ribosomal RNA, partial sequence	NR_043242.1
8.	<i>Bacillus pumilus</i> strain ATCC 14884 16S ribosomal RNA gene, partial sequence	MN456845.1
9.	<i>Bacillus cereus</i> ATCC 14579 16S ribosomal RNA gene, partial sequence	MG708176.1
10.	<i>Escherichia coli</i> strain ATCC 35469 16S ribosomal RNA gene, partial sequence	KP941759.1

3.7 Plant Growth promoting traits of the bacterial isolates

3.7.1 IAA production

The Gordon and Weber (1951) method was used to quantify the synthesis of indole-3-acetic acid. The bacterial inoculum was prepared by culturing the rhizobacterial isolates in 100 ml of Nutrient Broth (NB) medium (HiMedia, India) under continuous agitation at 180 rpm, at 28°C shaker incubator for 24 hrs. On the subsequent day, 100 µl of a bacterial inoculum, adjusted to a concentration of 10 CFU/ml (OD600 = 1), was introduced

into 10 ml of NB medium containing L-tryptophan (1000 ug/ml). Samples were collected at an interval of 24, 48, 72 and 96 hrs of incubation period and the following steps were performed:

- 5 ml of culture was collected in 50 ml falcon tubes (Tarsons, India) followed by centrifugation at 5500 rpm for 10 mins.
- To 1 ml of the culture supernatant, 2 ml Salkowski reagent (prepared using 50 ml of 35% HClO₄ and 1 ml of 0.5 M FeCl₃) was added in a test tube. NB with no bacterial growth was used as blank.
- The tubes were then incubated in dark at room temperature for 25 mins. The emergence of a red/pink colour, signify the presence of indolic compounds confirming indole-3-acetic acid (IAA) production and was measured using a UV-spectrophotometer (SpectroquantPharo 300, Merck, Germany) at 530 nm (Bessai *et al.*, 2022) and quantified using a standard curve of indole-3-acetic acid.

3.7.2 Phosphate Solubilization

Qualitative assessment of phosphate solubilization was conducted using the Pikovskaya (PVK) Agar Medium (HiMedia, India, M520) (Pikovskaya, 1948). The isolates were inoculated as spots onto the PVK agar medium and subsequently incubated at a temperature of 30°C for duration of 72 hrs. The development of transparent halo zones encircling the colonies indicates a positive outcome for phosphate solubilization activity (Nath *et al.*, 2012).

3.7.3 Zinc Solubilization

Qualitative evaluation of zinc solubilization was carried using the Zinc Solubilizing Agar medium (HiMedia, India, M2068). Each isolate was subjected to spot inoculation followed by incubation at a temperature of 30°C for a duration of 72 hrs. The formation of halo zones encircling the bacterial colonies signified zinc solubilization capabilities of the rhizobacterial isolates (Khanghahi *et al.* 2018).

3.7.4 Potassium Solubilization

Qualitative assessment of potassium solubilization was conducted using the Aleksandrov Agar medium (HiMedia, India, M1996). The rhizobacterial isolates were spot inoculated on petri plates containing Aleksandrov Agar medium and incubated at a temperature of 30°C for duration of 7 days. The presence of a distinct transparent halo zone

encircling the bacterial colonies indicated positive potassium solubilizer (Meena *et al.*, 2015).

3.7.5 Sulphur Solubilization

Qualitative evaluation of sulfur solubilization was executed utilizing a thiosulfate agar medium, following the method elucidated by Chaudhary *et al.* (2017). As an indicator, bromocresol purple was employed at a concentration of 0.025 g/L, imparting a purple hue to the solution. The rhizobacterial isolates were subjected to streaking on Petri dishes and subsequently placed under incubation at a temperature of 30°C for a duration of 24 hrs. In cases of positive results, a transformation in the color of the dye from purple to yellow was observed, denoting the sulfur solubilization activity exhibited by the isolates.

3.7.6 Siderophore Production

The qualitative assessment of siderophore production was carried out in accordance with the method detailed by Schwyn and Neilands (1987). The isolated rhizobacteria were streak inoculated on Tryptic Soya Agar (TSA) medium, followed by an incubation period at 30°C for 24 hrs. Upon the appearance of colonies, Chrome Azurol-S (CAS) medium was introduced onto the bacterial colonies and the samples were once again incubated at a temperature of 30°C for 24 hrs. The change in colour from green to formation of an orange/yellow halo zone encircling the bacterial isolate colonies confirmed a positive outcome for siderophore production.

3.8 Comparative Superoxide Dismutase activity of the interacting microbial partners during monoculture and dual-culture growth condition

Superoxide dismutase activity of the monoculture (bacterial isolates and pathogenic fungal isolates) and the dual culture bacterial fungal interacted samples was carried out employing the protocol of Adhikary *et al.*, (2022). Samples were collected at an interval of 24 hrs for 7 days from both the monocultures and the dual culture plates. 50 mg from each of the samples were grounded to powder in liquid nitrogen, transferred to a 2 ml tube and 2 ml of extraction buffer was added and subjected to centrifugation at 14000 rpm at 4°C for 30 mins. The supernatant was collected and the protein content was determined using Bradford's method. And the enzyme extract was stored at -20°C for future use. 1 ml of reaction mixture was then taken in a test tube and 20 µl of enzyme extract was added to it followed by 10 µl riboflavin (4.4 mg/ml). Extraction buffer was used in place of enzyme extract as a blank and the same procedure was followed. All the test tubes were then

illuminated for 10 mins under 20W florescent tubes. The increase in absorbance due to the formation of formazan was recorded at 560 nm and the results were expressed as units of SOD per μg of protein.

3.9 Relative quantification of expressions of key fungal Genes during antagonist bacterial and pathogenic fungal interaction

3.9.1 Isolation of the total RNA

Total RNA extraction was performed using TRI Reagent® (Sigma, USA). Fungal hyphae were harvested from interaction plates and monoculture plates and subsequently grinded into fine powder using liquid nitrogen. Approximately 100 mg of this powdered tissue was immediately combined with 1 ml of TRI Reagent® (Sigma, USA). The mixture was subjected to thorough mixing *via* repeated pipetting and allowed to incubate at room temperature for 10 mins. 200 μl of chloroform was added and gently mixed for 30 sec and allowed to stand at room temperature for 15 mins. The mixture was then subjected to centrifugation at 12,000 rpm for 15 mins at 4°C. The centrifugation process led to the separation of the mixture into 3 distinct phases: a red organic phase with proteins, an interphase with DNA and a colourless upper aqueous phase having RNA. The upper aqueous phase was then carefully transferred to a new 1 ml tube and 500 μl of 2-propanol was added. After thorough mixing, the tube was allowed to incubate at 4°C for 10 mins, followed by centrifugation at 12,000 rpm for 10 mins at 4°C. The supernatant was then discarded, leaving behind an RNA pellet, which was washed with 75% ethanol. This step was followed by another round of centrifugation at 12,000 rpm for 10 mins at 4°C. The supernatant was once again removed, and the RNA pellet was subjected to an air-drying step for 10-15 mins to eliminate residual ethanol. The resulting pellet was subsequently dissolved in 50 μl of RNase-free water, which had been pre-treated with 0.01% Diethyl pyrocarbonate (DEPC). The dissolved RNA was stored at -80°C for future use. The quality of the isolated RNA was assessed by running an analysis on a 1% denatured agarose gel, observing the presence of distinct 28S and 18S RNA bands. Additionally, the integrity of the RNA was evaluated using a Nanodrop ND1000 spectrophotometer (Thermo Scientific, USA).

3.9.2 Denaturing Agarose Gel Electrophoresis

To prepare a 1% agarose gel, 0.5 gms of agarose was mixed with 36 ml of autoclaved water treated with DEPC (a substance that deactivates RNases, enzymes that degrade RNA). The mixture was heated to dissolve the agarose and then cooled to around

60°C. To this, 5 ml of 10X MOPS buffer and 9 ml of 37% formaldehyde were added. The resulting mixture was poured into gel casting tray to solidify. And the gel was set up in a gel tank containing a buffer. Prior to starting the actual electrophoresis process, the gel was equilibrated in the buffer for about 30 mins. For the RNA samples electrophoresis, a mixture was created by combining 10 µl of RNA, 3 µl of 10X MOPS, 10 µl of formamide, 2 µl of ethidium bromide (a fluorescent dye) and 4 µl of 37% formaldehyde. This mixture was incubated at 65°C for 20 mins. After the incubation, the sample was quickly cooled in ice water for about 30 mins. Then, the mixture was then spun to ensure that all the sample components were at the bottom of the tube. To this solution, 3 µl of 10X RNA gel loading buffer was added. The prepared RNA sample was loaded into a well on the agarose gel. Electrophoresis was carried out at a voltage of 60V until the faster-moving dye, bromophenol blue, migrated about two-thirds of the way through the gel. Once this was achieved, the gel was viewed using a Gel Doc system (Bio-Rad USA). The image of the gel was captured for analysis.

3.9.3 Primer designing

Primers for expression analysis (Table 3.6) were designed by using the CDS sequence of each of the fungal genes from NCBI GeneBank database with the help of PrimerQuest Tool (IDT, 2023 Integrated DNA Technologies, Inc.).

Table 3.6. Primers used in the expression analysis of the fungal genes

Target	Primer	Sequence (5' - 3')	Length
Actin	Ag_Actin_qF	CCCGTCATCTAACAAACACAC	20
	Ag_Actin_qR	TATCGCAGGGTCAGGATAC	19
AbSte7	Ag_AbSte7_qF	CCCTTGAGATTGGTGTGAG	20
	Ag_AbSte7_qR	CCTCGCCATTATGACCTTG	19
AbPf2	Ag_AbPf2_qF	GCCATCCCACAGAAGAAAG	19
	Ag_AbPf2_qR	GGCAAATGTCGAGGATAGTG	20
Amk1	Ag_Amk1_qF	CCACTCCATGTTCTGTCTG	19
	Ag_Amk1_qR	GGTGAAGGTCTCGTAGTTTC	20
Amk2	Ag_Amk2_qF	GAAGGTCACCAACGTCTTC	19
	Ag_Amk2_qR	GGAATGTCCATGTCGTAGAG	20
Hog1	Ag_Hog1_qF	CATCATTACGGAGCTTCTGG	20
	Ag_Hog1_qR	GCAGGGTCTGGTGAAATTAG	20

3.9.4 First strand cDNA synthesis

The first strand cDNA synthesis was performed out with 1 µg of total RNA in a 20 µl reaction using Prime Script™ 1st Strand cDNA synthesis (TAKARA, India) following manufacturer's instructions. Fungal cDNA from the total RNA sample of pathogenic fungal monoculture and antagonistic bacterial-fungal interaction dual cultures were amplified with oligo-dT primer due to the presence of polyA tail in eukaryotic RNA.

3.9.5 Real-time Expression Analysis

The relative quantification of the expression profiles of the target fungal genes was performed by employing quantitative real-time PCR (qRT-PCR) in a QuantStudio 3 Real-Time PCR System (Applied Biosystems, Thermo Fisher Scientific, USA). Quantitative real-time PCR was done on the first strand cDNA using TB Green® Premix Ex Taq™ II (TliRNase H Plus, TAKARA, India). The total reaction volume was 10 µl containing 10

pmol of each primer and 50 ng cDNA template according to the manufacturer's protocol. The Real-time PCR was performed with three technical and biological replicates respectively with actin gene as the house keeping gene. The relative quantification (log₂ fold change) method was used to determine the relative gene expression of the respective genes (Livak and Schmittgen, 2001). The amplification profile was initial holding at 50°C for 2 mins followed by denaturation step at 95°C for 10 mins, 40 cycles of 95°C for 15 sec and 60°C for 1 min. Melt curve analysis was done to get a single amplification product. The results of the qRT-PCR were analyzed by Student's t-Test in MS Excel and $p < 0.05$ was considered to be significant.

3.10 Metabolite profiling during *in vitro* antagonist bacterial and pathogenic fungal interactions

LC-MS analysis was carried out to profile the secondary metabolites during antagonist bacterial- pathogenic fungal interactions.

3.10.1 Preparation of the culture for metabolite extraction

The pathogenic fungal isolate was grown on NA-PDA plates containing half strength NA-PDA medium for 5 days. Subsequently, the antagonist bacterial isolates were streaked on the petri-plates as shown in Fig. 3.1 and incubated at 28°C for 72 hrs.

3.10.2 Extraction of the secondary metabolites

Five 1 cm² portions from each of the bacterial-fungal interaction cultures were collected from the petri-plates by using sterile surgical blade. The bacterial cell/ fungal mycelium tissue was then extracted using a blend of organic solvents (10 ml of methanol, dichloromethane and ethyl acetate) in the ratio of 1 : 2 : 3 for 12 hrs at 28°C in a shaker incubator at 150 rpm followed by sonication for 15 min (Luo *et al.*, 2007). The extracts were then filtered and dried using rotary evaporator (IKA®, Germany). The semi dried extracts were re-suspended in 1 ml of HPLC grade methanol (Sigma, USA).

3.10.3 Analysis of metabolites using LC-ESI-MS

The methanol soluble extracts were subjected to LC-ESI-MS analysis for metabolite profiling during the *in vitro* bacterial-fungal interaction using Waters Alliance e2695/HPLC-Tandem Quadrupole Mass Detector (Waters Corporation, USA).

3.10.4 The Chromatographic conditions

An injection volume of 20 μ l of each sample was loaded into Waters Alliance e2695/HPLC system equipped with an auto sampler for automatic sample loading. The samples were then separated in a C18 column (250 \times 4.5 mm, pore size: 5 μ m) with gradient elution conditions consisting of mobile phase -acetonitrile (solvent A) and 0.01% formic acid in water (gradient mode, solvent B). The gradient profile is shown in Table 3.7 below. The fractions were then ionized in positive mode and further detected using an ESI- Tandem Quadrupole Mass Detector connected to the HPLC system (Waters Corporation, USA). The range of the scan was 150-1200 m/z.

Table 3.7 Chromatographic conditions for metabolite profiling using gradient elution

Time (min)	Solvent A (%)	Solvent B (%)	Flow rate (ml/min)
0	5	95	1.5
1	5	95	1.5
6	30	70	1.5
12	60	40	1.5
16	60	40	1.5
20	80	20	1.5
24	80	20	1.5
26	5	95	1.5
30	5	95	1.5

3.10.5 Data extraction and identification of the compound

Peaks originating from both the Electrospray Ionization (ESI) positive and negative modes were acquired, with the m/z (mass-to-charge) ratio depicted on the x-axis and the relative abundance (%) on the y-axis, all corresponding to distinct retention times. The molecular masses for each peak, spanning various retention times, were ascertained through the identification of different adducts, including M+H, M+NH₄, M+Na+2H, M+Na, M+ACN+H, M+ACN+Na, 2M+ACN+H, 2M+H, M+CH₃OH+H, M+2Na-H, M+K, M+2K+H, 2M+K and 2M+Na. The determined molecular masses were compared with the molecular weights of compounds from different databases and available literature to assign the compound name.

3.11 TLC analysis of the crude metabolite extract of the bacterial isolates

The crude metabolite extracts of the rhizospheric bacterial isolates were subjected to thin layered chromatographic analysis. The bacterial isolates were streaked in NA media and incubated at 28°C for 72 hrs. Similar; methodology was followed as described in the section 3.10.2 for the crude methanol extracts of the bacterial isolates. Thin layer chromatographic plate (Merck Millipore, Germany) coated with silica gel 60 was cut into desired size and used as a stationary phase. A horizontal line was drawn with pencil at the bottom of side of the plate and samples were carefully loaded along the line. The chromatographic plate was then dried and placed in the chromatographic chamber loaded with the mobile phase, Chloroform: Methanol: Water-39:15:3 (v/v) in such a way that only the tip of the bottom side of the chromatographic plate touches the mobile solvent. The mobile phase was allowed to rise for 30 mins till the fractions were separated and the solvent front was noted. The plate was air dried and pure water was sprayed to visualize the sample front.

3.12 Whole genome sequencing and *de novo* assembly of the potential bacterial isolate

The genomic DNA of the potential bacterial isolates was extracted by CTAB method. The quantitative & qualitative analysis was then done by the fluorescent (Qubit fluorometer4.0) and agarose gel electrophoresis for quality assurance. The libraries were then prepared for amplicons using the manufacturer instructions of NEBNext Ultra II FS DNA library preparation kit for Illumina (Fig. 3.2).

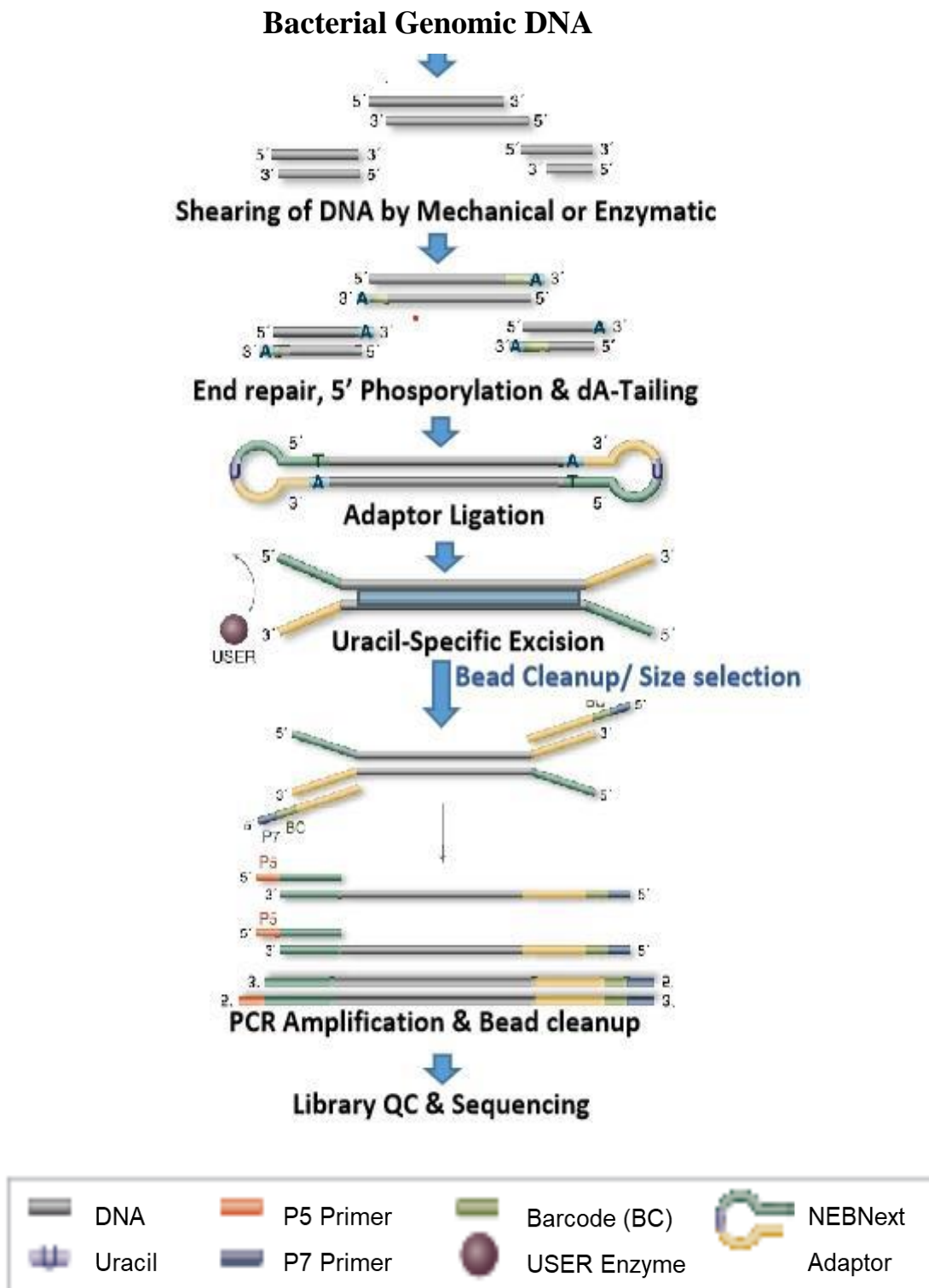


Fig. 3.2. Workflow demonstrating the use of NEBNext Ultra II FS DNA Library Prep Lit Illumina

The process of Library Preparation for Amplicon Sequencing

1.Fragmentation/End repair:- Fragmentation and end repair occurs during the 37°C incubation step with 100 ng of amplicons and NEBNext Ultra II FS Enzyme Mix to get the fragment size of 200-450 bp for 5 mins.

2. Adaptor Ligation:- Ligate the digested and end repaired fragments by using NEBNext Ultra II Ligation Master Mix and NEBNext Adaptor for Illumina and Incubate at 20°C for 15 mins in a thermal cycler with the heated lid off following by adding user enzyme and mix well and incubate at 37°C for 15 mins with the heated lid set to $\geq 47^\circ\text{C}$.

3. Clean up of Adaptor-Ligated DNA:- Clean the ligated products by Adding 0.8X AmpureXP beads (Beckmen coulter) and instructions user manual of library preparation kit.

4.PCR Enrichment of Adaptor-Ligated DNA:- Enrich the purified Adaptor- ligated DNA by using NEBNext Ultra II Q5 Master Mix and Index Primer Mix to add Illumina flow cell annealing sequences, multiplexing indices and sequencing primer annealing regions to all fragments and to increase concentrations of sequencing libraries.

5. PCR Enrichment of Adaptor- ligated DNA:- Clean the ligated products by adding 0.9X AmpureXP beads (Beckmen coulter) and instructions user manual of library preparation kit.

6. Assess Library Quality on a Tape station:- After purification check the concentration by using Qubit and quality by using tape station on D1000 screen tape.

7. Sequencing:-These libraries were sequenced in a 2*150 bp paired-end run using the NovaSeq 6000 with v1.5 reagents (300 cycles).

After sequencing the libraries, raw data so obtained were subjected to downstream analysis (Fig: 3.3). The raw data is obtained as read one and two fastq format that has been subjected to further analysis. Raw sequencing data is quality trimmed using Trim-galore to remove low quality reads ($q < 30$) and adaptors. The quality trimmed reads have been mapped on the reference to get the sequencing depth. On the other hand, that reads has been subjected to de novo assembly using Unicycler assembler with default parameters. After preparation of the assembly it has been annotated using PROKKA prokaryotic genome annotator using Bacteria as reference. The gene ontology and pathway annotation is performed with eggNOG and KOALA respectively. The secondary metabolite producing gene prediction has been performed using AntiSMASH.

The pan genome phylogeny has been prepared across all the available draft assembly of the different strains of this bacteria using Roary. The average nucleotide identity has been performed with the closest strain using the FastANI tool.

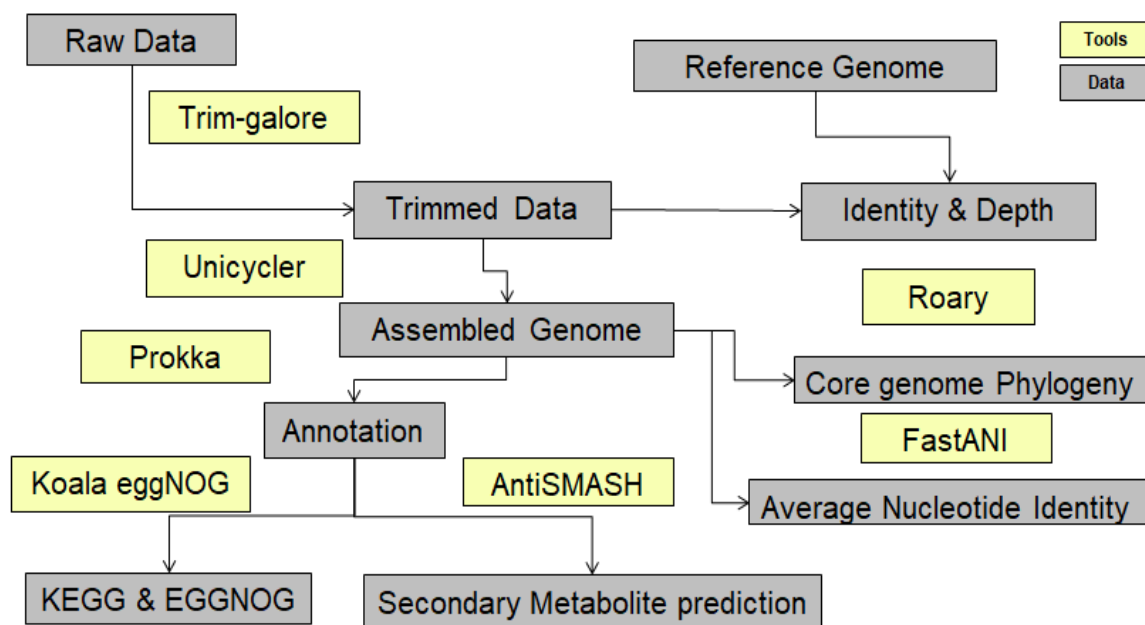


Fig. 3.3. Workflow of the downstream analysis of the raw data to achieve the *de novo* bacterial genome with functional annotation

3.13 Differential expressions of genes involved in the biosynthesis of key bacterial secondary metabolites in the monoculture and interacted dual culture sample in different time intervals

3.13.1 Isolation of the total RNA

Total RNA was extracted from the monoculture bacterial samples and the bacterial fungal interacted dual culture samples using the same methodology as described in the section 3.9.1

3.13.2 Denaturing Agarose Gel Electrophoresis

Agarose gel electrophoresis was performed using the same methodology as described in the earlier section 3.9.2

3.13.3 Primer designing

Primers for expression analysis (Table 3.8) were designed by using the bacterial gene sequences from NCBI GeneBank database with the help of PrimerQuest Tool (IDT, 2023 Integrated DNA Technologies, Inc.).

Table 3.8 Primers used for the expression analysis of the bacterial genes

Gene	Primer	Sequence (5' - 3')	Length
16s RNA	Ag_16s_qF	CGGTGAAATGCGTAGAGATG	20
	Ag_16s_qR	GGACTACCAGGGTATCTAATCC	22
srfAB	Ag_srfAB_qF	ATAAGATCCGCCTTCTCCTC	20
	Ag_srfAB_qR	CTTTGCGGACGTCCTTTATC	20
dhbF	Ag_dhbF_qF	CGAGATTCATTTCCCTGACC	20
	Ag_dhbF_qR	GTGATGACGCATTAGGAGAC	20
fenF_1	Ag_fenF_1_qF	CGTTTGAAGAGAGAGGTTGAG	20
	Ag_fenF_1_qR	AGGATGCCGTTACACTTG	18
bacD	Ag_bacD_qF	GGCGTAATATGGGATGTCTC	20
	Ag_bacD_qR	CGAGTATGACGACTGGTATG	20
ItuA	Ag_ItuA_qF	GGATATGCCTGCGGATTATG	20
	Ag_ItuA_qR	GTTGCTCCTGTGTCTTCTTC	20

3.13.4 First strand cDNA synthesis

The first strand cDNA synthesis was performed out with 1 µg of total RNA in a 20 µl reaction using Prime Script™ 1st Strand cDNA synthesis (TAKARA, India) following manufacturer's instructions. Bacterial cDNA from the total RNA sample of bacterial monoculture and bacterial-fungal interaction dual cultures were amplified with Random 6mers (50 µM) as per manufacturer's instructions.

3.13.5 Real-time Expression Analysis

The relative quantification of the expression profiles of the target bacterial genes was performed using the same methodology as described in the earlier **section 3.9.5** using 16S RNA gene as house-keeping gene.

3.14 Effect of bacterial priming on plant growth and development

3.14.1 Preparation of the bacterial inoculum and seed bio-priming assay

The seeds of cabbage and rapeseed were surface sterilized with 0.1% hypochlorite solution for 1 min followed by three times washing with autoclaved distilled water. The overnight grown rhizo-bacterial cultures were centrifuged at 5500 rpm for 15 mins and the supernatant was discarded and the bacterial cells were re-suspended in autoclaved saline solution (0.85% w/v) maintaining a concentration of 1×10^7 bacterial cells/ml. The seeds were then submerged in the bacterial suspension 6 hrs followed by air dried inside laminar chamber. The primed seeds were then kept for germination over an autoclaved filter-paper in a petri-plate with 2 ml autoclaved distilled water (Paul *et al.*, 2020). 30 seeds per petri- plates were kept for germination for each bio-priming treatment with three biological replications. Unprimed sterilized seeds were used as a mock. The plates were sealed to maintain appropriate humidity and were kept at 28°C incubator for germination. Seed germination percentage was calculated after 7 days of germination following the protocol given by Costa *et al.* (2020).

$$\text{Germination \%} = \frac{\text{Number of seeds germinated}}{\text{Total number of seeds}} \times 100$$

Along with germination percentage, the root length and shoot length of the germinated seeds were calculated in cm and recorded.

3.14.2 Greenhouse pot culture experiments

The bio-primed germinated seeds of cabbage along with the unprimed germinated seed, mock was transferred aseptically to 17 cm diameter plastic pots having 4 times autoclaved potting mixture (Garden soil: Vermicomposting-80:20) for further experiments. The plants were watered at an interval of 48 hrs. After 30 days, agronomic data such as the shoot height, root length, number of leaves and leaf area index (leaf area/ land area) were recorded. Two extra sets of mock plants were simultaneously maintained for fungicide treatment and fungal infection assay along with mock and other bio-primed plants.

3.15 Evaluation of the disease suppression efficiency of the bacterial isolates

3.15.1 Bio-control Assay

For bioassay, leaves of the 45 days old cabbage bio-primed plants as mentioned in the section 3.14.2 were carefully rubbed with sterilized cotton to remove the waxy cuticle layer and foliar sprayed with the same bacterial inoculum with same concentration as mentioned in the section 3.14.1. A set of mock plants were sprayed with commercial fungicide (Mancozeb). All the plants were then covered with plastic bags to retain high humid condition for 48 hrs. Following this, pathogenic fungal spore suspension of concentration 1×10^7 spore/ml (maintained using haemocytometer) was sprayed in set of treatments except the absolute mock which was sprayed with sterile distilled water. All the plants were again covered with transparent plastic bags to retain high humid condition for disease development for 48 hrs and the following parameters were recorded after 5 days post inoculation (dpi) of the fungal spore treatment—number of leaf with lesion, number of lesion per leaf, lesion size and disease was rated in the scale of 0-3 as described by Bal and Kumar, (2014) and also the disease severity index was calculated. Leaf samples were also harvested to analyze the physiological and biochemical changes (Chlorophyll content, RLWC, ELI%, proline content, total phenolics and SOD activity) in cabbage after 5 dpi of the fungal spore treatment.

3.15.2 Total Chlorophyll Estimation

Fresh leaf samples weighing 50 mg each from the treatments were collected and were subjected to crushing in 2 ml of 80% acetone followed by centrifugation at a force of 6000 rpm for a duration of 15 mins. Subsequently, the absorbance of the resulting supernatant was measured at wavelengths of 662 nm, 644 nm, and 440 nm. These absorbance measurements were performed relative to a blank composed of 80% acetone. The quantification of chlorophyll content was carried out in accordance with Saini *et al.*, (2023) using the formula:

$$\text{Chl a} = 9.78A_{662} - 0.99A_{644}$$

$$\text{Chl b} = 21.40A_{644} - 4.65A_{662}$$

$$\text{Total Chlorophyll} = \text{Chl a} + \text{Chl b}$$

3.15.3 Relative Leaf water Content

Relative Leaf Water Content (RLWC) analysis was executed according to the method previously outlined by Saini *et al.* (2023). Initially, a mass of 50 mg of fresh leaves (referred to as fresh mass, FM) was weighted. These leaves were subsequently immersed in distilled water for duration of 2 hrs. Following the incubation, the tissues were carefully removed from the water and weighed after gently wiping away any excess moisture. This recorded weight was termed as the turgid weight (TW). After the weighing process, the leaves were subjected to oven drying at a temperature of 60°C for a period of 48 hrs and the dried leaves were weighed (DW). The Relative Leaf Water Content (RLWC) was calculated employing the following formula:

$$RLWC = \frac{TW - DW}{TW - FW} \times 100$$

3.15.4 Electrolyte leakage indexing (ELI %)

The determination of the Electrolyte Leakage Index (ELI) was conducted following the method outlined by Saini *et al.*, (2023). Initially, leaves were washed carefully and 50 mg of leaves from each of the treatment were weighted and immersed in 10 ml of distilled water for a duration of 18 hrs in test tubes and the initial conductivity (L_0) of the solution were recorded. Subsequently, test tubes containing both distilled water and the leaf tissues were subjected to autoclaving at a temperature of 120°C for a period of 20 mins. Following autoclaving, the conductivity of the solution (L_t) was again noted. Electrolyte Leakage Index (ELI %) was calculated utilizing the following formula:

$$ELI\% = L_0 / L_t \times 100$$

3.15.5 Total proline content

50 mg of fresh leaf material (FM) was subjected to homogenization in 2 ml of a 3% sulfosalicylic acid solution followed by centrifugation at 12,000 rpm for duration of 10 mins. To 1 ml of the resulting supernatant, a mixture consisting of 1 ml of acid ninhydrin and 1 ml of glacial acetic acid was added. This amalgamation was subsequently boiled for a period of 1 hr at a temperature of 100°C. The reaction was brought to a halt by placing the test tubes containing the sample mixture in an ice bath. Following this, 2 ml of toluene was introduced into the mixture and vigorously mixed to facilitate the separation of the layers. The upper layer was carefully taken, and its absorbance was measured at a wavelength of 520

nm. To determine the concentration of proline in the samples, a standard curve of L-proline was employed (Saini *et al.*, 2023).

3.15.6 Total phenol content

The quantification of total phenol content was conducted employing the Folin-Ciocalteu colorimetric assay, as described by Saini *et al.* (2023) with modifications. 50 mg leaf samples were subjected to homogenization in 80% methanol, followed by an incubation period at room temperature 24 hrs. The resultant supernatant was collected after centrifugation at 3000 rpm for 10 mins. To 100 μ l of the supernatant, 0.2 ml of Folin-Ciocalteu reagent and 2 ml of distilled water were added. The resulting mixture was then incubated for 3 mins at room temperature. Following this, 1 ml of 20% sodium carbonate was introduced to the mixture and the mixture was again incubated 1 hr at room temperature. The quantification of total phenol content was accomplished by measuring the absorbance at a wavelength of 765 nm. The quantification was performed using a standard curve of gallic acid.

3.15.7 Superoxide dismutase activity

SOD activity of the leaf samples from each of the treatments were carried out employing the protocol of Adhikary *et al.*, (2022) as described in section 3.8.

3.16 Comparison of the necrosis level

Detached leaves from 30 days old cabbage plant were used to determine the level of necrosis post infection with fungal spore (10^7 spore/ml) using trypan blue staining method (Fernandez-Bautista *et al.*, 2016). Similar methodology was used for foliar spray with the bio-inoculum and for the spraying of fungal spores as described in the section 3.14.1. After 5 dpi leaves from each of the treatments were washed with distilled water gently. The leaves were then immersed in trypan blue solution (as detailed in APPENDIX II) and incubated for 30 mins followed washing with dist. water. The leaves were then destained in 70% ethanol for overnight followed by immersion in glycerol for 6 hrs. The excess glycerol was subsequently drained, and leaves were paper dried and photographs were taken.

CHAPTER IV

RESULTS AND DISCUSSIONS

The aim of this research focused on examining the rhizospheric bacteria associated with healthy cabbage plants. The primary objectives were to understand these bacteria's characteristics, their potential to enhance plant growth and their ability to combat diseases. The study involved various aspects, including identifying and describing the rhizospheric bacteria, investigating their ability to counteract fungal pathogens, elucidating the mechanisms by which they achieve this through differential expressions of genes and the production of metabolites and finally, confirming their positive effects on both plant growth and disease management.

4.1 Isolation of the pathogenic fungi from diseased leaf of cabbage

Isolation of the pathogenic fungi was done following the methodology as described in section 3.2.1 from the diseased leaf of cabbage (Fig. 4.1). A pure fungal isolate was recovered from mixed fungal cultures grown in PDA medium supplemented with streptomycin (75 mg/ml) that showed typical *Alternaria* like colony characteristics. The fungal isolate was isolated from the disease sample collected from the Horticulture Orchard, AAU, Jorhat and was designated as AG1F in further experiments. To establish the pathogenicity of AG1F, detached cabbage leaf was subjected to inoculation with a spore suspension of the fungal isolate. This led to the development of characteristics like chlorosis around the site of inoculation and black concentric ring spots on the cabbage leaf, consistent with symptoms of the disease (Fig. 4.2 A- D). Subsequently, when the diseased cabbage leaf with the black spot was introduced to the PDA medium, the re-isolation of fungi resembling AG1F, thereby establishing the Koch's postulates. Similar observation was also observed with leaves of rapeseed confirming the wide range of host of the fungal isolate (Fig. 4.2 E-H). Similar observations were also reported by Rahimloo and Ghosta (2015).

4.1.1 Morphological characterization of the pathogenic fungi

Morphological investigations of the phyto-pathogenic fungal strain AG1F were conducted, based on its growth on Potato Dextrose Agar (PDA) medium. Initially, AG1F displayed a slightly yellowish to light brown colour on the PDA plate, which subsequently darkened as it progressed. The colony exhibited a cottony mycelial texture, maintaining a rounded form and possessing rugged margins. The fungal isolate exhibited a distinctive pattern of zonation, achieving a diameter of more than 8 cm during a 20-day

cultivation period on PDA at 28°C (Fig. 4.3 A). Under a light microscope, AG1F exhibited a dichotomous branching configuration, characterized by septate hyphae (Fig. 4.3 B). The conidia of AG1F took on a cylindrical-oblong shape, displaying a golden yellow hue and a smooth surface (Fig. 4.3 C). These conidia were observed to be melanized with muriform in structure. Macioszek *et al.* (2018) have also showed that different isolates of *Alternaria brassicae* exhibited diverse cultural attributes, including variability in colony colour (white, off-white, to light brown). The colony's morphological traits encompassed variations in texture (cottony to fluffy and even feathery). Colony growth rates showed variation, encompassing slow, medium and fast growth. Colony margins also displayed diversity, ranging from wavy and smooth to rough.

4.1.2 Molecular characterization of the fungal isolate

The molecular characterization of the pathogenic fungal isolate was conducted by using the Internal Transcribed Spacer (ITS) primers by sequencing of the ITS region of the fungal DNA.

4.1.2.1 Isolation and spectral analysis of fungal genomic DNA

The genomic DNA extracted from the pathogenic fungal isolate AG1F was evaluated using agarose gel electrophoresis within a 0.8% agarose gel matrix. The presence of intact bands within the gel substantiated the successful isolation of genomic DNA possessing sound structural integrity; devoid of any RNA impurities (Fig. 4.4 A). Assessing DNA quality stands as a pivotal consideration when engaging in molecular studies.

4.1.2.2 Spectral analysis of genomic DNA (Nanodrop reading)

The quantification and purity analysis of DNA sample was executed using the NanoDrop-1000 spectrophotometer, relying on absorbance readings at 260 nm for DNA concentration determination and 280 nm for assessing protein contamination. The 260/280 ratio of 1.89 for the fungal, AG1F DNA sample indicated the presence of pure and high-quality DNA, with a concentration of 1126 ng/μl. Gardes and Bruns (1993) conducted a similar investigation for fungal DNA extraction, finding the resulting DNA quality and quantity to be dependable and satisfactory for each fungal isolate. The absorbance ratios at 260/280 nm ranged from 1.77 to 1.99, with DNA concentrations spanning 215.75 to 260.26 ng/μl.

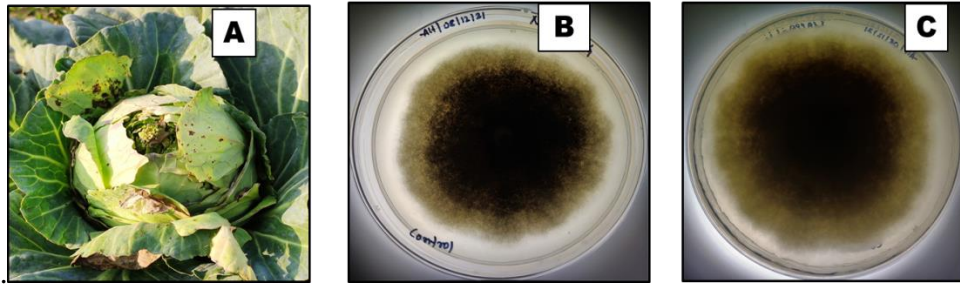


Fig. 4.1. Pathogenic fungi, AG1F isolated from an infected cabbage leaf (A), AG1F- front view (B) and AG1F- back view (C)

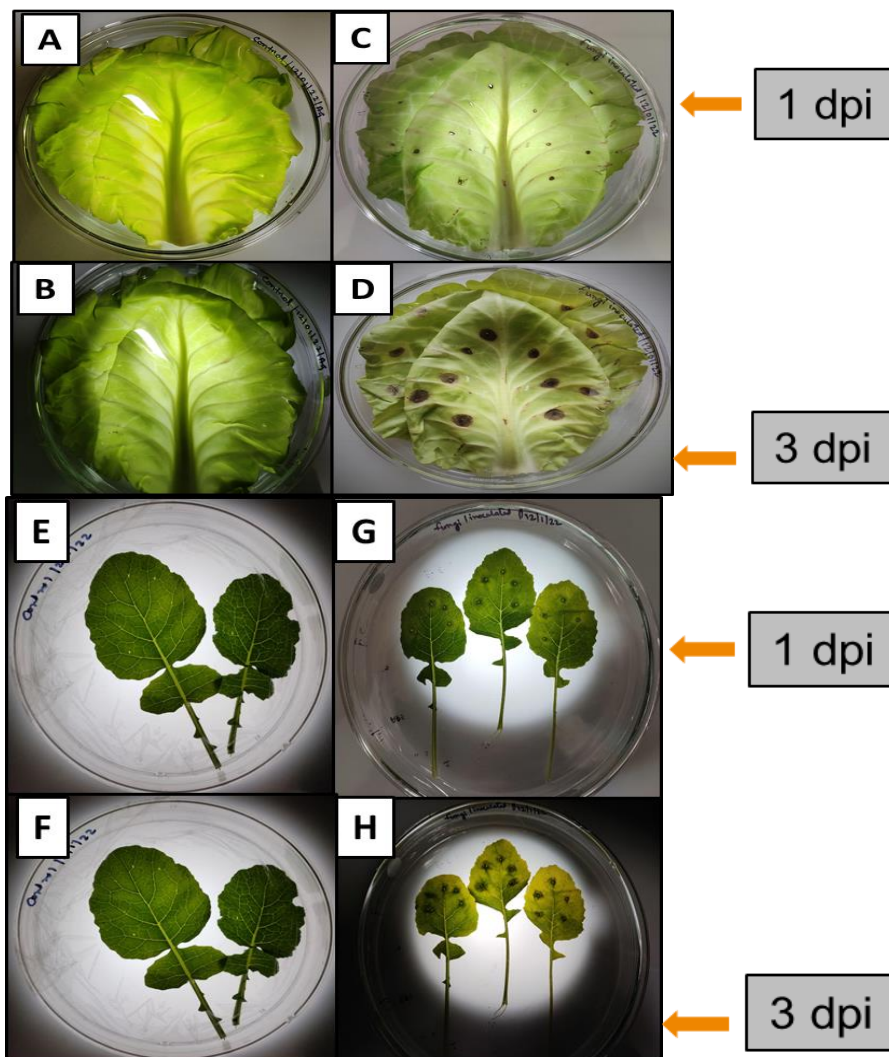


Fig. 4.2. Detached leaf assay showed similar black spot symptoms upon inoculated with the spore suspension of AG1F. (A & B) Cabbage – Mock; (C & D) AG1F Inoculated Cabbage leaf; (E & F) Rapeseed – Mock; (G & H) AG1F Inoculated Rapeseed leaf. # Mock- sterile H₂O inoculated and dpi- days post inoculation.

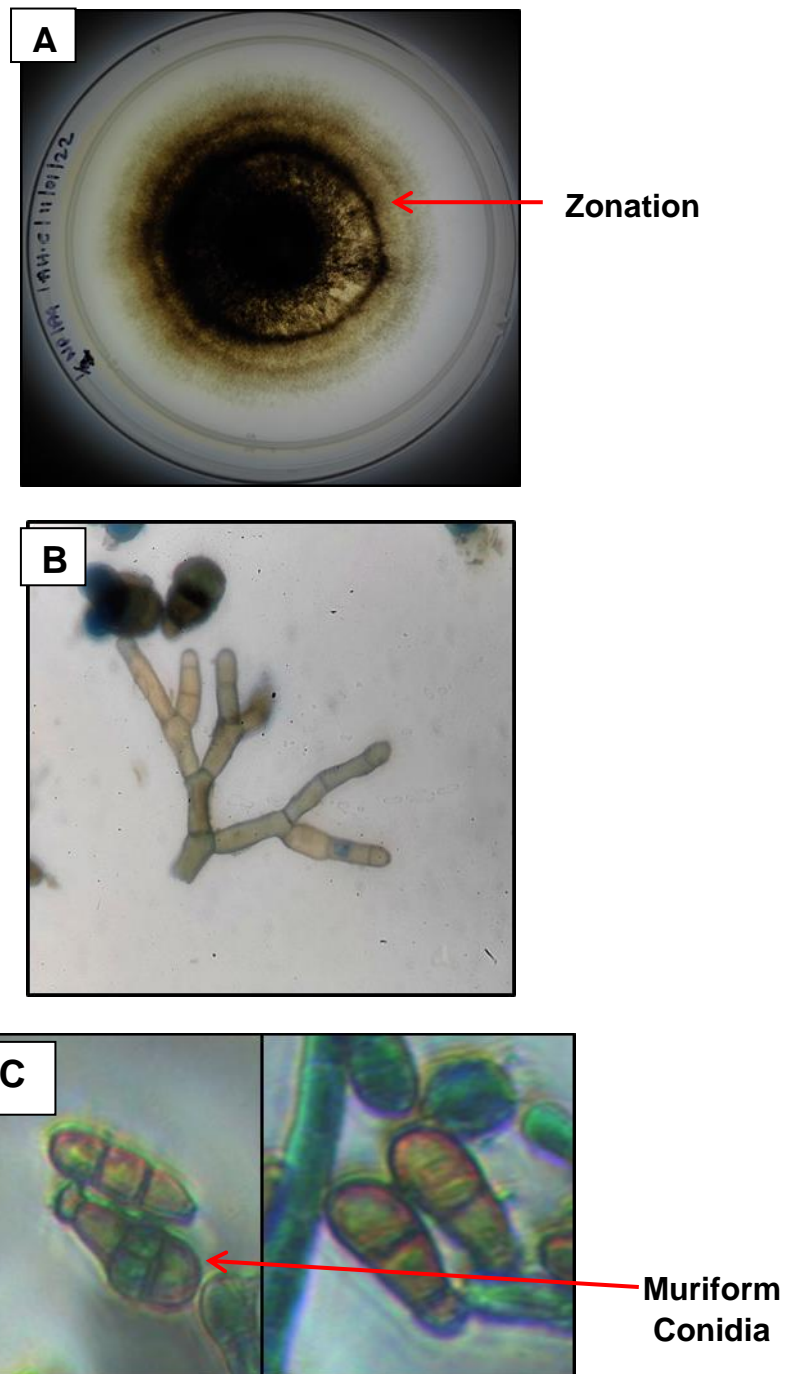


Fig. 4.3. Macroscopic and microscopic characteristics of the pathogenic fungal isolate, AG1F. A. Colony morphology on PDA medium; rounded shaped, yellowish-brown in colour with rough margins; B. Under light microscope, AG1F showed dichotomous branching with septate hyphae, C. The conidia of AG1F are club to oblong in shape, golden yellow, melanited with both longitudinal and transverse section (muriform).

4.1.2.3 PCR amplification of the genomic DNA

PCR amplification of the genomic DNA obtained was performed, targeting the Internal Transcribed Spacer (ITS) region of the ribosomal DNA, employing ITS1 and ITS4 primers. The ITS regions exhibit a notable level of divergence, even within species closely akin to each other. This characteristic renders them suitable as markers for discerning relationships among species of the same genus and closely related fungal genera (Hao *et al.*, 2010).

Following electrophoresis on a 1.2% agarose gel, the PCR products displayed bands with an approximate size of around 700 base pairs (~700 bp) (Fig. 4.4 B). Several other studies have also reported that the ITS region commonly varies within the range of 550 to 750 base pairs. This attribute renders it amenable to high-throughput sequencing methodologies (Choi *et al.*, 2007; Das *et al.*, 2015).

4.1.2.4 ITS rDNA sequencing and phylogenetic analysis

The polymerase chain reaction (PCR) amplification of the Internal Transcribed Spacer (ITS) region yielded fragments of approximately 700 base pairs (bp) in length. Subsequently, the PCR product underwent sequencing using an ABI 377 automated DNA Sequencer (Applied Biosystems, USA). The obtained sequence was aligned using the Clustal W algorithm within MEGA X and the sequence's homology was scrutinized through nucleotide BLAST (nBLAST) analysis on the NCBI platform to identify potential matches. The BLAST outcomes for the fungal isolate AG1F indicated a homology range of 90-99% with entries accessible in the NCBI database.

The phylogenetic tree was constructed for the fungal ITS region. The isolate AG1F was clustered with the reference Ascomycota division and was closely related to *Alternaria brassicicola* with 97% bootstrap confidence (Fig. 4.4 C). The consensus sequence of the isolated sample generated using BioEdit (v7.2) software was submitted to the National Center for Biotechnology Information (NCBI) database that identified the fungal isolate as *Alternaria brassicicola* AG1F, with the specific accession number designated as OR186688. The Internal Transcribed Spacer (ITS) region has been widely acknowledged as a robust marker for delineating fungal systematics and phylogeny (Begerow *et al.*, 2010; Bellemain *et al.*, 2010; Schoch *et al.*, 2012). However, challenges in distinguishing between two fungal species using the ITS marker have been highlighted by multiple researchers (Wiekes and Wiederhold, 2018; Azuddin *et al.*, 2021).

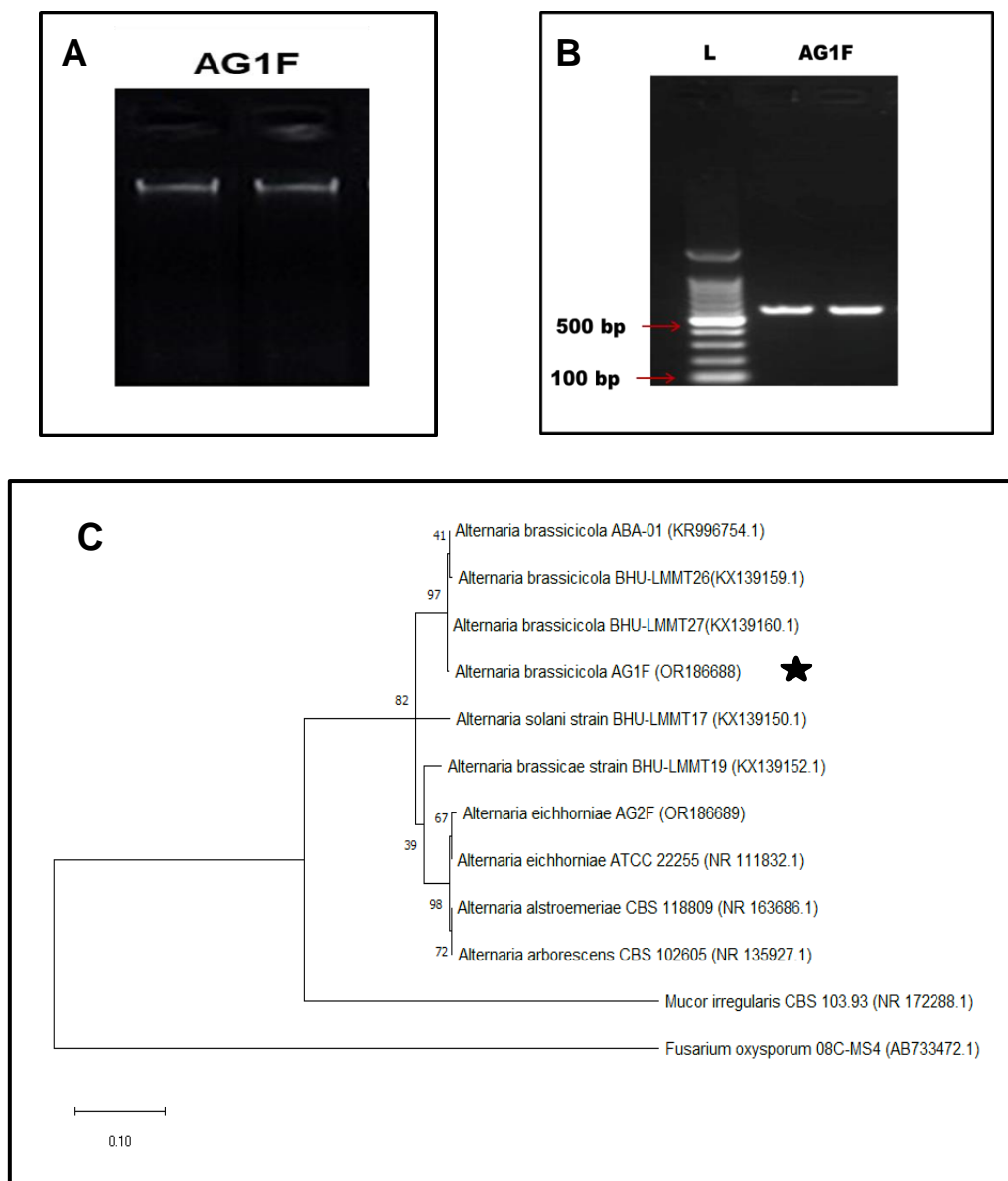


Fig. 4.4. PCR amplification of target ITS gene of the fungal isolate detected on agarose gel and the phylogenetic tree. A. Genomic DNA isolated from the fungal isolate, AG1F; B. PCR amplified ITS genomic region with size ~700 bp detected employing 100 bp DNA ladder (Himedia, India); C. The phylogenetic relationship between the pathogenic fungal isolate, AG1F and the type strains of the related species is shown by employing maximum likelihood tree-based method using Tamura Nei model on the ITS fungal gene. Branch node count represents the bootstrap percentage obtained from 1000 bootstrap replications. The reference sequences were retrieved from GenBank database and accession numbers are given within brackets.

4.2 Isolation of rhizospheric bacteria associated with healthy cabbage plant

A total of twenty-two bacterial isolates were recovered from the rhizospheric soil of disease free cabbage plant collected from different parts of Jorhat, Assam. Pure culture of all the twenty- two isolates were maintained growing a single colony on NA medium at 28°C for further use.

4.3 Screening of the rhizospheric bacterial isolates for antagonistic interaction with the pathogenic fungi, *Alternaria brassicicola* AG1F

All the twenty- two bacterial isolates were screened for their antagonistic property in a dual culture plate assay following the methodology as mentioned in section 3.4.1(Fig. 3.1). Among the twenty- two bacterial isolates, only two bacterial isolates showed antagonistic interaction with the phyto-pathogenic fungi, AG1F and were denoted as AG1B and AG2B respectively (Fig. 4.5).

Two previously isolated bacterial isolates *Serratia marcescens* D1 and *Bacillus subtilis* Scb-1 were obtained from the Microbial Biotechnology Lab, Department of Agricultural Biotechnology, Assam Agricultural University, Jorhat (Hazarika *et al.*, 2019; Hazarika *et al.*, 2020) and were also screened for antagonistic interaction against AG1F. Both the bacterial isolates can successfully reduce the growth of the pathogenic fungal isolate, AG1F (Fig. 4.6).

4.3.1 Effect of the bacterial isolates on the radial growth of the pathogenic fungi

The antagonistic effect exerted by the four bacterial isolates, AG1B, AG2B, *Serratia marcescens* D1 and *Bacillus subtilis* Scb-1 on the pathogenic fungi, AG1F in dual culture condition was studied for four consecutive days (24, 48, 72 and 96 hrs respectively) after bacterial inoculation. This showed that there is a significant increase in the colony diameter in the monoculture condition of *A. brassicicola* AG1F. But the growth of the fungi got restricted when co- cultured with each of the antagonistic bacterial isolates (Fig. 4.7). Similar kinds of results have also been reported by Zhang *et al.* (2022) and Hazarika *et al.* (2019).

Similar, observations were also found when the four bacterial isolates, AG1B, AG2B, *Serratia marcescens* D1 and *Bacillus subtilis* Scb-1 was co- cultured with other phyto-pathogenic fungi viz. *Alternaria brassicae* 2542, *A. brassicicola* 8344, *A. eichhorniae* AG2F, and *Fusarium oxysporum* respectively (Fig. 4.8).

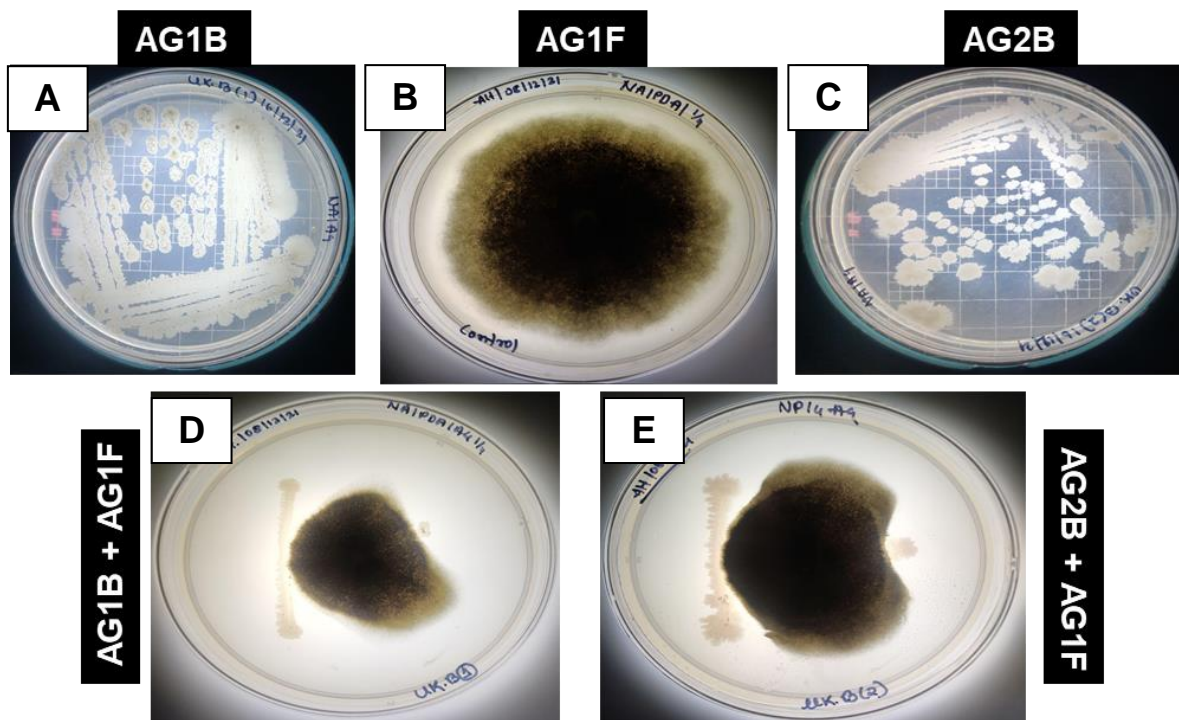


Fig. 4.5. Antagonistic activity exerted by the rhizospheric bacterial isolates AG1B and AG2B against the pathogenic fungi, AG1F in dual culture condition. A and C are the pure culture of the bacterial isolates, AG1B and AG2B respectively; B represents the monoculture of the pathogenic fungi, AG1F; D and E represents antagonistic interactions between each of the bacterial isolates AG1B and AG2B with the pathogenic fungi, *Alternaria brassicicola* AG1F.

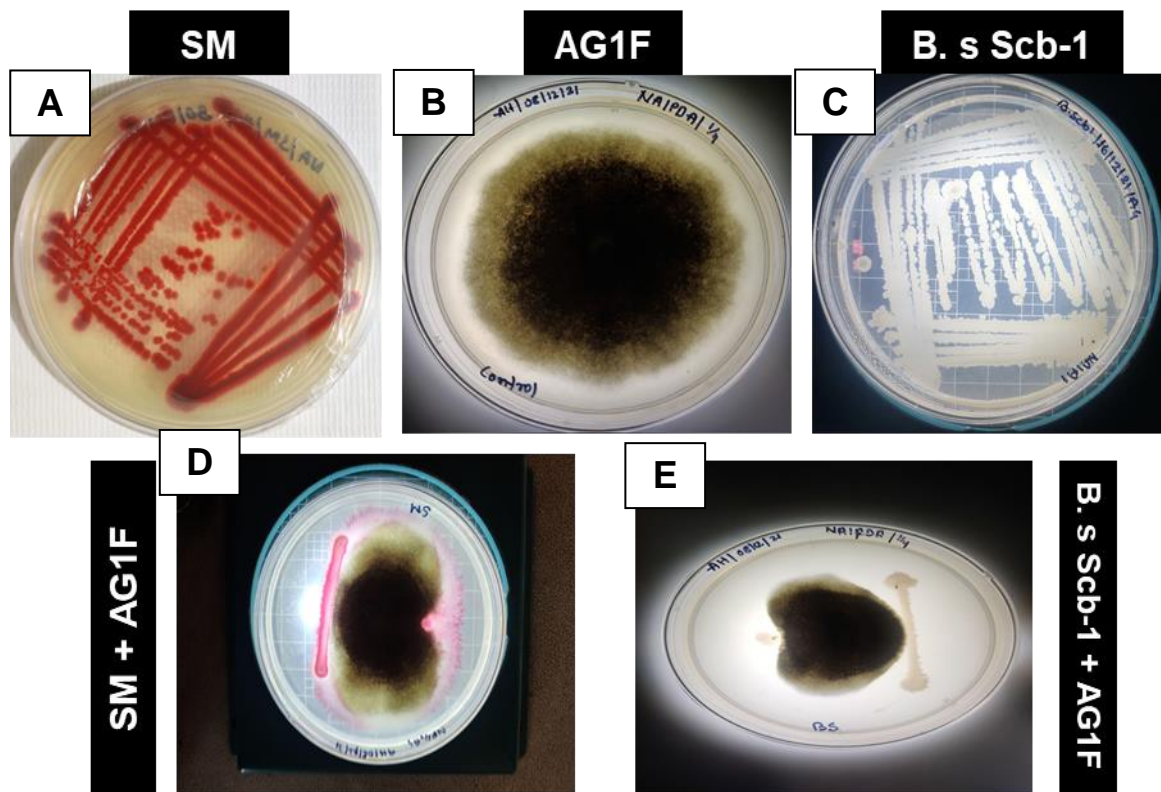


Fig. 4.6. Endo-fungal bacterial isolate, *Serratia marcescens* D1 (SM) and endophyte bacterial isolate, *Bacillus subtilis* Scb-1 shows significant growth reduction of the pathogenic fungi, AG1F in dual culture experiment. A and C are the pure culture of the bacterial isolates, SM and *B. subtilis* Scb-1 respectively; B represents the monoculture of the pathogenic fungi, AG1F; D and E represents antagonistic interactions between each of the bacterial isolates SM and *B. subtilis* Scb-1 with the pathogenic fungi, *Alternaria brassicicola* AG1F.

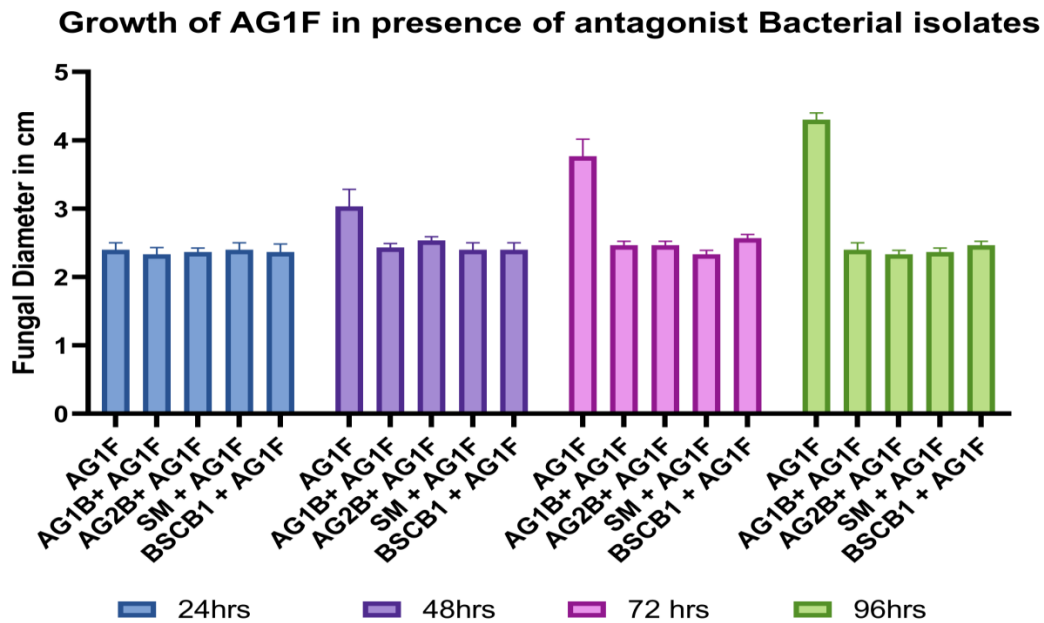
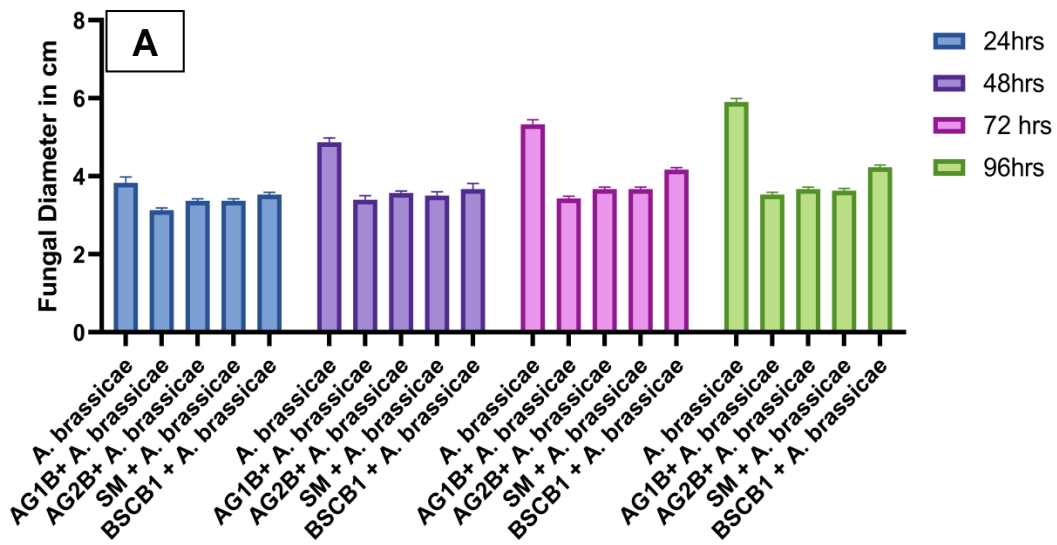
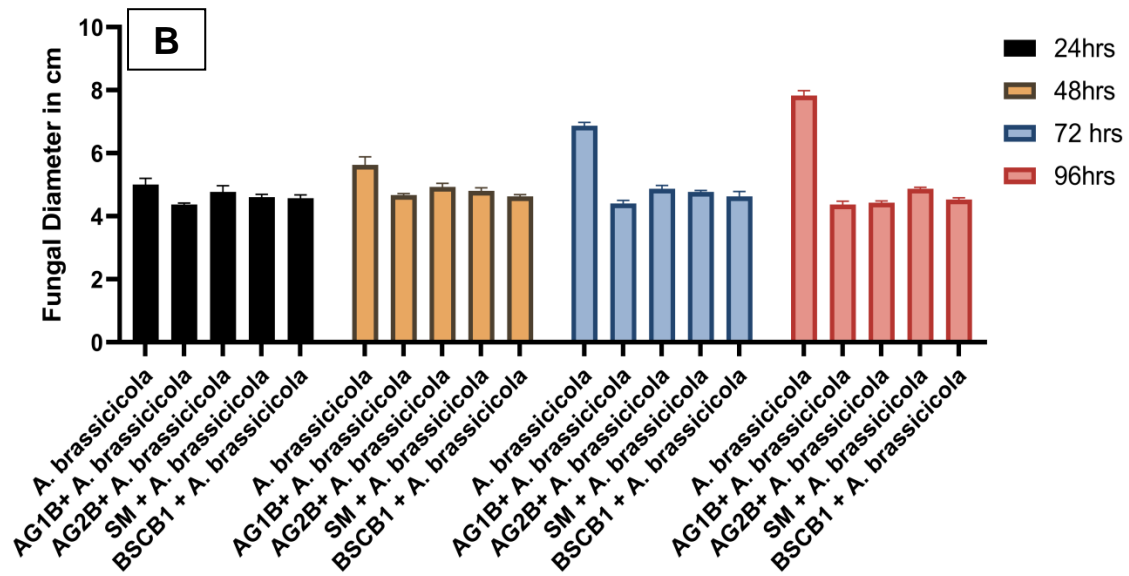


Fig. 4.7. The growth of the pathogenic fungal isolate, *Alternaria brassicicola* AG1F gets retarded upon co-culture with the bacterial isolates with each of the four bacterial isolates, AG1B, AG2B, *Serratia marcescens* D1 (SM) and *Bacillus subtilis* Scb-1 (BsScb1). This growth reducing effect of the bacterial isolates was recorded for four consecutive days (24 hrs, 48 hrs, 72 hrs & 96 hrs) post inoculation with the antagonist bacterial culture. AG1F represents the monoculture of the pathogenic fungi and the rest four were the respective dual-cultures. Results were analyzed using three biological replications with each of three technical replications and the error bar is representing the standard deviation.

Growth of *Alternaria brassicae* 2542 in pregence of Antagonist Bacteria



Growth of *Alternaria brassicicola* 8344 in pregence of Antagonist Bacteria



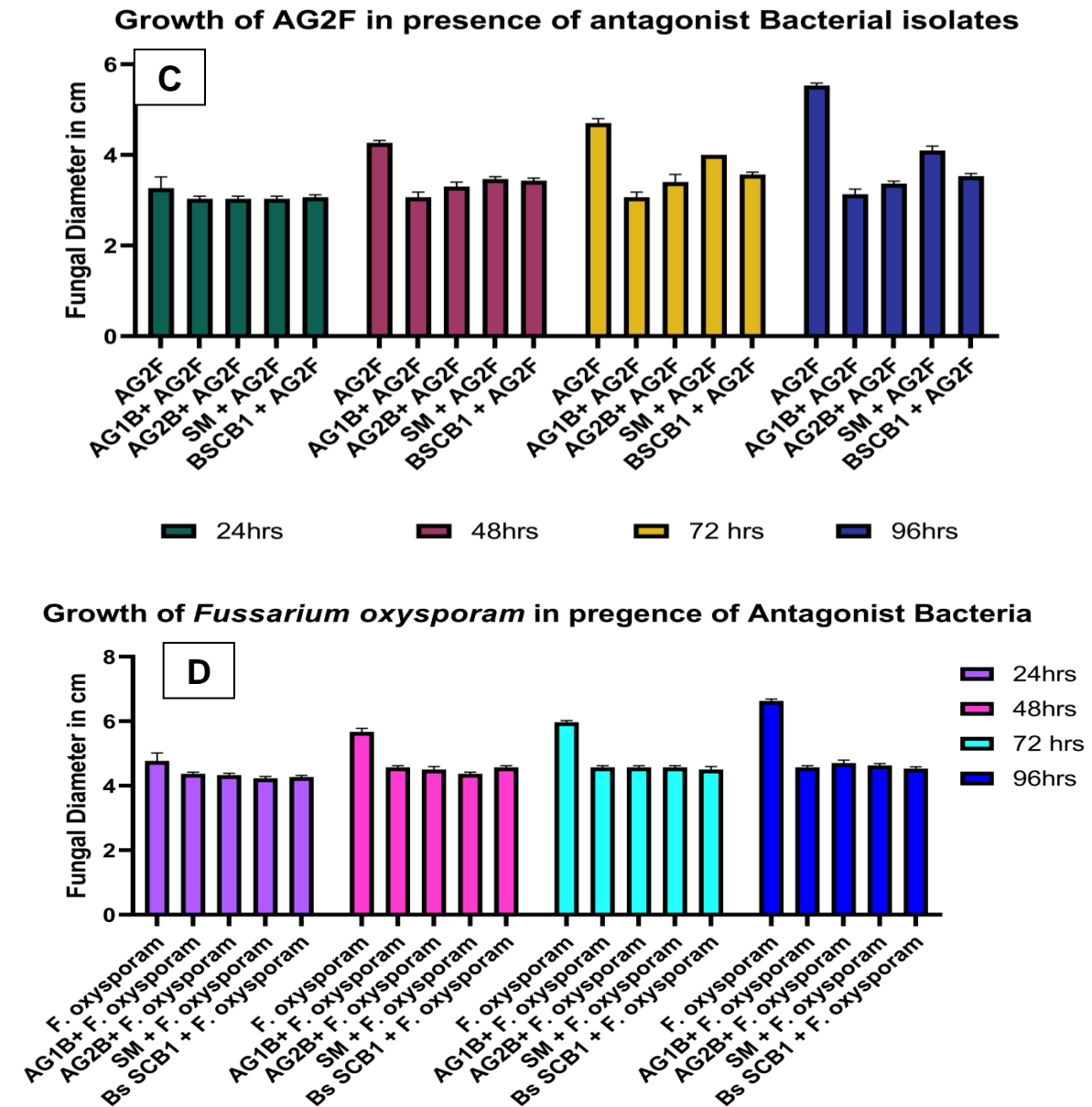


Fig. 4.8. The growth of the different pathogenic fungal isolates gets retarded upon co-culture with each of the four bacterial isolates, AG1B, AG2B, *Serratia marcescens* D1 (SM) and *Bacillus subtilis* Scb-1. (BsScb1). This growth reducing effect of the bacterial isolates was recorded for four consecutive days (24 hrs, 48 hrs, 72 hrs & 96 hrs) post inoculation with the antagonist bacterial culture. A, B, C & D represent growth reduction effects of the bacterial isolates on *Alternaria brassicae* 2542, *A. brassicicola* 8344, *A. eichhorniae* AG2F, and *Fusarium oxysporum* respectively. Results were analyzed using three biological replications with each of three technical replications and the error bar is representing the standard deviation.

4.3.2 Impact of antagonist bacteria on radial growth of fungi after 20 days of co-culture

When the four bacterial isolates, AG1B, AG2B, *Serratia marcescens* D1 and *Bacillus subtilis* Scb-1 was co- cultured with *A. brassicicola* AG1F till the monoculture fungal plate reach its full growth (20 days), it showed that among the four bacterial isolates, AG1B, AG2B, and *Bacillus subtilis* Scb-1 showed significant growth reduction of AG1F except *S. marcescens* D1 (Fig. 4.9). *S. marcescens* D1 could initially reduce the growth of AG1F but for a later period the fungi surpass the negative effects of bacteria. This could be because of the mycophagy nature of *S. marcescens* D1.

The percentage inhibition (PI) was also calculated. AG1B showed the highest inhibitory effect, with a percentage inhibition of 76.47%, against the pathogenic fungi *A. brassicicola* AG1F followed by AG2B and *B. subtilis* Scb-1 with an inhibition percentage of 70.59% (Fig. 4.10). Gkarmini *et al.* (2015) has also reported PI of beneficial bacteria on *Rhizoctonia solani*.

S. marcescens D1 showed the least percentage inhibition of 29.42%. Therefore, as *S. marcescens* D1 was not showing the desired effect for a longer period. Therefore, it was not included for the rest of the study.

4.3.3 Inhibitory effect of the bacterial cell free supernatant on fungal radial growth

Agar well diffusion assay was conducted as described in the earlier section 3.4.2. The cell free supernatant of each of the three bacterial isolates AG1B, AG2B and *Bacillus subtilis* Scb-1 could be able to reduce the radial growth of the fungi, *A. brassicicola* AG1F in PDA medium. Autoclaved distilled H₂O was used as a control check. The boiled supernatant (denoted as H in Fig. 4.11) of each of the bacterial isolates also could be to reduce the fungal growth suggesting the heat stability of the active ingredients present in each of the bacterial supernatants. The PDA medium (100 ml in molten state) was poisoned with 1 ml of each of the bacterial cell free supernatant. It was then poured in petriplates and upon solidification the fungi, *A. brassicicola* AG1F was inoculated. NB broth (1ml) added to PDA medium (100 ml in molten state) was used for the control check and data was recorded on the 10th day. This study also showed the growth reduction of the pathogenic fungi as compared to the control (Fig. 4.11).

This suggests that the bacterial isolates are secreting some active metabolites that have potential antifungal activity. Liang *et al.* (2023) and Hazarika *et al.* (2019) have also reported the antifungal effect of the bacterial cell free supernatant.

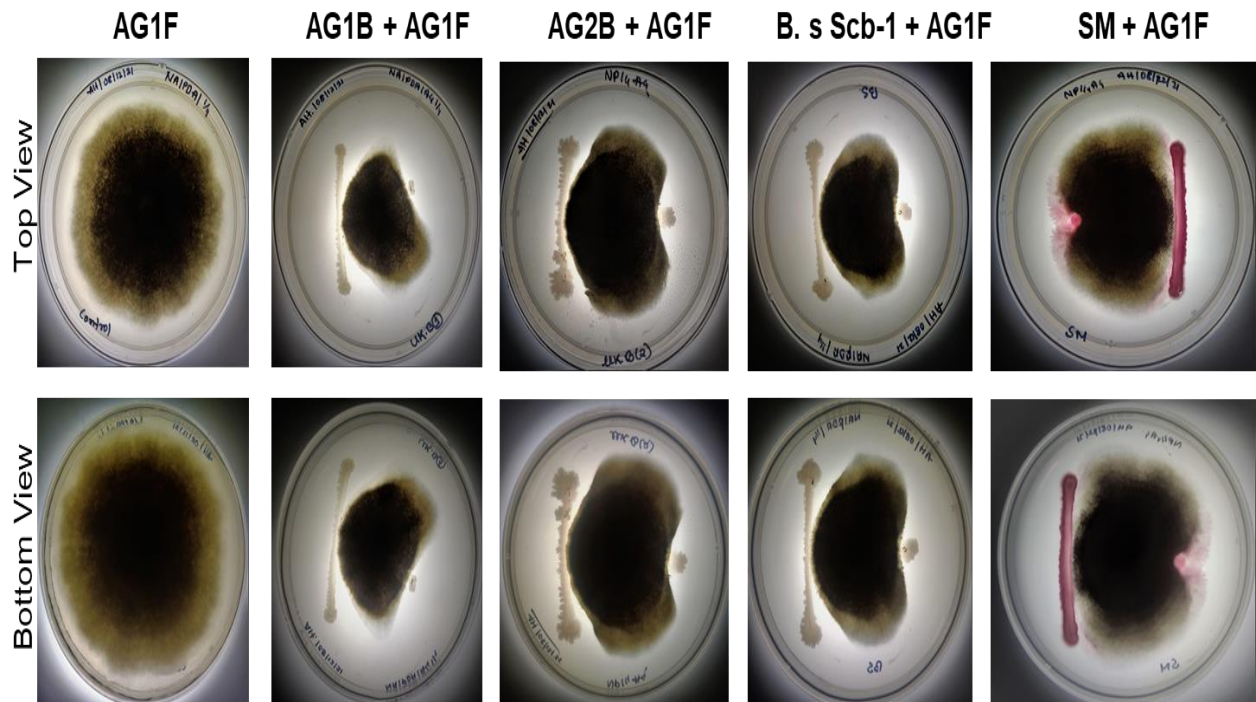


Fig. 4.9. Colony morphology of the pathogenic fungal isolate, AG1F when co cultured with antagonistic bacterial isolates after 20 dpi. (A) represents the monoculture of the pathogenic fungi, *Alternaria brassicicola* AG1F ; (B-E) antagonistic interactions between each of the bacterial isolates AG1B, AG2B, and *Bacillus subtilis* Scb-1 *Serratia marcescens* D1 (SM) with the pathogenic fungi, *Alternaria brassicicola* AG1F

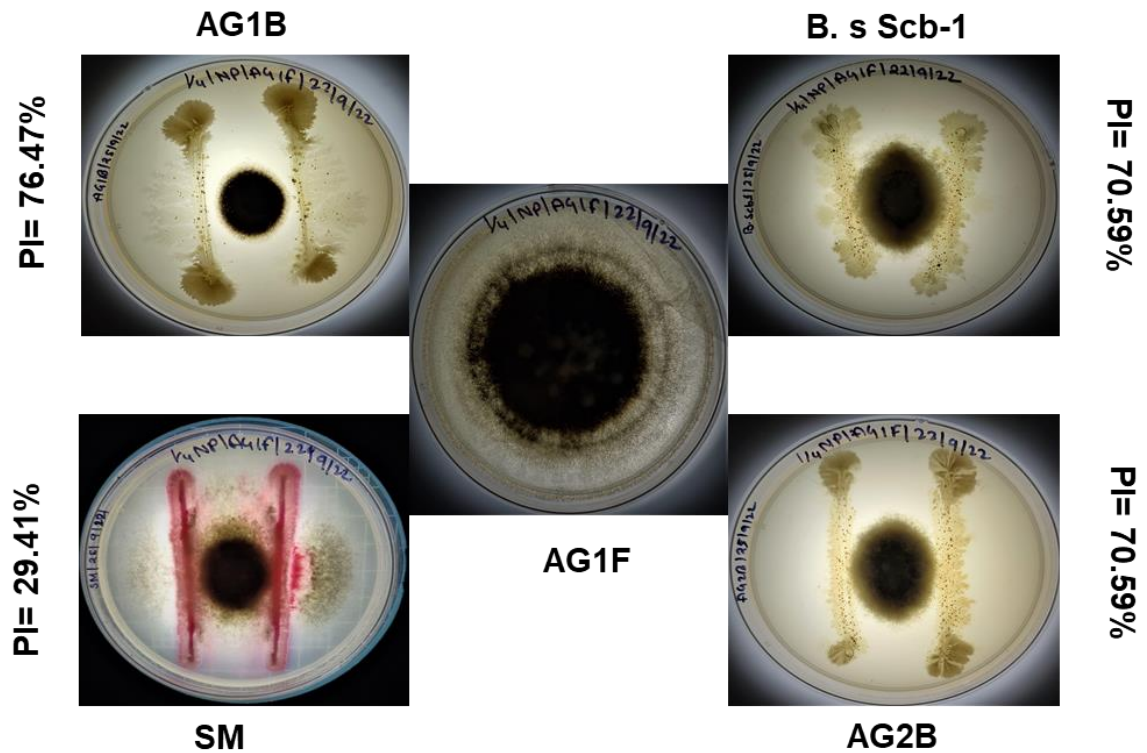
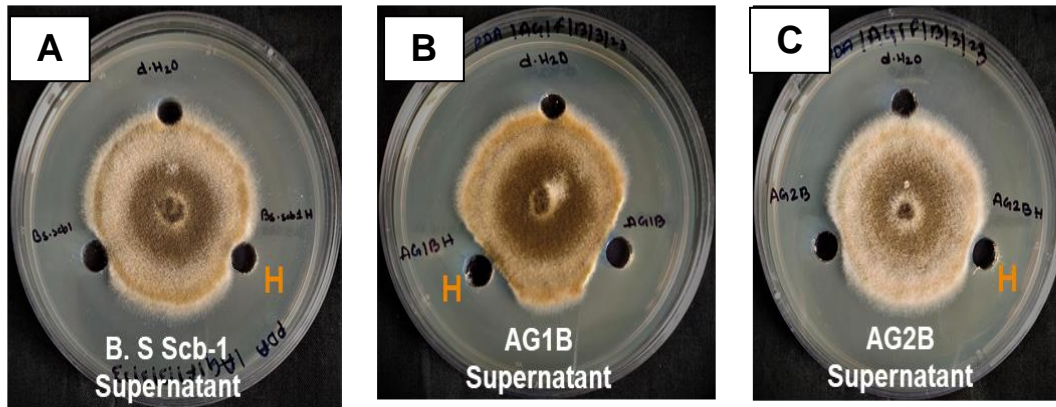


Fig. 4.10. Percentage inhibition (PI) Assay. AG1B showed the highest inhibitory effect, with a percentage inhibition of 76.47%, against the pathogenic fungi *A. brassicicola* AG1F followed by AG2B and *B. subtilis* Scb-1 with an inhibition percentage of 70.59%. *S. marcescens* D1 (SM) showing the least percentage inhibition of 29.42% probably due to its mycophagy nature. Results were analyzed using three biological replications with each of three technical replications.

Well Diffusion Method



Poisoned Food Assay 10 dpi

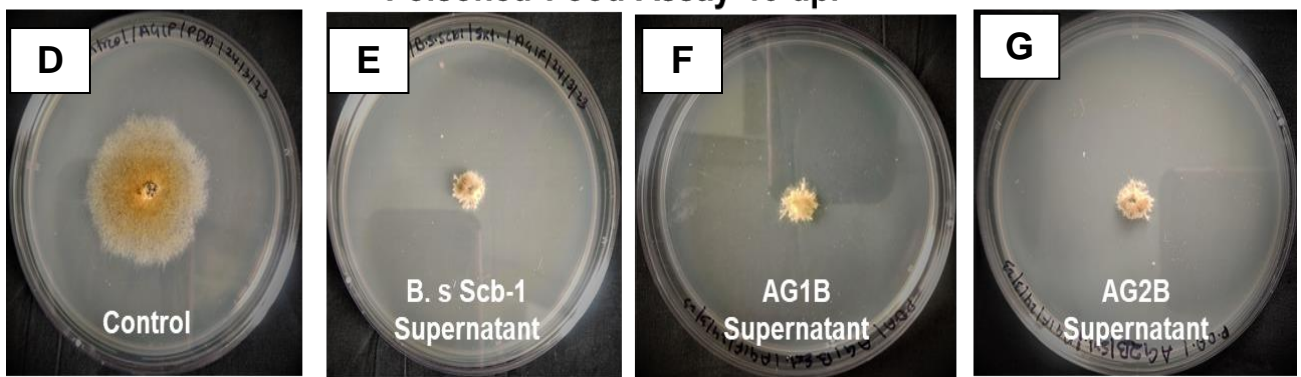


Fig. 4.11 Effects of the cell free supernatant of the bacterial isolates against the fungi, AG1F. (A -C) represents the well diffusion inhibitory effects of the bacterial supernatant. (D-E) results of the poisoned food assay

4.3.4 Antagonistic effect of the bacterial secreted volatile organic compounds (VOCs)

When the bacteria (AG1B, AG2B and *B. subtilis* Scb-1) inoculated plates were inverted on the fungal inoculated plate followed by proper sealing with parafim, it showed that all the bacterial isolates have released volatile antifungal compound that has resulted in the growth reduction of the fungi, *A. brassicicola* AG1F (Fig. 4.12). Upon incubation for longer period (360 hrs), the volatiles may get dispersed that resulted in the increase in fungal diameter for the AG2B and *B. subtilis* Scb-1 treatment. Interestingly, the effect of AG1B secreted volatiles was prominent after 360 hrs, Similar studies on bacterial antifungal volatiles have been reported by Zhang *et al.* (2020) and Hazarika *et al.* (2019).

4.4 Microscopic observation of the in vitro bacterial-fungal interactions

Microscopic studies was done following the methodology as describes in this section 3.5.

4.4.1 Visualization of the in vitro interaction between antagonist bacterial isolates (AG1B, AG2B and *B. subtilis* Scb-1) and the pathogenic fungi, *A. brassicicola* AG1F under light microscope

Under light microscope, the hyphae of AG1F from the monoculture plate showed normal morphology of the hyphae and noted their regular lengths, smooth surfaces, and intact structures. However, in the bacterial interaction plate, the mycelia of AG1F displayed wrinkled surfaces and deformities (Fig. 4.13). This suggests the antifungal nature of each of the bacterial isolates (Tendulkar *et al.*, 2007).

4.4.2 Visualization of the in vitro interaction between antagonist bacterial isolates (AG1B, AG2B and *B. subtilis* Scb-1) and the pathogenic fungi, *A. brassicicola* AG1F under Scanning Electron Microscope (SEM)

The hyphae from the interaction zone showed notable morphological anomalies, characterized by surface wrinkling and structural deformities under SEM as compared with the hyphae from the monoculture condition. The hyphae became thick and clumped forming protoplast balls (Fig. 4.14). Similarly, the conidia from the dual culture interaction plate showed abnormal deformities, rough and wrinkled surface. The AG1B treated conidia also exhibited bubble like morphology with pore formation (Fig 4.15). Similar kind of observation has been reported by Zhang *et al.* (2022) upon treatment of the pathogenic fungal hyphae with the bacterial fengycin.

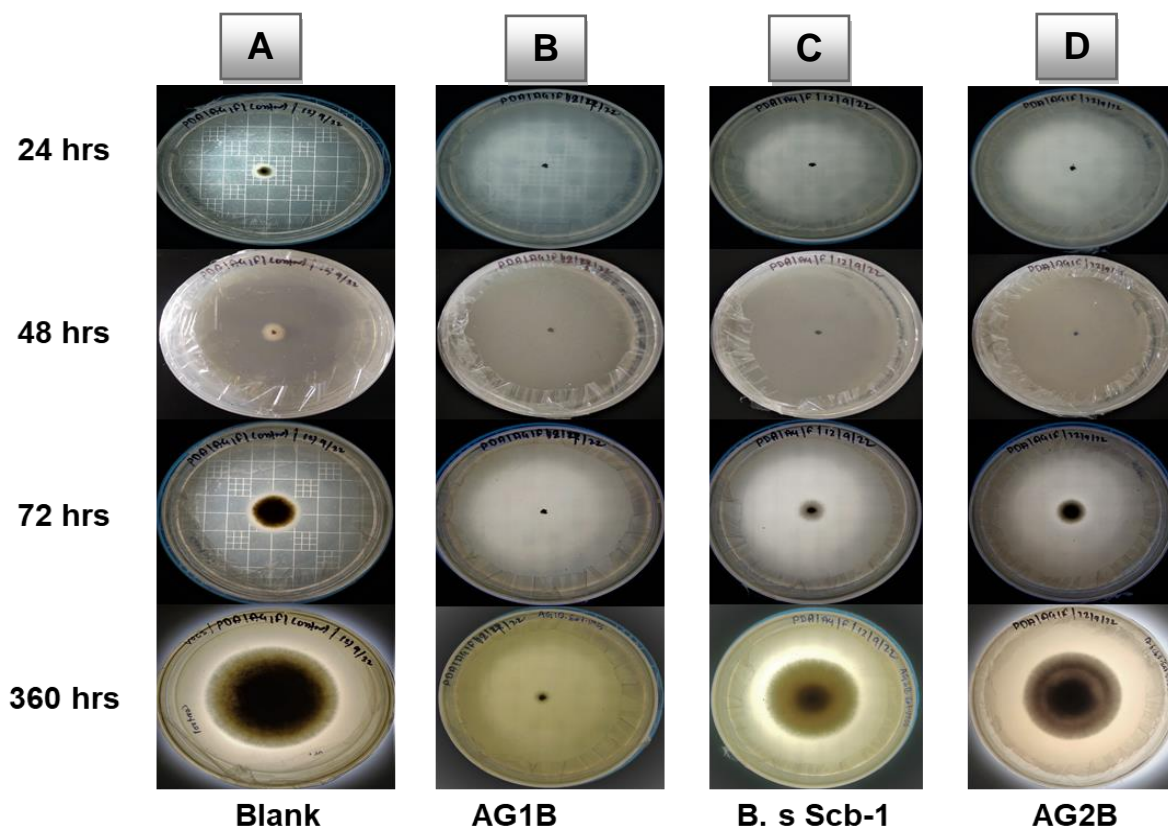


Fig. 4.12. Effect of Bacterial Volatiles on the linear growth of the pathogenic fungal isolate, AG1F. (A) Monoculture of AG1F in different time intervals; (B, C, & D) represents AG1B, *B. s Scb-1* and AG2B released volatile has showed a significant reduction in the colony diameter of the pathogenic fungi, AG1F upon cultured for 15 days the effect of volatiles decreases (C & D). AG1B have the highest growth reduction effect on fungi.

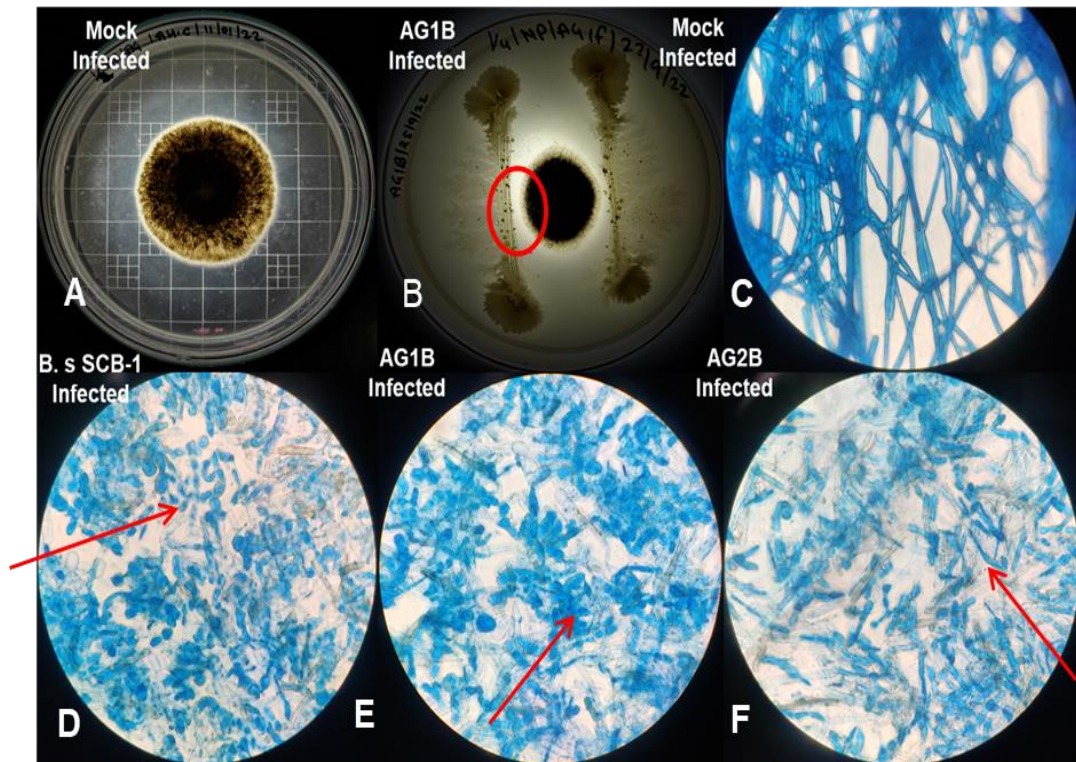


Fig. 4.13. Light microscopic study of the antagonistic effects of the bacterial isolates *B. subtilis* Scb-1, AG1B and AG2B on *Alternaria brassicicola* AG1F. (A & B) Representative monoculture and dual-culture with the interacting zone; (C) Monoculture, AG1F showing the normal hyphae with normal hyphae; (B, C & D) The mycelia of AG1F interacted with each of the three bacterial isolates respectively showed hyphae with abnormal feature. Hyphae became clumped and shrunken.

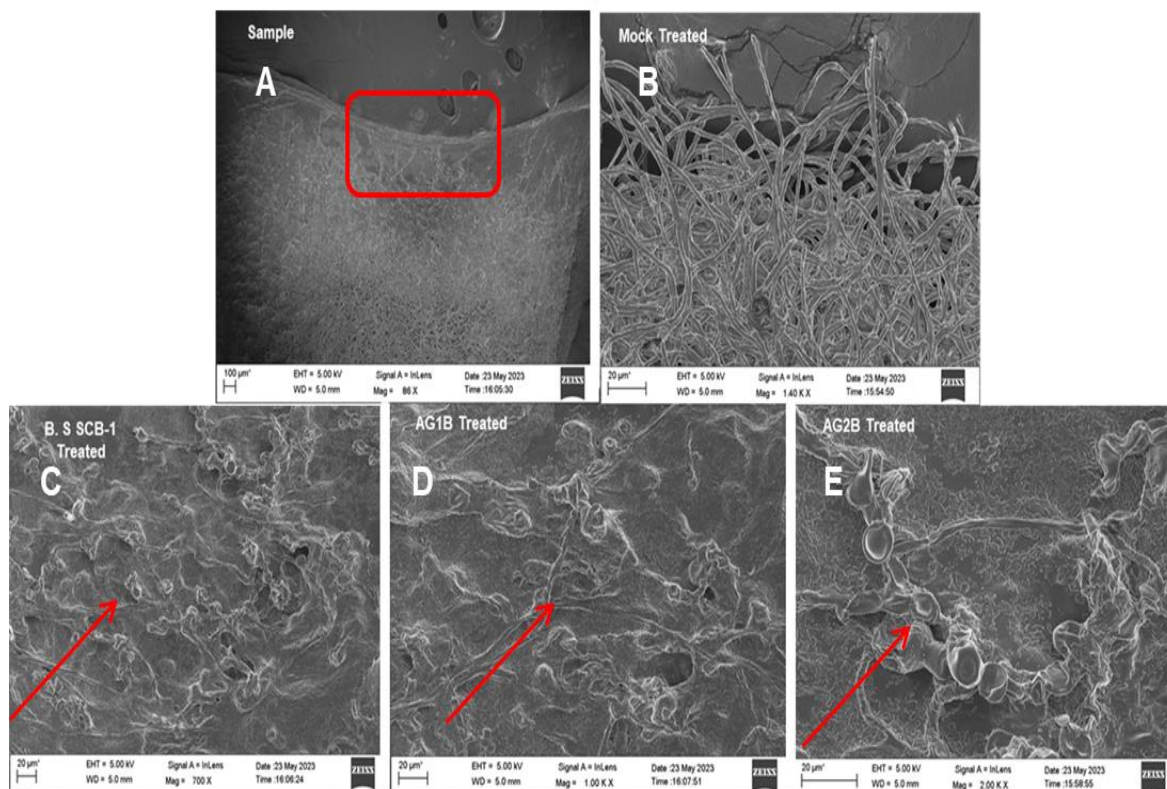


Fig. 4.14. SEM study of the antagonistic effects of the bacterial isolates *B. subtilis* Scb-1, AG1B and AG2B on *Alternaria brassicicola* AG1F. (A) Representative interacting zone; (B) Monoculture, AG1F showing the normal hyphae with regular lengths, smooth surfaces and intact structures; (B, C & D) The mycelia of *AG1F* interacted with each of the three bacterial isolates respectively showed wrinkled surfaces and deformities. Abnormal swelling and formation of protoplast balls of hyphae also appeared in the treated group.

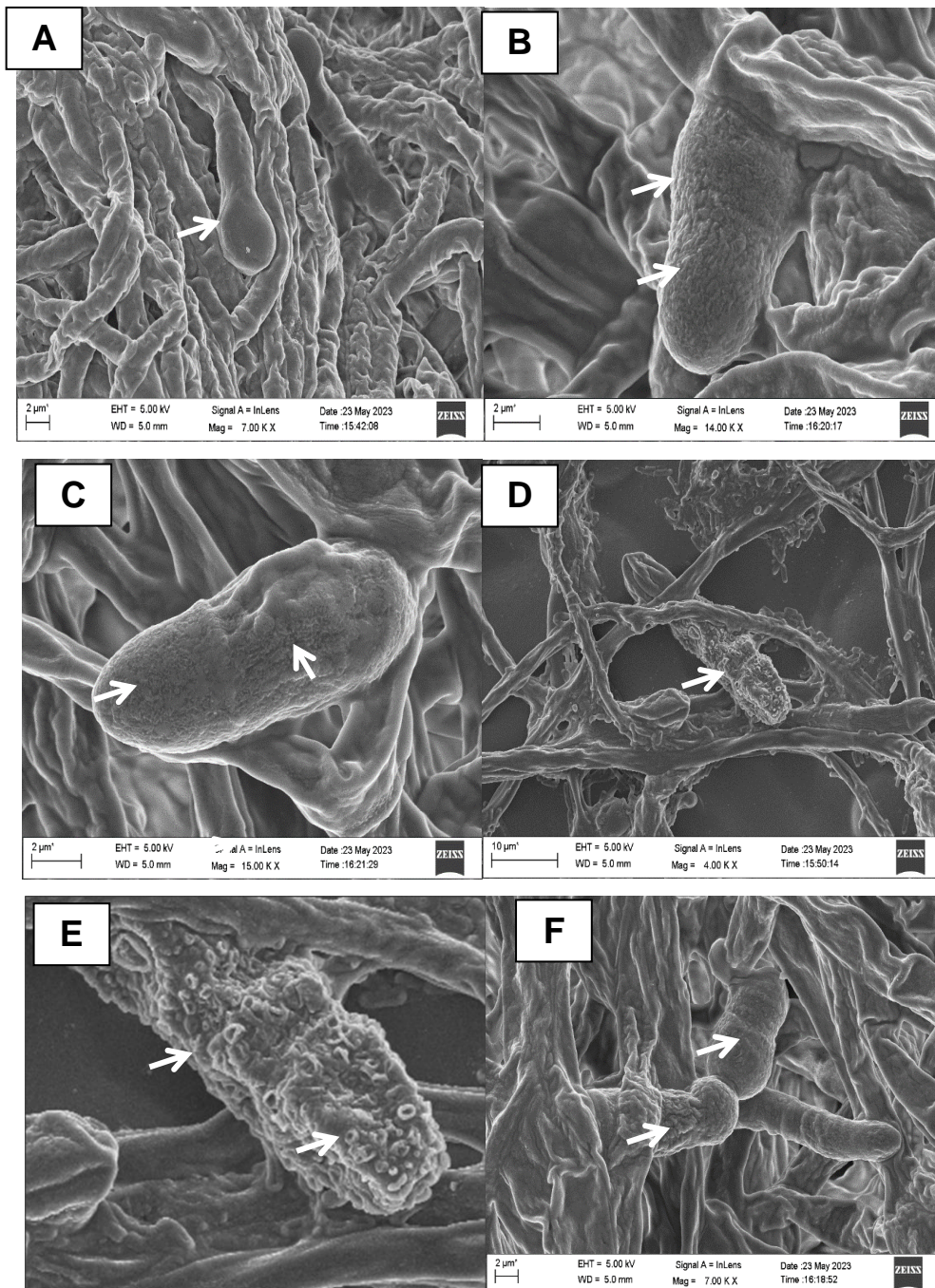


Fig. 4.15. SEM study of the antagonistic effects of the bacterial isolates *B. subtilis* Scb-1, AG1B and AG2B on the conidia of *Alternaria brassicicola* AG1F. (A) Club shaped Conidia of AG1F with smooth surface; (B & F) Conidia of AG1F showing morphological abnormalities with wrinkled and rough surface when interacted with *B. subtilis* Scb-1 and AG2B respectively; (C, & D) Conidia of AG1F showing similar morphological abnormalities with wrinkled and rough surface with deformities resulting in pore like or bubble like structure (Zoomed View of D) on the conidia when interacted with AG1B.

4.5 Characterization of the bacterial isolates having antifungal property

The rhizospheric bacterial isolates AG1B and AG2B showing antagonistic interaction with the pathogenic fungal isolate, *A. brassicicola* AG1F were further characterized based on their morphological, biochemical and molecular properties.

4.5.1 Morphological characteristics of the bacterial isolates

Both the bacterial isolates AG1B and AG2B are gram positive showing round colony morphology when grown in NA medium. Under SEM, the bacterial isolates AG1B and AG2B showed rod in shape with size of 1.735 μm , 644.5 nm and 3.094 μm , 821.8 nm respectively (Fig. 4.16). Some of the morphological features have been shown in the Table 4.1 below:

Table 4.1 Morphological characteristics of the bacterial isolates

Sl. No.	Characteristics	AG1B	AG2B
1	Gram's Staining	Gram Positive	Gram Positive
2	Cell Shape	Rod	Rod
3	Colony morphology	Round,slimmy,rough surface	Round; rough surface
4	Oxygen requirement	Aerobic	Aerobic
5	Pigment	Negative	Negative

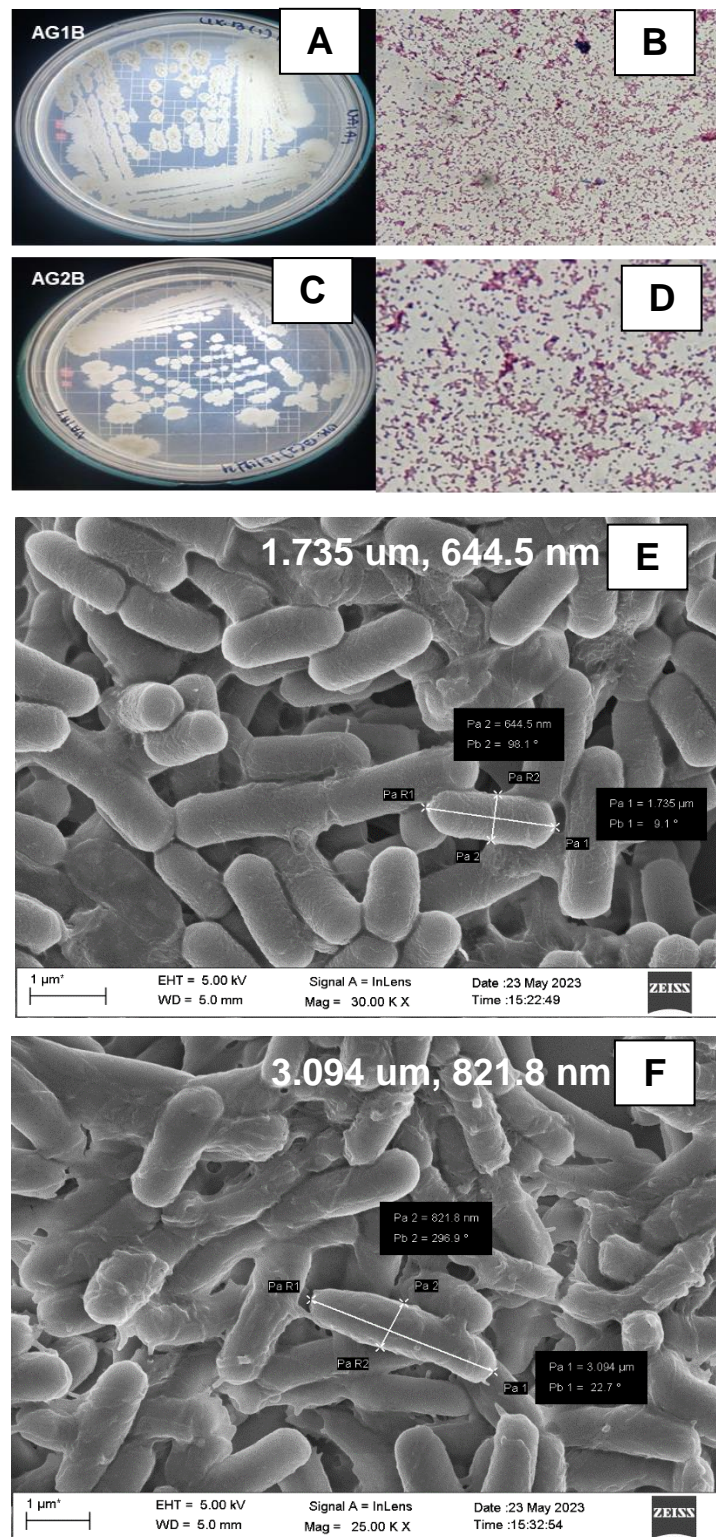


Fig. 4.16. Morphological characteristics of the bacterial isolates AG1B and AG2B. (A & C) represents the colony morphology of AG1B and AG2B respectively in NA medium at 28 $^\circ\text{C}$, (B & D) Gram's staining of the bacterial isolate, AG1B and AG2B respectively; (E & F) Scanning electron microscopic image of bacterial isolates AG1B and AG2B.

4.5.2 Biochemical characteristics of the bacterial isolates

The bacterial isolates with promising antifungal activity were subjected to biochemical characterization. And the results obtained are shown in the Table 4.2.

Table 4.2 Results of biochemical characterization of the bacterial isolates

Sl. No.	Test/ Sugar	AG1B	AG2B
1	Indole	Negative	Negative
2	Methyl Red	Negative	Negative
3	Voges Proskauer's	Negative	Negative
4	Citrate Utilisation	Positive	Positive
5	Glucose	Positive	Positive
6	Adonitol	Negative	Negative
7	Arabinose	Positive	Positive
8	Lactose	Negative	Negative
9	Sorbitol	Negative	Negative
10	Mannitol	Positive	Positive
11	Rhamnose	Negative	Negative
12	Sucrose	Positive	Positive
13	Xylose	Negative	Negative
14	Maltose	Negative	Positive
15	Fructose	Negative	Positive
16	Dextrose	Positive	Positive
17	Galactose	Negative	Negative
18	Raffinose	Negative	Negative
19	Trehalose	Negative	Positive
20	Melibiose	Negative	Positive
21	Mannose	Negative	Negative
22	Inulin	Negative	Negative
23	Sodium gluconate	Negative	Negative
24	Glycerol	Negative	Negative
25	Salicin	Negative	Negative

26	Dulcitol	Negative	Negative
27	Inositol	Negative	Negative
28	Arabitol	Negative	Negative
29	Erythritol	Negative	Negative
30	Alpha- methyl-glucoside	Negative	Negative
31	Rhamnose	Negative	Negative
32	Cellobiose	Negative	Negative
33	Melezitose	Negative	Negative
34	Alpha-Methyl-D-Mannoside	Negative	Negative
35	Xylitol	Negative	Negative
36	ONPG	Negative	Positive
37	Esculin hydrolysis	Positive	Positive
38	D Arabinose	Negative	Positive
39	Malonate Utilization	Negative	Negative
40	Sorbose	Negative	Negative
41	Lysine Utilization	Negative	Negative
42	Ornithine Utilization	Negative	Negative
43	Urease	Positive	Positive
44	Phenylalanine deamination	Negative	Negative
45	Nitrate Reduction	Negative	Negative
46	H ₂ S production	Positive	Positive
47	Catalase	Positive	Positive

4.5.3 Molecular characteristics of the rhizobacterial isolates

The molecular characterization of the rhizospheric bacterial isolate was conducted by using the 16S rRNA gene primers by sequencing of the 16S rRNA region of the bacterial DNA.

4.5.3.1 Isolation and spectral analysis of bacterial genomic DNA

The genomic DNA extracted from the rhizospheric bacterial isolates AG1B and AG2B was evaluated using agarose gel electrophoresis within a 0.8% agarose gel matrix. The presence of intact bands within the gel substantiated the successful isolation of genomic

DNA possessing sound structural integrity; devoid of any RNA impurities (Fig. 4.17 A). Assessing the quality of DNA is very important while engaging in molecular studies.

4.5.3.2 Spectral analysis of genomic DNA (Nanodrop reading)

The quantification and purity analysis of DNA samples were executed using the NanoDrop-1000 spectrophotometer, relying on absorbance readings at 260 nm for DNA concentration determination and 280 nm for assessing protein contamination. The 260/280 ratio of DNA sample of AG1B and AG2B are 1.85 and 1.89 respectively, indicating the presence of pure and high-quality DNA, with a concentration of 1225 ng/ μ l and 1254 ng/ μ l respectively.

4.5.3.3 PCR amplification of the genomic DNA

PCR amplification was done by using the 16S rRNA specific primers. Following PCR, the product was visualized on a 1.2% agarose gel that showed approximately 1500 bp PCR product (Fig. 4.17 B) indicating positive amplification of 16S rRNA gene.

4.5.3.4 16S rRNA gene sequencing and phylogenetic analysis

The polymerase chain reaction (PCR) amplification of 16S rRNA gene yielded fragments of approximately 1500 bp in length. Subsequently, the PCR product underwent sequencing using an ABI 377 automated DNA Sequencer (Applied Biosystems, USA). The obtained sequence was aligned using the Clustal W algorithm within MEGA X and the sequence's homology was scrutinized through nucleotide BLAST (nBLAST) analysis on the NCBI platform to identify potential matches. The BLAST outcomes for the bacterial isolate AG1B and AG2B indicated a homology range of 90-99% with entries available in the NCBI database.

The phylogenetic tree was constructed for the 16S rRNA gene. The isolate AG1B and AG2B was clustered with the reference Bacillaceae family and were closely related to *Bacillus amyloliquefaciens* and *Bacillus subtilis* respectively with 70% and 78% bootstrap confidence (Fig. 4.17 C). The consensus sequence of the isolated sample generated using BioEdit (v7.2) software was submitted to the National Center for Biotechnology Information (NCBI) database that identified the bacterial isolates as *Bacillus amyloliquefaciens* AG1B and *Bacillus subtilis* AG2B with the specific accession number designated as OR186676 and OR186677 respectively.

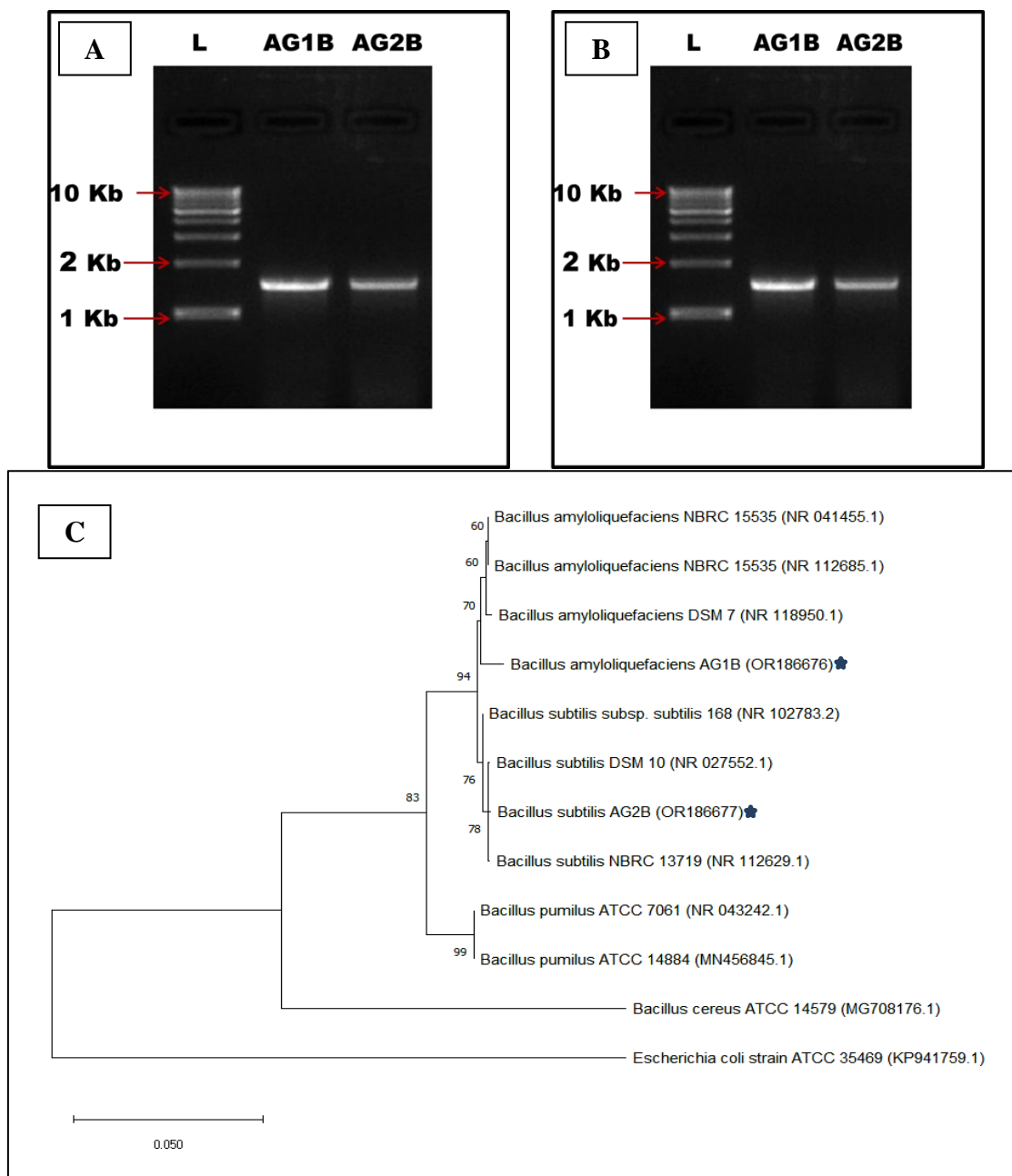


Fig. 4.17. PCR amplification of target 16s rRNA gene of the bacterial isolates detected on agarose gel and the phylogenetic tree. (A) Genomic DNA isolated from each of the bacterial isolates, AG1B and AG2B; (B) PCR amplified 16s rRNA genomic region with size ~1.5Kb detected using 1 Kb DNA ladder (Himedia, India); (C) The phylogenetic relationship between the each of the bacterial isolates AG1B & AG2B (denoted with *) and the type strains of the related species is shown by employing maximum likelihood tree-based method using Tamura Nei model on the 16S rRNA gene. Branch node count represents the bootstrap percentage obtained from 1000 bootstrap replications. The reference sequences were retrieved from GenBank database and accession numbers are given within brackets.

4.5.4 Screening of the plant growth promoting traits of the bacterial isolates

The two rhizobacterial isolates *Bacillus amyloliquefaciens* AG1B and *Bacillus subtilis* AG2B along with the endophytic bacterium, *Bacillus subtilis* Scb-1 were studied for their plant growth promoting traits.

4.5.4.1 Indole-3-Acetic acid (IAA) production

All the three bacterial isolate, *B. amyloliquefaciens* AG1B, *B. subtilis* AG2B and *B. subtilis* Scb-1 are able to produce IAA and the concentration of IAA was found to be 152.56 ± 0.87 $\mu\text{g/ml}$, 97.89 ± 0.52 $\mu\text{g/ml}$ and 58.64 ± 0.87 $\mu\text{g/ml}$ respectively. Idris *et al.* (2007) reported that *B. amyloliquefaciens* FZB42 harbours genes for IAA production. Mutation of the genes decreases the plant growth potential of the bacterium.

4.5.4.2 Phosphate Solubilization.

B. amyloliquefaciens AG1B, *B. subtilis* AG2B and *B. subtilis* Scb-1 exhibited mild phosphate solubilization efficiency as very minimal halo zone as shown in the Fig.4.18A. Ghosh *et al.*, (2016) studied the phosphate-solubilizing *Burkholderia* strains (*B. tropica* P4 and *B. uname* P9), that colonize in the rhizoids of *Lycopodium*. You *et al.*, (2020) isolated *Burkholderia cenocepacia* CR318 and elucidated its role in enhancing corn growth through the solubilization of inorganic tricalcium phosphate and potassium. Furthermore, Tian *et al.* (2021) explored the potential of phosphate-solubilizing microbes for mitigating soil phosphorus deficiency and therefore can be an environmentally sustainable alternative to conventional chemical fertilizers, promoting both greener agricultural practices and enhanced yield efficiency.

4.5.4.3 Zinc Solubilization

B. subtilis Scb-1 showed the highest zinc solubilization followed by *B. subtilis* AG2B and *B. amyloliquefaciens* AG1B (Fig.4.18B). Zinc holds a crucial function in the synthesis of chlorophyll. Rhizobacteria with the capability to solubilize zinc oxide, zinc phosphate and zinc carbonate have been documented in prior studies (Saravanan *et al.*, 2007).

4.5.4.4 Potassium Solubilization

None of the bacterial isolates showed could solubilize potassium. In response to the constraints posed by chemical fertilizers, potassium solubilizing microorganisms

(KSM) are being employed in commercial applications as biofertilizers and inoculants (Sattar *et al.*, 2019).

4.5.4.5 Sulphur Solubilization

All the three bacterial isolates, *B. amyloliquefaciens* AG1B, *B. subtilis* AG2B and *B. subtilis* Scb-1 showed yellow halo zone formation confirming that it could solubilize the thio-sulphate present in the medium (Fig.4.18 C). Sulfur, existing in the sulfate form, stands as a fundamental nutrient imperative for plant growth. Bacteria possessing the capacity to convert reduced sulfur compounds into sulfate play a crucial role in facilitating sulfur nutrition for plants (Rani *et al.*, 2023).

4.5.4.6 Siderophore production

Siderophore activity has been shown by all three bacterial isolates, *B. amyloliquefaciens* AG1B, *B. subtilis* AG2B and *B. subtilis* Scb-1 (Fig.4.18D). Siderophore production by microorganisms has garnered significant attention for its diverse applications across agricultural disciplines, including soil science, environmental sciences, and plant pathology. Siderophores are organic compounds characterized by their low molecular weight (< 10 kDa) and high specific affinity for iron chelation (Oswald, 2010). Bacteria produce siderophores falling into four distinct groups: catecholates, hydroxamates, salicylates, and carboxylates (Rajkumar *et al.*, 2010). These compounds play a pivotal role in the sequestration of iron from various organic sources. Prominent genera of siderophore-producing bacteria encompass *Rhizobium*, *Arthrobacter*, *Azospirillum*, *Pseudomonas*, *Azotobacter*, *Bacillus*, *Acinetobacter*, *Alcaligenes*, *Beijerinckia*, *Burkholderia*, and *Enterobacter* (Ghazy and Nahrawy, 2021; Sinha and Parli 2020; El-Nahrawy *et al.*, 2019; Bashan *et al.*, 2014; Grobelak and Hiller 2017; Ghavami *et al.*, 2016).

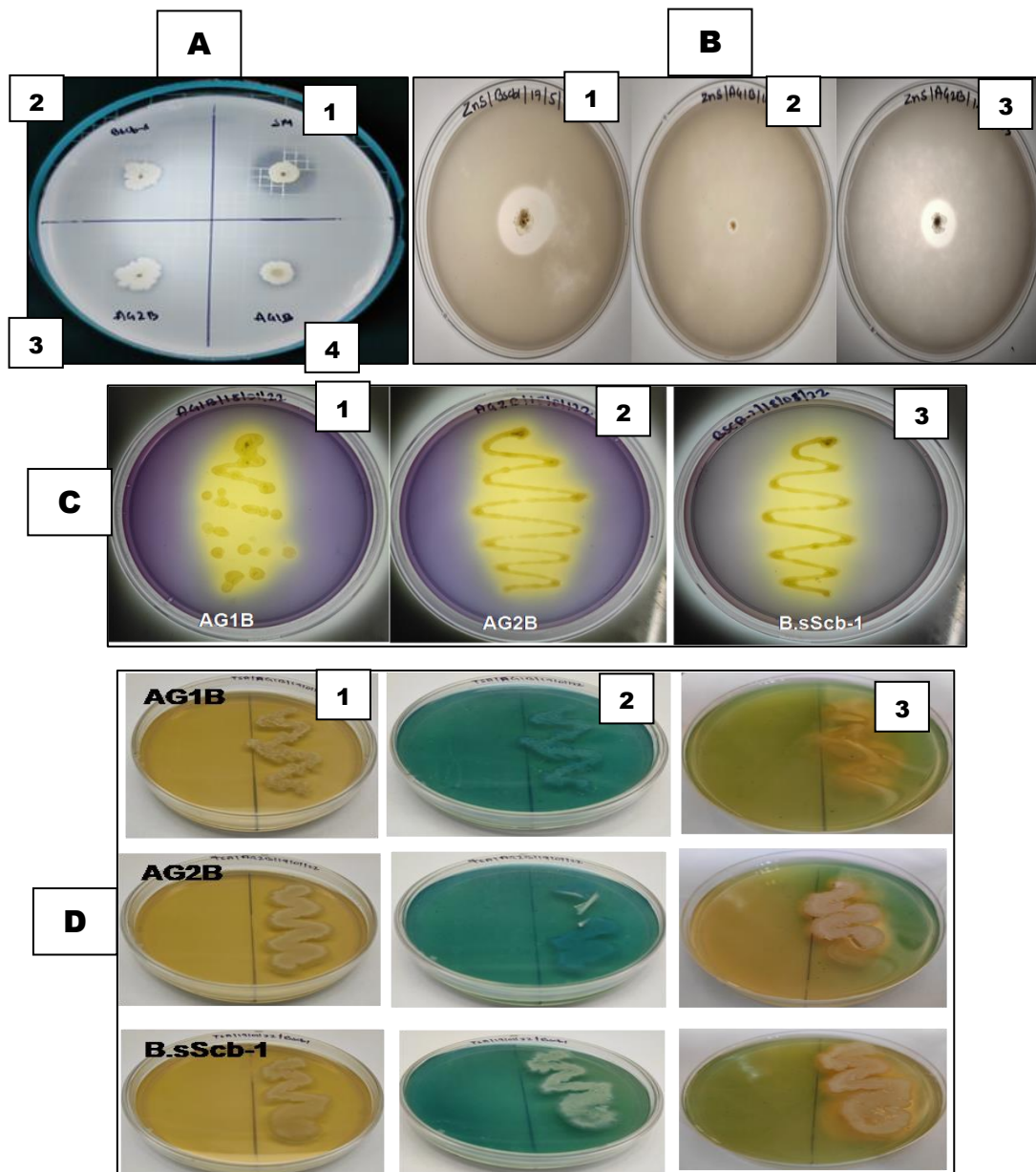


Fig. 4.18. Plant growth promoting traits of the bacterial isolates. (A) Bacterial isolates - *B. subtilis* Scb-1 (2), AG1B (3), AG2B (4) showing the solubilization of phosphates. *Serratia marcescens* D1 (1) was taken as a positive control; (B) Zinc solubilizing efficiency of the bacterial isolates *B. s* Scb-1 (1), AG1B (2) and AG2B (3); (C) Sulphur solubilizing efficiency of the bacterial isolates AG1B (1), AG2B (2), and *B. s* Scb-1 (3); (D) Siderophore production by the bacterial isolates AG1B, AG2B, and *B. subtilis* Scb-1. (1) Represents the growth of the individual bacterial isolates on Tryptic Soya Agar; (2) Addition of CAS Agar. The CAS/HDTMA complexes exhibit a strong affinity for ferric iron, resulting in the formation of a blue color complex.; (3) However, when a potent iron chelator like a siderophore extracts iron from the dye complex, the color undergoes a transition from blue to orange-yellow. All the experiments were repeated thrice.

4.6 Comparative analysis of SOD activity of the interacting microbial partners during monoculture and dual culture condition

The investigation revealed a significant increase in the activity of superoxide dismutase (SOD) during the dual culture scenario involving *A. brassicicola* AG1F in conjunction with each of *B. subtilis* Scb-1, *B. amyloliquefaciens* AG1B, and *B. subtilis* AG2B, as opposed to their individual monoculture conditions (Fig. 4.19). This observation strongly suggests an increased generation of reactive oxygen species (ROS) as an outcome of the interactions between these bacterial and fungal entities. Superoxide dismutase (SOD) is an enzyme that plays a pivotal role in detoxifying superoxide radicals (*O_2^-), a type of ROS, by converting them into less harmful hydrogen peroxide (H_2O_2) and molecular oxygen (O_2). Elevated SOD activity in the dual culture condition points to an escalated rate of superoxide radical generation, which is likely a result of the intricate interplay between the bacteria and the fungus. This study clearly showed the increase in SOD activity in the dual culture condition with the increase in incubation time. This also indicates the increase in ROS generation with time. Dullah *et al.* (2021) has also reported similar increase in SOD activity during fungal- fungal interaction. Hassett *et al.*, (1995) reported that FeSOD is the key enzyme maintaining the oxidative stress in *Pseudomonas aeruginosa*.

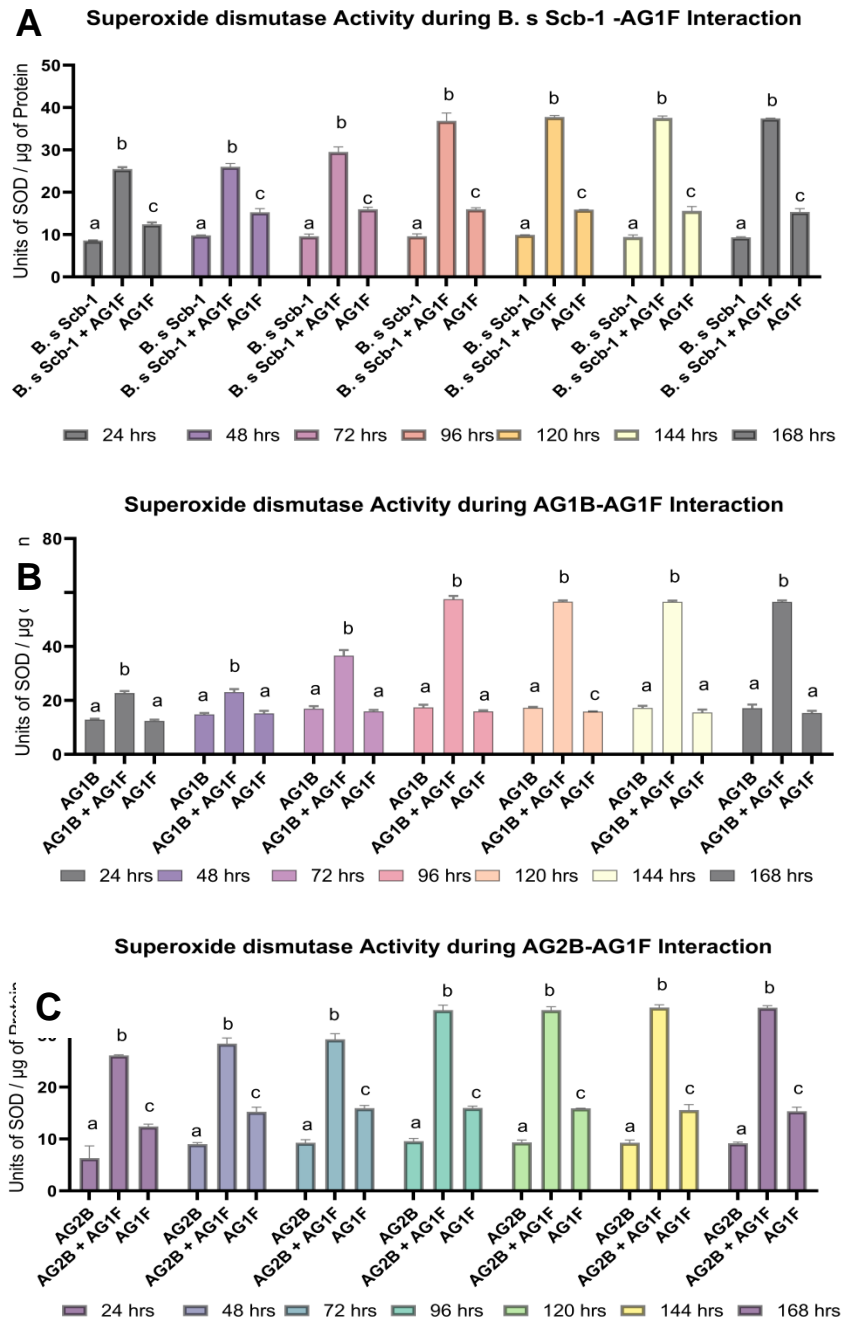


Fig. 4.19. Comparative profile of the Superoxide Dismutase Activity. (A) SOD activity during the antagonistic interaction between *Bacillus subtilis* Scb-1 and *Alternaria brassicicola* AG1F and their respective monoculture condition; (B) SOD activity during the antagonistic interaction between *B. amyloliquefaciens* AG1B and *A. brassicicola* AG1F and their respective monoculture condition; (C) SOD activity during the antagonistic interaction between *B. subtilis* AG2B and *A. brassicicola* AG1F and their respective monoculture condition. (Level of significance with $p \leq 0.05$).

4.7 Differential expression analysis of key fungal genes during antagonist bacterial and pathogenic fungal interactions

Quantitative Real time PCR (qRT-PCR) analysis of five fungal genes important for maintaining pathogenicity and cellular homeostasis was performed during the dual culture of each of *Bacillus subtilis* Scb-1, *B. amyloliquefaciens* AG1B and *B. subtilis* AG2B with *Alternaria brassicicola* AG1F in different time intervals (24 hrs and 72 hrs of dual-culture condition). The genes used in this study viz., AbSte7, Amk1 (regulates the gene expression of hydrolytic enzyme in fungi for plant cell invasion), Amk2, Hog1 and MAP kinase gene related to the pathogenicity of the fungus and maintaining cell wall integrity; and AbPf2 gene encode a transcription factor which is also related to the pathogenicity of the fungi, *Alternaria brassicicola*. It can be clearly seen from the Fig. 4.20 (A, B and C) that there is a transcriptional up-regulation of all the genes during 24 hrs of dual culture condition. However, gene related to the pathogenicity of the fungi, *Alternaria brassicicola* AG1F gets significantly down regulated after 72 hrs of dual culture condition. This might be due to the compounding effect of bacterial antifungal compounds secreted during the exponential phase of bacterial growth. Interestingly the gene related to maintain cellular integrity, Amk2 and Hog1 showed significant up-regulation. The probable reason could be for the defense against bacterial metabolites that targets cell membrane damaged. The microscopic observation in this study also showed deformities in hypha and conidia membrane in the dual culture condition. On contrary, in the interacting between *B. subtilis* Scb-1 and *A. brassicicola* AG12F, the expression of Hog1 gene showed more than 10 fold up-regulations during the 24 hrs incubation. Whereas, the expression becomes low when incubated for the 72 hrs. Previous studies have also showed that the mutation in genes related to the pathogenicity and cell wall integrity of *A. Brassicicola* decreases its pathogenicity and the fungus became sensitive to phytoalexins (Joubert *et al.*, 2010, Cho *et al.*, 2013, Xu *et al.*, 2013, Lu *et al.*, 2019).

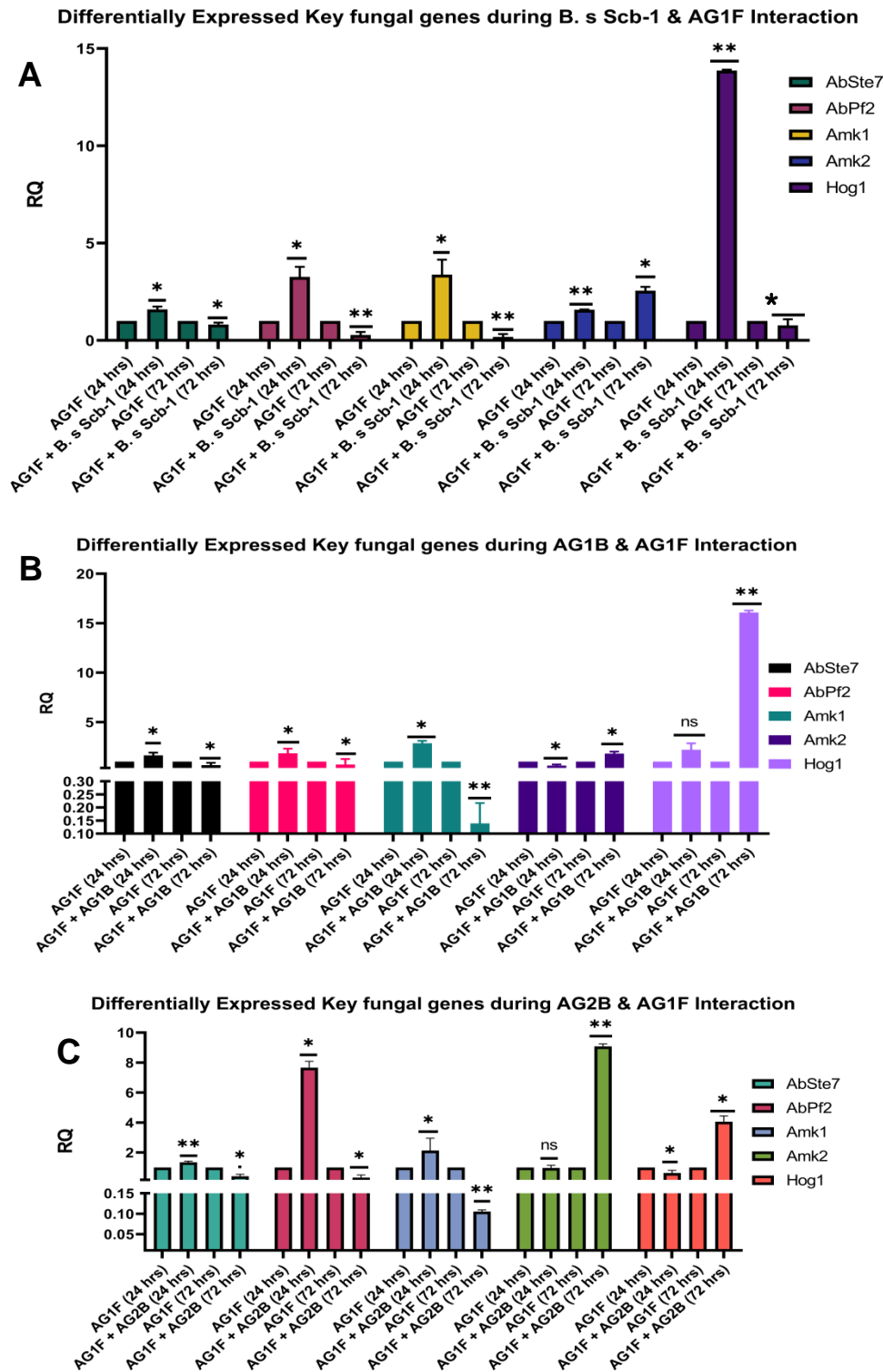


Fig. 4.20. Differential expression of key fungal genes during the interaction between each of (A) *Bacillus subtilis* Scb-1, (B) *B. amyloliquefaciens* AG1B and (C) *B. subtilis* AG2B with *A. brassicicola* AG1F in different time intervals. (l 95 of significance with $p \leq 0.05$ is denoted with * and $p \leq 0.001$ is denoted with **).

4.8 Metabolite profiling during *in vitro* antagonist bacterial and pathogenic fungal interactions

To study into the bacterial secondary metabolites with antifungal properties each of the bacterial isolates *Bacillus subtilis* Scb-1, *B. amyloliquefaciens* AG1B and *B. subtilis* AG2B was allowed to interact with *Alternaria brassicicola* AG1F for 72 hrs. Followed by sample collections, metabolite extractions, LC-MS analysis and data interpretation.

Interestingly, in each of the dual culture plates multiple fractions of surfactin (C13 to C16) have been identified with molecular weight ranging from 1008.8 to 1050.1 g/mol respectively. Along with surfactin, other lipopeptides like iturin D (1049.9 g/mol) was also detected in the samples. All these compounds have been previously reported in many studies with potential antifungal effect. The result from the LC-MS study is validating the membrane damage (lipopeptide mediated) of the fungi and these metabolites might have a role in the regulation of important fungal genes for pathogenicity and cell wall integrity. Compounds identified from the LC-MS in all the conditions with antifungal property have been listed below in Table 4.2.

4.9 Thin Layer Chromatography (TLC) of the crude bacterial metabolite extracts

The methanol extracts of each of the bacterial cell free extracts were subjected to TLC characterization using chloroform: methanol: water-39:15:3 (v/v) as the mobile phase. After the solvent front reached a certain height, the TLC plate was carefully air dried and sprayed with water that reflects the lipopeptide fronts in the TLC plate. The retention factor (R_f) value was calculated. The R_f of all the fractions belonging to the respective sample as shown in Fig. 4.21 ranges from 0.90 to 0.92.

Meena *et al.* (2021) has also reported the similar R_f value using standards of iturin, surfactin and purified surfactin isolated from *Bacillus velezensis* KLP2016 using the same mobile phase.

Therefore, the results obtained from the LC-MS study was further validated by TLC characterization.

Table 4.3 List of bacterial secondary metabolites having antifungal property detected in this study by using LC-ESI-MS

Compound Name	Adduct Ions	Relative intensity	Predicted Mol. Wt. (g/mol)
Surfactin, C14	M+ H, M+Na	100	1022.8
Macrolactin A	M+H	100	403.3
Suractin C15	M+ H, M+K	100	1036.8
Suractin C13	M -1	100	1008.8
Suractin C16	M-1	100	1050.1
Iturin A	M+H, M+2H, M+NH ₄	100	1043.9

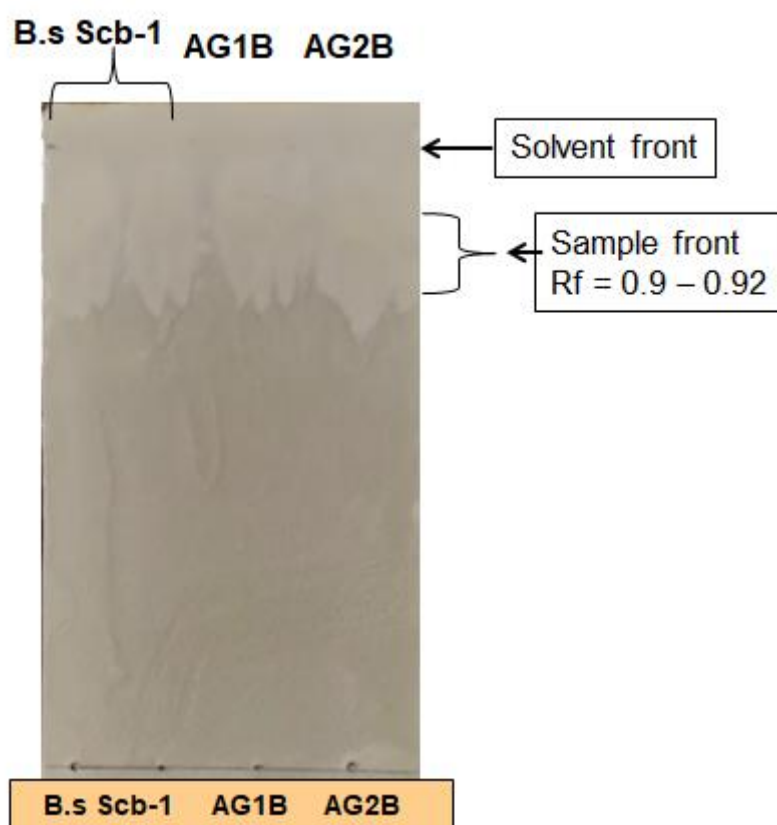


Fig. 4.21. TLC confirmation of the bacterial lipopeptide.

4.10 Whole genome sequencing and *de novo* assembly of *Bacillus amyloliquefaciens* AG1B

The whole genome sequencing of the potential bacterial isolate AG1B showing percentage inhibition of 76.47 % against the fungal pathogen, *Alternaria brassicicola* AG1F was done, and *de novo* assembly of the genome was performed. This showed the genome of 3,894,346 bp in size (Fig. 4.22) with 38 scaffolds, of which the largest scaffold is 1,118,293 bp in size and N50 value of 9,92,324 bp with identity of 99.3% having 1295X depth coverage. The gene ontology and functional annotation of the genome resulted in 3716 CDS. 4 rRNA and 80 tRNA regions (Fig. 4.23 and 4.24). The important gene for plant growth promotion and the secondary metabolite gene was predicted using AntiSMASH and showed in the Table. 4.4.

Table 4.4 List of important genes conferring to plant growth promoting and antifungal compound production

Genes	Associated Functions
trpB, trpA, trpC	IAA synthesis
moaA, moaB	Nitrogen utilization
corA_1, corA_2, mgtE	Magnesium Utilization
pstA, pstB, pstS	Phosphate solubilisation
epsF2, epsO, epsN, epsM, epsL, epsK, epsD	Exopolysaccharide production
dhbC, dhbF	Siderophore synthesis
srfAB, srf AA, srfAC	Surfactin synthesis
fenF	Fengycin synthesis
baeB, baeC, baeD, baeE_2, acpl, pksG_1	Bacillaene and other polyketide synthesis
Itu_A	Iturin synthesis
bacD	Bacillomycin D synthesis
tmrB	Tunicamycin resistant protein (Confirms its rhizobacterial nature)
yuaD, yuaF	Putative metal-sulfur cluster biosynthesis (Confirms its rhizobacterial nature)

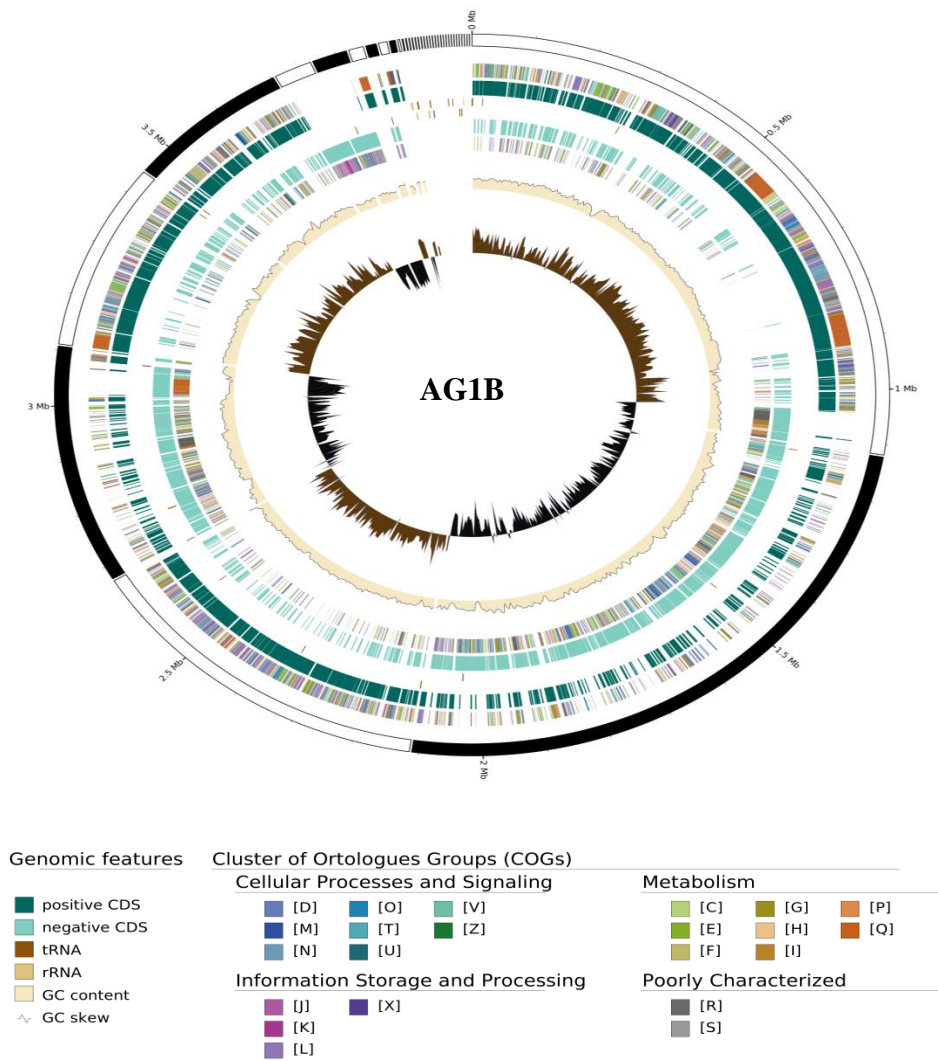
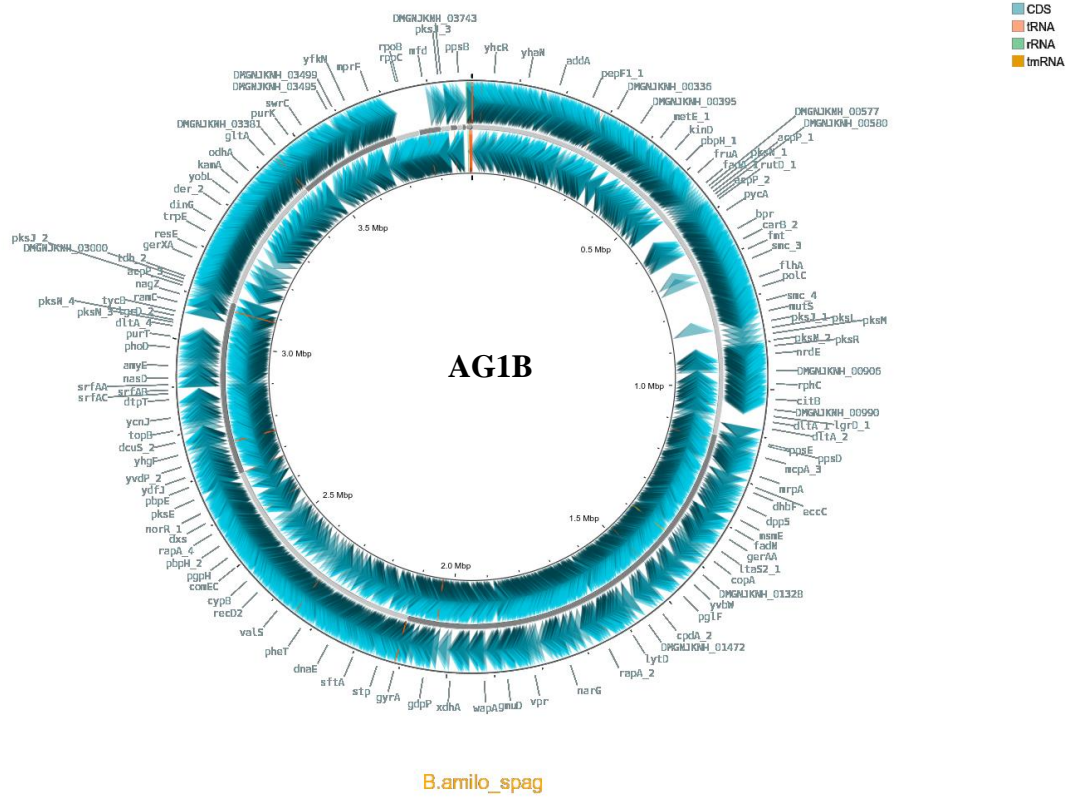


Fig. 4.22. Circular map of the *de novo* assembled whole genome of AG1B



Index	No
Total Base	3894346
CDS	3716
rRNA	4
tRNA	80

Fig. 4.23. Gene ontology study of the genome of AG1B

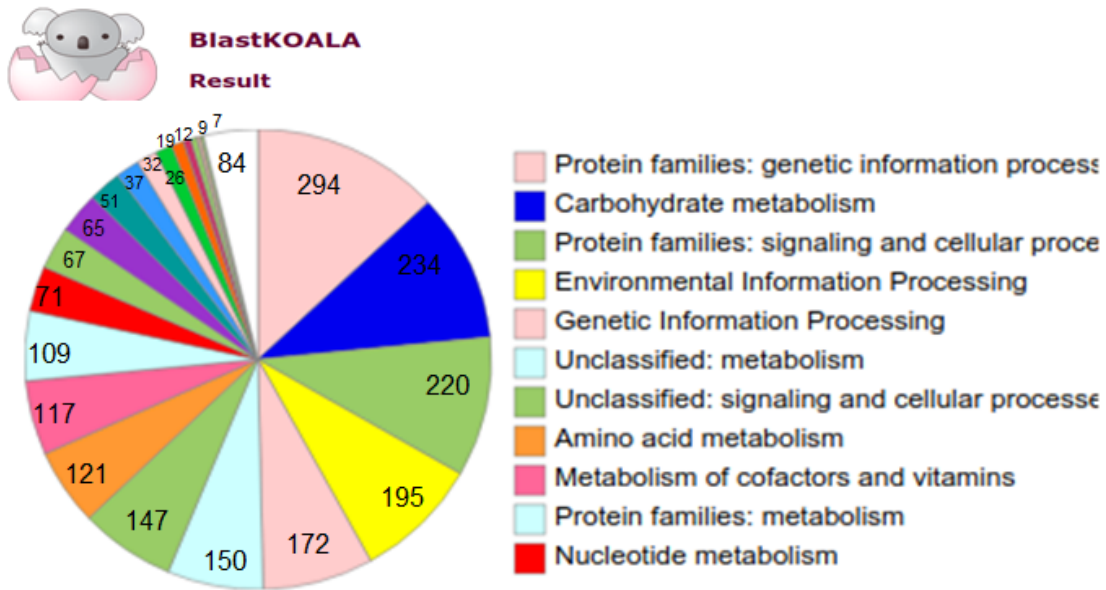
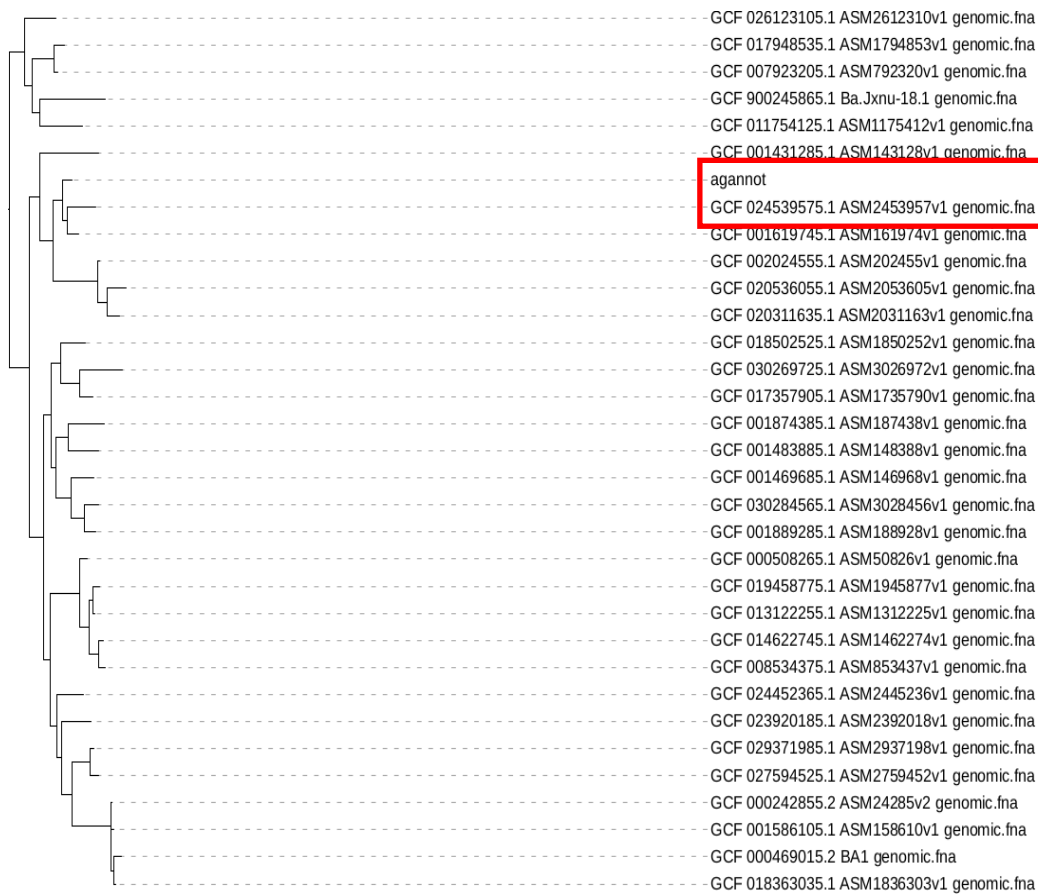


Fig. 4.24. Genes associated with the pathway using KEGG

The pan genome phylogeny has been prepared across all the available draft assembly of the different strains of this bacterium using Roary. The average nucleotide identity has been performed with the closest strain using the FastANI tool. The annotated genome matched with *Bacillus amyloliquefaciens* BA11 and showed 99.45 % ANI score.



FastANI Results

Successfully queried every assembly. Results are sorted by ANI Match, with the highest match at the bottom.

Note: No ANI output is reported for a genome pair if the ANI value is much below 80%. See the documentation for more information.

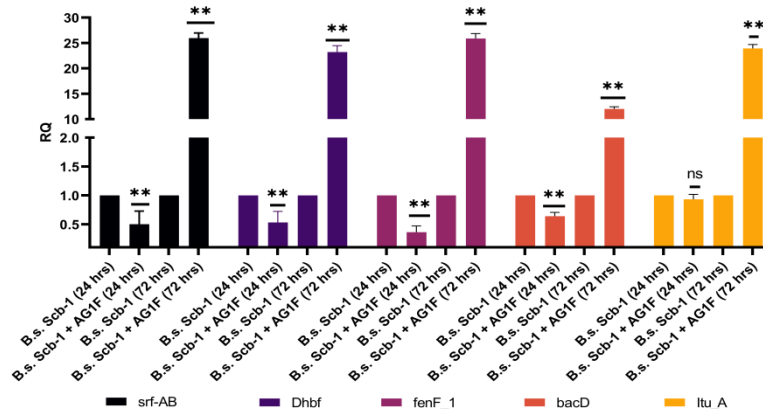
QUERY	REFERENCE	ANI ESTIMATE	MATCHES	TOTAL	VISUALIZATION
assembly	ref	99.4533	1266	1287	PDF

Fig. 4.25. Pan Genome phylogeny showing the Average Nucleotide Identity score of 99.4533

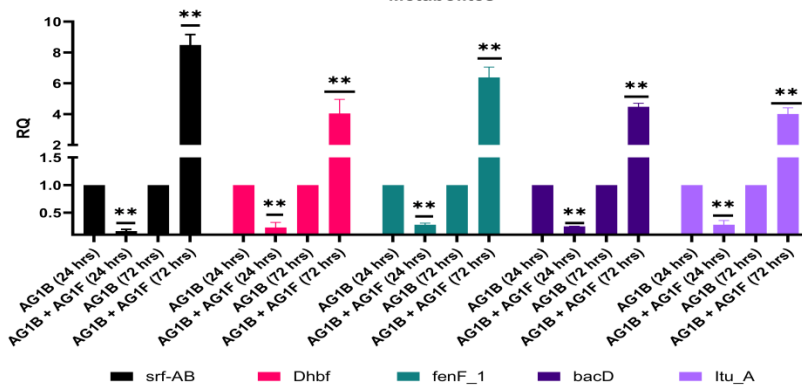
4.11 Differential expression analysis of genes involved in the biosynthesis of bacterial secondary metabolites in the monoculture and interacted dual culture conditions in different time intervals

Quantitative Real time PCR (qRT-PCR) analysis of five genes involved in the biosynthesis of bacterial secondary metabolites was performed during the dual culture of each of *Bacillus subtilis* Scb-1, *B. amyloliquefaciens* AG1B and *B. subtilis* AG2B with *Alternaria brassicicola* AG1F in different time intervals (24 hrs and 72 hrs of dual-culture condition). The genes used in this study viz., SrfAB (involved in surfactin biosynthesis); dhbF (siderophore synthesis); fenF (fengycin synthesis), bacD (bacillomycin synthesis); and ItuA (iturin synthesis). All are related to the production of antifungal metabolites. It can be clearly seen from the Fig. 4.26 (A, B and C) that there is a transcriptional down-regulation of all the genes during 24 hrs of dual culture condition. However, all five genes in all the dual culture condition significantly up regulated after 72 hrs of dual culture condition. As the bacterial secondary metabolite synthesis starts in the exponential phase of bacterial growth so there is a significant down- regulation of the secondary metabolites biosynthesis genes. While, during 72 hrs of incubation the bacteria reach the exponential phase and thus we have seen transcriptional; up-regulation of all the gene during the antagonistic bacterial fungal interaction. The results of the qRT-PCR analysis further confirm the LC-MS based metabolite prediction. Moreover it can be concluded that due to involvement of these antifungal metabolite synthesis genes, each of the bacteria are able to show antagonism against the pathogenic fungi.

Differentially Expressed Genes Involved in the Biosynthesis of Key Bacterial Secondary Metabolites



Differentially Expressed Genes Involved in the Biosynthesis of Key Bacterial Secondary Metabolites



Differentially Expressed Genes Involved in the Biosynthesis of Key Bacterial Secondary Metabolites

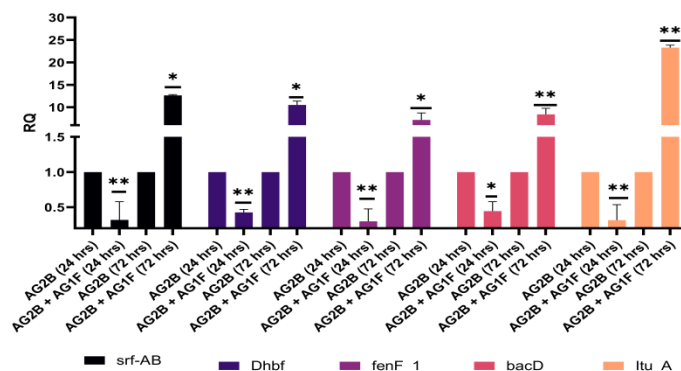


Fig. 4.26. Differential expression of key genes involved in the biosynthesis of bacterial secondary metabolites during the interaction between each of (A) *Bacillus subtilis* Scb-1, (B) *B. amyloliquefaciens* AG1B and (C) *B. subtilis* AG2B with *Alternaria brassicicola* AG1F in different time intervals. (Level of significance with $p \leq 0.05$ is denoted with * and $p \leq 0.001$ is denoted with **).

4.12 Evaluation of the plant growth promoting efficacy of *Bacillus subtilis* Scb-1, *Bacillus amyloliquefaciens* AG1B, and *Bacillus subtilis* AG2B

All the three bacterial isolates, *B. subtilis* Scb-1, *B. amyloliquefaciens* AG1B, and *B. subtilis* AG2B were found to have plant growth promoting traits. Therefore, these isolates were used to evaluate their plant growth promotion ability in pot culture experiments.

4.12.1 Effect of bacterial priming on seed germination after 7 days

The seeds of cabbage and rapeseed were collected and by following the procedure as described in section 3.14.1 seeds were bio-primed. Bio-primed seeds of cabbage and rapeseed showed better germination percentage as compared to the control with increased shoot and root length.

Seeds of cabbage were procured from Sungro Seed Company, and they have listed that the average germination percentage of the cabbage (Savitri) seed to be 70%. Interestingly, the bio-primed seeds showed an increase in germination percentage of 80% whereas the un-primed seed remained around 70% (Fig.4.27 A). The result of this experiment positively correlates with the IAA production capacity and bio-control activity of each of the bacterial isolates. The practice of seed bio-priming has gained significant interest due to its capability to stimulate seed germination and offer initial support for seedling growth, particularly in challenging environmental conditions. Seeds of carrots showed better germination and growth when bio-primed with potential bacterial isolates (Fidoro *et al.*, 2023).

Similarly, seeds of rapeseed (TS-67) also showed increased germination percentage and increased root and shoot length (Fig. 4.27 B) as compared with the un-primed seeds as mock.

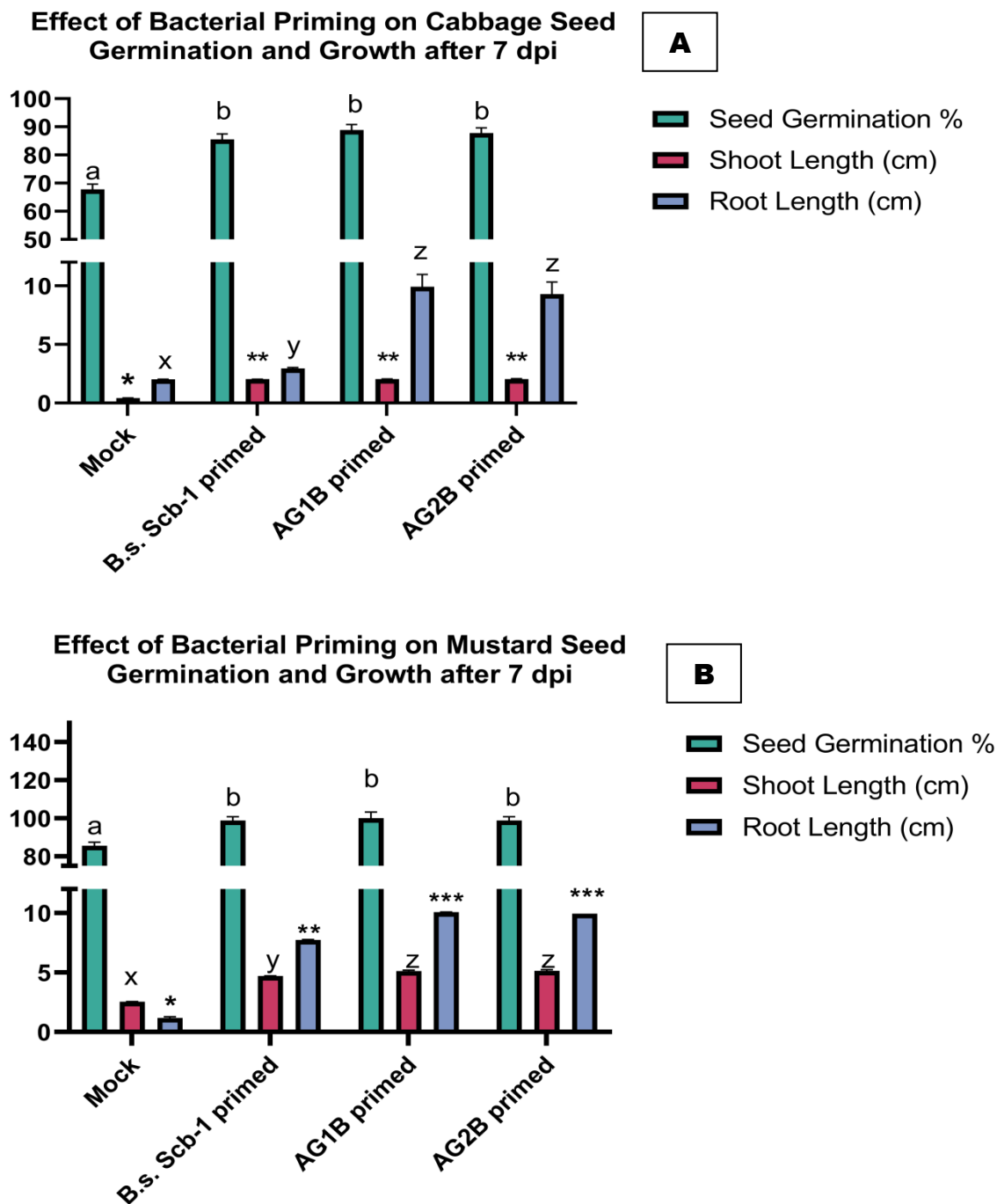


Fig. 4.27. Bio-priming increased the germination percentage, root and shoot length of cabbage (A) and rapeseed (B). The values represent the cumulative of results of three independent biological replications with three technical replications. (Statistical significance was calculated using SPSS 25.0 software by one-way Analysis of Variance (ANOVA). Duncan multiple range test was performed to study the level of significance among the treatments ($p \leq 0.05$).

4.12.2 Effect of bacterial priming on cabbage after 30 days

The bio-primed seeds of cabbage after germination was carefully transplanted to soil for pot culture experiments. The unprimed plants were divided into two groups and one group was kept at mock and the other group was treated with commercial fungicide.

The bacterial treated plant showed significant plant growth promotion (Fig. 4.28). The bio-primed plants showed an increase in shoot and root length as compared with the unprimed mock plant. Similarly, the number of leaves has also increased in the bio-primed plants that have also increases the leaf area index (Fig. 4.29).

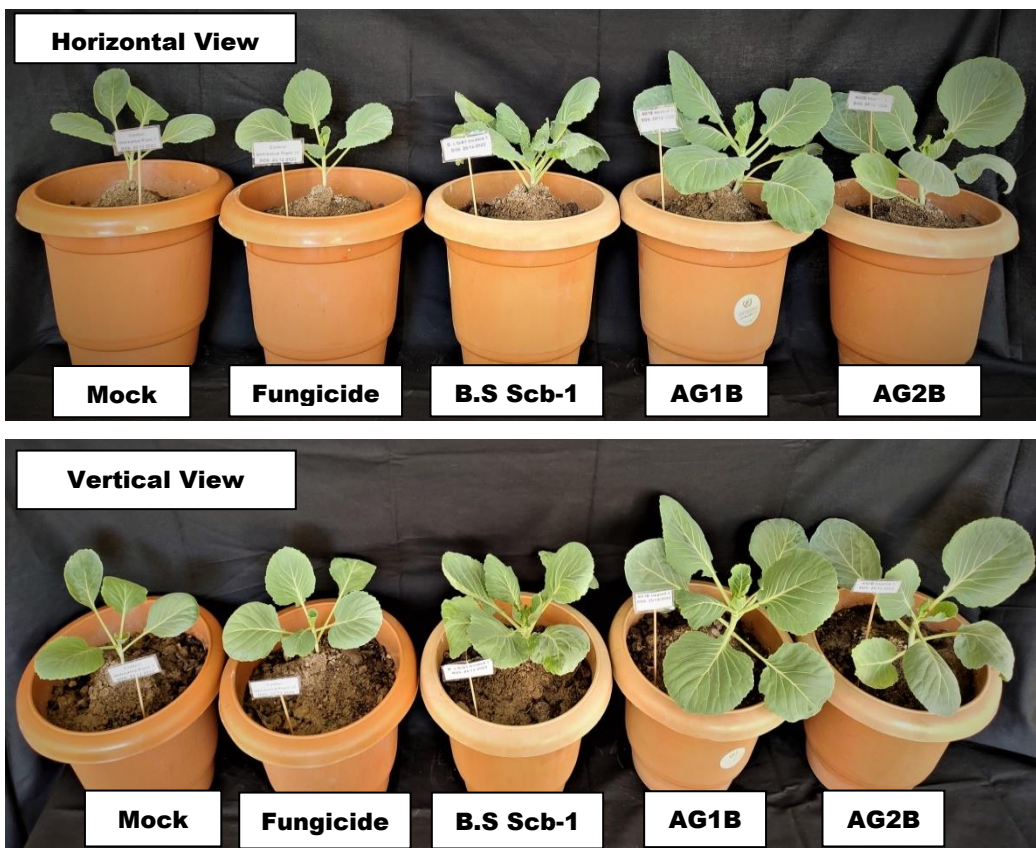


Fig. 4.28. Bacterial Priming enhances the growth of cabbage

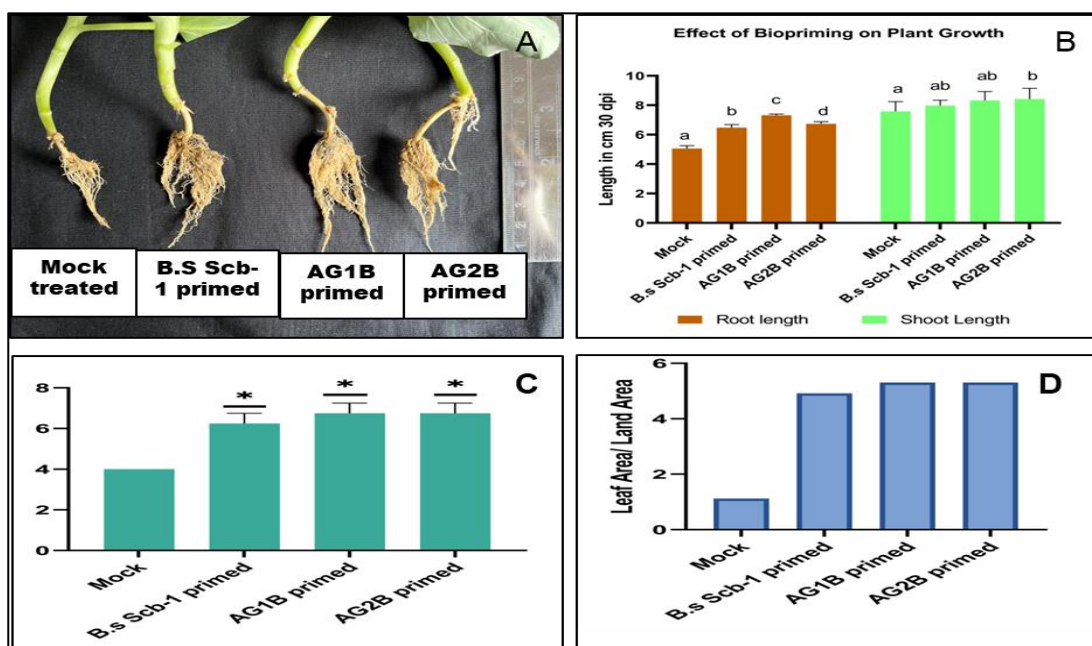


Fig. 4.29. Bacterial priming enhances the root length (A- Representative Image of the increased root length), shoot length (B), leaf count (C) and leaf area index (D). (Statistical significance was calculated using SPSS 25.0 software by one-way Analysis of Variance (ANOVA). Duncan multiple range test was performed to study the level of significance among the treatments ($p \leq 0.05$)

4.12.2 Elucidating the biocontrol efficiency of each of *Bacillus subtilis* Scb-1, *Bacillus amyloliquefaciens* AG1B and *Bacillus subtilis* AG2B against *Alternaria brassicicola* AG1F in cabbage

4.12.2.1 Impact of Foliar Application of Bio-inoculants on Disease Suppression in Cabbage

A foliar application with each of the *Bacillus subtilis* Scb-1 (B.s Scb-1 treated), *Bacillus amyloliquefaciens* AG1B (AG1B treated), and *Bacillus subtilis* AG2B (AG2B treated) was done on a 45 days old bio-primed cabbage plant. The mock was sprayed with distilled water and divided into two groups. One is for absolute control (Mock) and the other is for positive control of disease development (Fungi Infected, FI) and the other control group was treated with fungicide (Fungicide treated). Following this, all the plants were sprayed with the spore suspensions of *Alternaria brassicicola* AG1F. The results were recorded after seven days of post inoculation with the fungi. This showed that the foliar application of the bio-inoculum efficiently reduces the disease severity index as compared to that of the fungi infected plant. Moreover, there was less number of lesion count and size (Table 4.5 and Fig. 4.30).

Table 4.5 Outcome of the foliar application of the bio-inoculum on disease management

Sample	No. of leaves with lesion	No. of lesion/ leaf	Lesion Diameter	Disease Severity Index
Mock inoculated	0	0	0	0
Fungi Infected (FI)	6	4.33	1.67	93.33
Fungicide treated	2	1.33	0.2	13.33
B. s Scb-1 treated + FI	1	1	0.2	6.67
AG1B treated + FI	1	1	0.2	10.00
AG2B treated + FI	1	1.33	0.2	13.33

4.12.2.2 Comparison of the necrosis level

Trypan blue staining of the leaf collected from each of the treatments was done to visualize the level of necrosis. This showed that the pathogen can only cause necrosis in the untreated plant leaf. The rest of the leaf treated with bio-inoculum has no visible necrosis (Fig. 4.31).

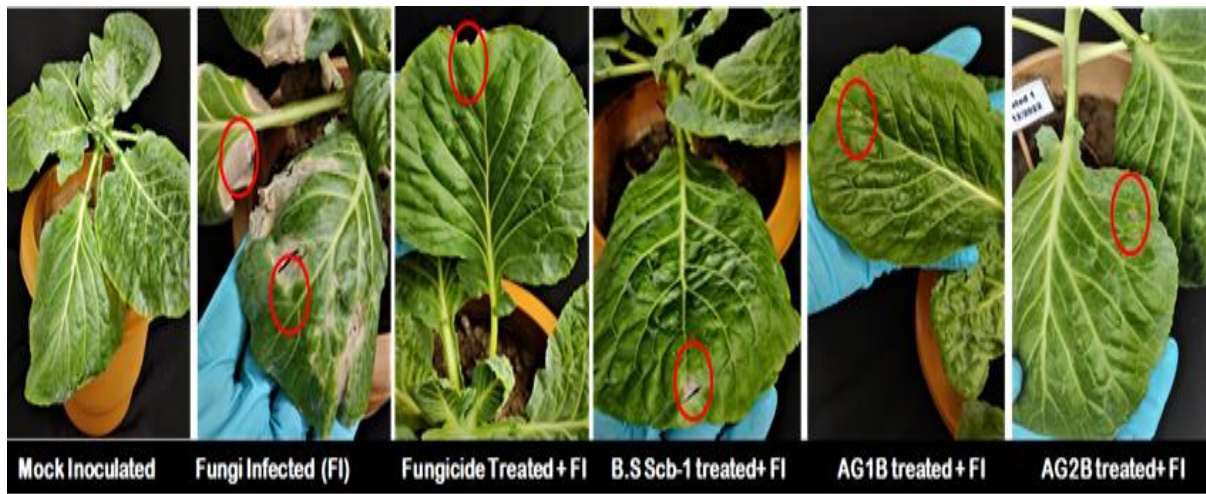


Fig. 4.30 Phenotypic observation of the effect of foliar application of bio-inoculums on disease management

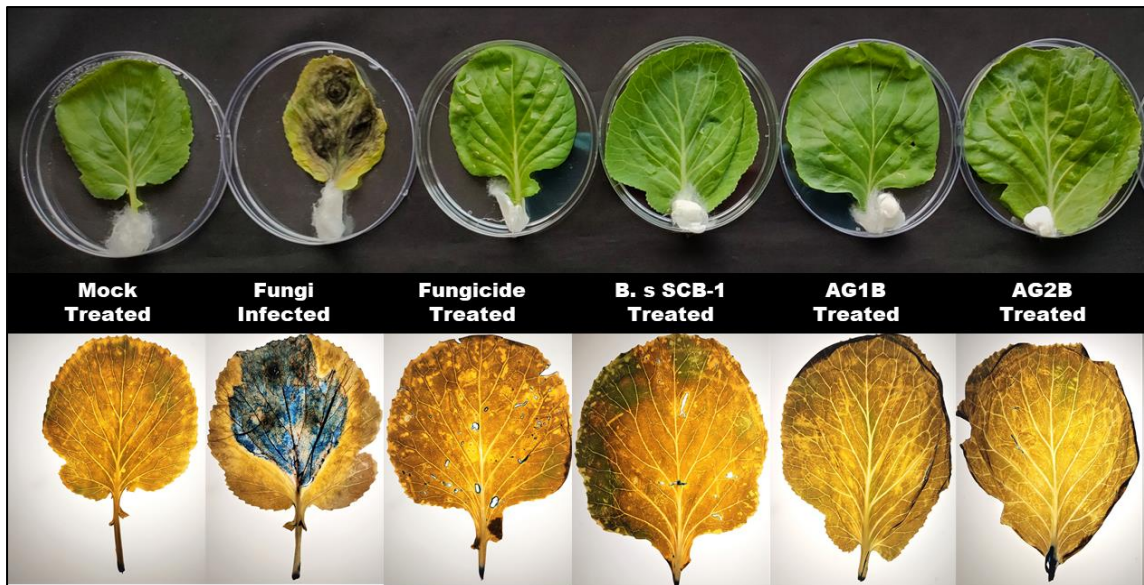


Fig. 4.31. Trypan blue staining of the leaf showing the level of necrosis;

Mock- is the absolute control with no fungal or bacterial inoculation; Fungi treated – the positive control for disease incidence inoculated with the fungal spore of *Alternaria brassicicola* AG1F; Fungicide treated – the fungicide treated plant inoculated with fungal spore of *Alternaria brassicicola* AG1F; B.s Scb-1 treated – *B. subtilis* Scb-1 treated plant inoculated with fungal spore suspensions of *Alternaria brassicicola* AG1F; AG1B treated – *B. amyloliquefaciens* AG1B treated plant inoculated with fungal spore suspensions of *Alternaria brassicicola* AG1F; AG2B treated – *B. subtilis* AG2B treated plant inoculated with fungal spore suspensions of *Alternaria brassicicola* AG1F

4.12.2.3 Analysis of the physiological and biochemical changes during biotic stress alleviation

During stress, plant alters its physiological and biochemical properties. Therefore, study of these physiological and biochemical changes are very crucial during the tripartite interaction between the beneficial bacteria, the pathogenic fungi and the host plant. All the analysis was done from the leaf sample collected after 7 days post infection.

4.12.2.3.1 Total chlorophyll estimation.

One of the most important outcomes of infection with necrotropic fungal pathogen like *Alternaria brassicicola* is the damage of the chloroplast system and the decrease in total chlorophyll level (Macioszek *et al.*, 2020). The results of the total chlorophyll content in this study clearly showed the positive impact of bio-priming and foliar application of the bacterial cultures prior to the fungal infection. The total chlorophyll content of cabbage leaf treated with each of the bacterial isolates (*Bacillus subtilis* Scb-1, *Bacillus amyloliquefaciens* AG1B, and *Bacillus subtilis* AG2B) prior to infection with *Alternaria brassicicola* AG1F was found to be almost similar with the absolute control leaf sample (Mock). Whereas, the chlorophyll content in the fungi infected gets significantly reduced (Fig. 4.32 A).

4.12.2.3.2 Relative leaf water content.

The relative leaf water content of cabbage leaf treated with each of the bacterial isolates (*Bacillus subtilis* Scb-1, *Bacillus amyloliquefaciens* AG1B and *Bacillus subtilis* AG2B) prior to infection with *Alternaria brassicicola* AG1F was found to be significantly higher than that of the fungi infected leaf sample (Fig. 4.32 B).

4.12.2.3.3 Electrolyte leakage indexing (ELI%)

The ELI % of the fungi infected leaf sample was found to be the highest (33.33%) but in the bacterial treated samples ELI % was found to be very minimum, same as that of the absolute control sample. This suggested that in the fungi infected leaf sample the fungi might have secreted cell wall degrading enzymes or any toxins, having potential to damage in the host cell membrane that counts for the high electrolyte leakage. There is very less electrolyte leaking in the bacterial treated leaf samples suggesting their potential bio-control efficacy (Fig. 4.32 C).

4.12.2.3.4 Total proline content

Proline is an osmolyte and a stress marker molecule. High proline content corresponds to the stress condition. Therefore, in the fungi infected sample the content of the proline was found to be maximum (0.56 µg/mg F.W of the sample) then that of all the

bacterial treated samples and the mock suggesting that the bacterial treated plants exhibited no biotic stress (Fig. 4.32 D).

4.12.2.3.5 Total phenol content

The total phenol content in the bacterial treated samples was found to be higher than that of the fungi infected sample. This might be due to the bacterial mediated defense of the host plant (Fig. 4.32 E).

4.12.2.3.6 Superoxide dismutase activity

SOD is the key enzyme to detoxify the effects of ROS and other free radicles. The SOD activity of the fungi infected leaf sample was found to be higher than that of the bacterial treated plant and the mock. This suggested that there is higher ROS generation in the fungi infected leaf samples (Fig. 4.32 F).

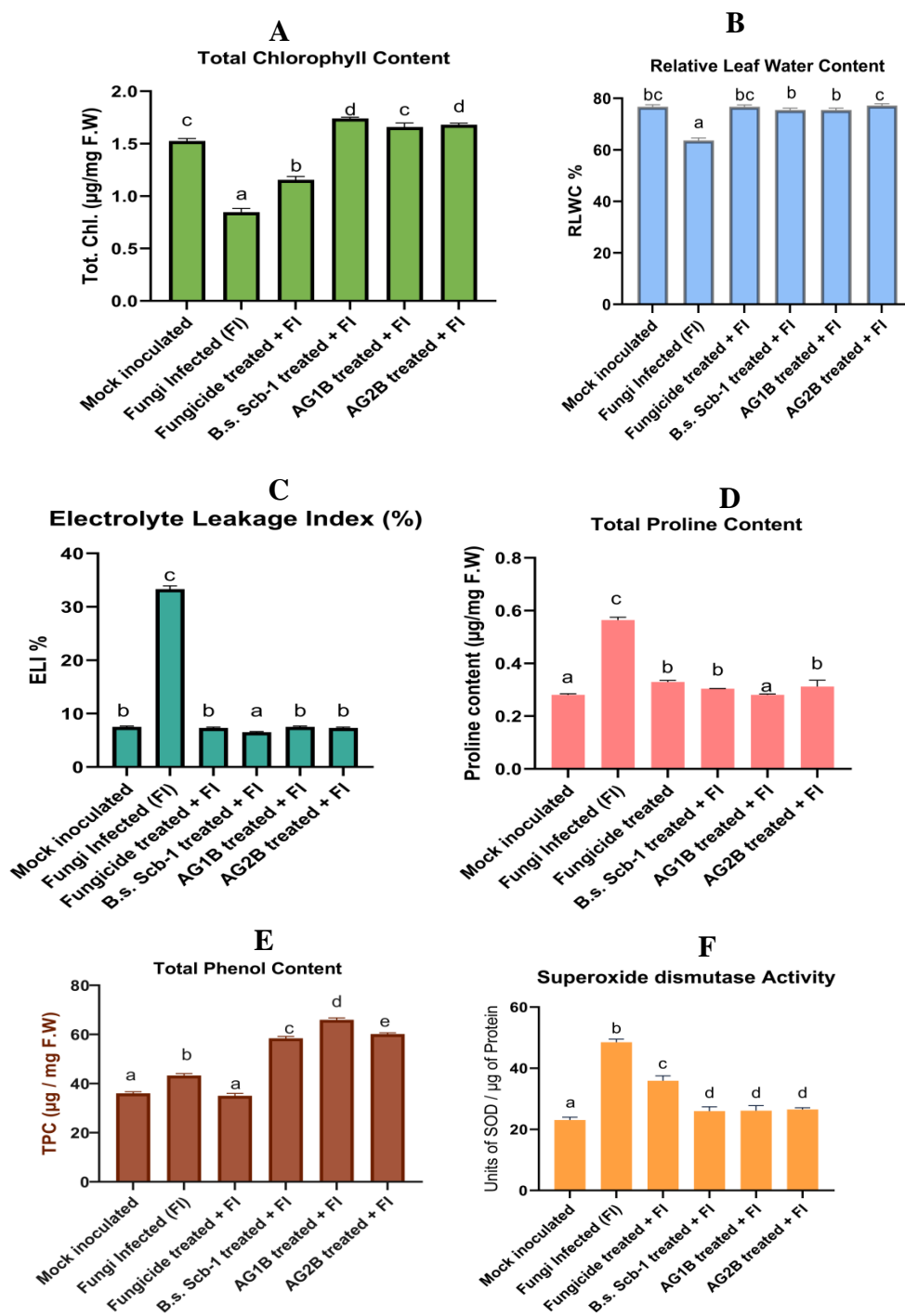


Fig. 4.32 Physiological and biochemical changes during biotic stress alleviation.(A) Total chlorophyll content;(B) Relative leaf water content; (C) Electrolyte leakage indexing; (D) Total proline content; (E) Total phenol content; (F) SOD activity

CHAPTER V

SUMMARY AND CONCLUSION

This study aimed to investigate the rhizospheric bacteria associated with the roots of healthy cabbage plants and assess their role in promoting plant growth and suppressing diseases. A total of twenty-two bacterial isolates were obtained from the rhizospheric soil of healthy cabbage plants and screened for their antagonistic interactions against a necrotrophic fungal pathogen isolated from diseased cabbage leaves. Among these isolates, two showed antagonistic activity against the plant pathogenic fungi in an *in vitro* dual culture assay. Morphological, biochemical and molecular characterizations were performed on the rhizo-bacterial isolates. The fungal pathogen was also characterized based on its morphological and molecular properties. Microscopic analysis revealed deformities and membrane damage in the fungal hyphae during the dual culture condition. Metabolite profiling conducted during the dual culture using LC-MS indicated the production of bacterial secreted lipopeptides and polyketide compounds, which may have caused the observed membrane damage in the fungi. Key secondary metabolite biosynthesis genes exhibited significant up-regulation in the dual culture condition, corroborating the results of metabolite profiling. Conversely, down-regulation of essential fungal MAP kinase genes, responsible for maintaining pathogenesis and homeostasis, was observed during the dual culture. Furthermore, bacterial primed rapeseeds and cabbage seeds exhibited improved germination indices, and the resulting plantlets demonstrated significant growth enhancement. Foliar application of the bacterial isolates effectively reduced fungal disease incidence, confirming their potential for biocontrol. The key outcomes of the current investigation are outlined as follows:

1. Cabbage leaves exhibiting disease symptoms and rhizospheric soil from healthy cabbage plants were collected from various locations within the Jorhat district of Assam.
2. A necrotrophic fungal pathogen was isolated from the affected cabbage leaf and subsequently identified as *Alternaria brassicicola* AG1F through morphological and molecular characterization.
3. Twenty-two bacterial cultures were isolated from soil samples of the rhizosphere, and their potential for antagonistic interaction against the fungal pathogen *A. brassicicola* AG1F was assessed.

4. Among the twenty-two bacterial isolates, only two, designated as AG1B and AG2B, exhibited antagonistic interaction. Additionally, a previously isolated endophyte identified as *Bacillus subtilis* Scb-1 also demonstrated similar antagonistic interaction against the fungus *A. brassicicola* AG1F.
5. The bacterial isolates with antagonistic properties, AG1B and AG2B, were characterized based on their morphological, biochemical and molecular attributes, leading to their identification as *Bacillus amyloliquefaciens* AG1B and *Bacillus subtilis* AG2B, respectively.
6. Among the three bacterial isolates, *B. amyloliquefaciens* AG1B exhibited highest inhibitory effect, with a percentage inhibition of 76.47%, against the pathogenic fungi *A. brassicicola* AG1F followed by *B. subtilis* AG2B and *B. subtilis* Scb-1 with an inhibition percentage of 70.59%.
7. The cell-free supernatant derived from the bacterial isolates exerted inhibitory effects on fungal growth. The metabolites present in these cell-free extracts displayed resilience to heat. Additionally, the volatile organic compounds (VOCs) released by the bacterial isolates exhibited substantial reductions in fungal growth.
8. The bacterial isolates *B. amyloliquefaciens* AG1B, *B. subtilis* AG2B and *B. subtilis* Scb-1 exhibited significant antagonistic activity against several other plant pathogenic fungal isolates, including *Alternaria brassicae* 2542, *A. brassicicola* 8344, *A. eichhorniae* AG2F and *Fusarium oxysporum*.
9. Light microscopic and scanning electron microscopic examinations unveiled distinctive alterations in the hyphae of *A. brassicicola* AG1F during co-cultivation with *B. amyloliquefaciens* AG1B, *B. subtilis* AG2B and *B. subtilis* Scb-1. These changes included anomalous deformation, irregular swelling, and the development of protoplast balls within the hyphal structure. Moreover, the conidia of *A. brassicicola* AG1F exhibited surface irregularities such as wrinkling, pore-like formations, or bubble-like structures.
10. Elevated superoxide dismutase (SOD) activity was observed in the dual culture condition of *A. brassicicola* AG1F with each of *B. amyloliquefaciens* AG1B, *B. subtilis* AG2B and *B. subtilis* Scb-1, in comparison to their respective monoculture conditions. This observation implies increased production of reactive oxygen species (ROS) during the bacterial-fungal interactions.
11. Metabolite profiling carried out through LC-ESI-MS during the dual culture experiment revealed the synthesis of anti-fungal compounds, specifically surfactin

and iturin. Additionally, the examination of gene expression through qRT-PCR indicated an increase in the transcription of genes responsible for the synthesis of bacterial lipopeptides when the bacteria were co-cultured with the pathogenic fungi.

12. Furthermore, the qRT-PCR analysis revealed significant reduction in the expression of pivotal fungal genes linked to pathogenic traits, alongside an increase in the expression of genes related to maintaining cellular homeostasis, in the context of the dual culture environment. These findings collectively indicate the inhibitory impact of bacterial secondary metabolites on the pathogenicity of the fungi, *A. brassicicola* AG1F.
13. All the three bacterial isolates, *B. amyloliquefaciens* AG1B, *B. subtilis* AG2B, and *B. subtilis* Scb-1 showed plant growth promoting traits. These traits encompassed the synthesis of indole-3-acetic acid (IAA), the ability to solubilize phosphate, sulfur, and zinc, as well as the production of siderophores.
14. Whole genome sequencing and *de novo* assembly of the potential bacterial isolate, *B. amyloliquefaciens* AG1B revealed a genome size of 3.89 Mbp. Functional assessment of this genome unveiled the presence of genetic elements associated with plant growth promotion, synthesis of antifungal compound and genes confirming its affiliation to rhizospheric soil.
15. *B. amyloliquefaciens* AG1B, *B. subtilis* AG2B and *B. subtilis* Scb-1 primed seeds of cabbage and mustard showed increase in the germination percentage, shoot and root length.
16. Cabbage plants subjected to bio-priming exhibited improved agronomic attributes, including enhanced shoot and root lengths, increased leaf count and a higher leaf area index.
17. The application of each of the bio-inoculum (*B. amyloliquefaciens* AG1B, *B. subtilis* AG2B and *B. subtilis* Scb-1) via foliar spray method resulted in a reduction in both the count and dimensions of lesions on cabbage plants when exposed to spore suspensions of *A. brassicicola* AG1F. This approach effectively demonstrated disease management capabilities of the bacterial isolates.
18. Following the foliar application of each of the bio-inoculum (*B. amyloliquefaciens* AG1B, *B. subtilis* AG2B and *B. subtilis* Scb-1) and exposure to spore suspensions of *A. brassicicola* AG1F, an assessment of physiological and biochemical

parameters in cabbage plants provided an additional validation for the disease management effectiveness of the bio-inoculum.

In summary, this study's notable findings encompass the characterization of rhizospheric bacteria and their antagonistic effects against fungal pathogens, elucidation of the underlying mechanisms involving metabolite production and gene expression and validation of their positive impacts on plant growth and disease management (Fig. 5.1). While several transcriptomics studies have highlighted differential gene expression patterns in the host plant and the pathogenic fungi, very less research has been documented concerning on the expression profiles of bacterial secondary metabolite genes in the context of dual culture conditions. This study has the potential to uncover distinct gene expression profiles associated with the production of secondary metabolites possessing antifungal attributes within bacteria during the dual culture experiment. Moreover, there is a need to undertake the purification and comprehensive characterization of various lipopeptides extracted from the bacterial culture supernatants. This step is essential to assess their effectiveness against a diverse spectrum of fungal pathogens. Furthermore, the process of enhancing the expression of pivotal genes involved in bacterial secondary metabolite synthesis holds potential for large-scale production of these metabolites for commercial applications. Subsequently, conducting field trials using the identified bacterial isolates becomes imperative to validate and confirm their efficacy under field conditions. Collectively, this study has introduced a sustainable alternative to conventional pesticides and fertilizers, offering an eco-friendlier method to enhance plant vitality and fitness.

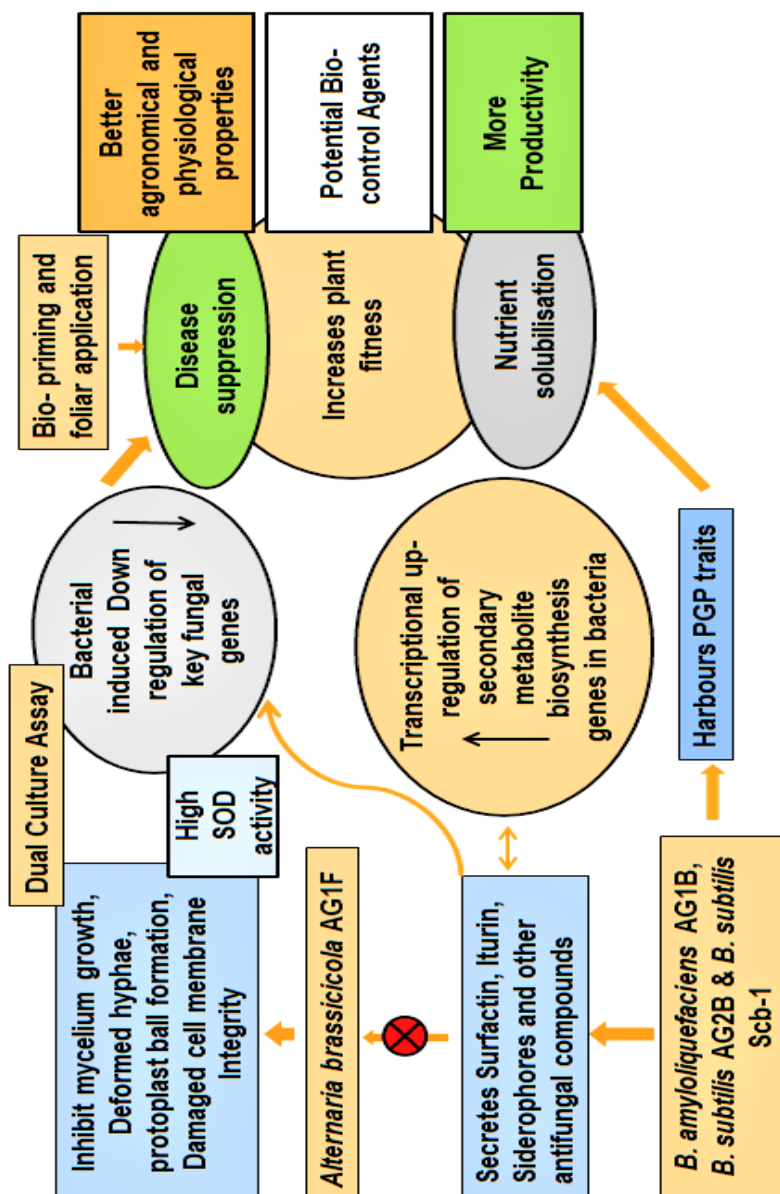


Fig. 5.1. Overall summary of this research work

BIBLIOGRAPHY

- Adhikary, A.; Saini, R.; Kumar, R.; Singh, I.; Ramakrishna, W. and Kumar, S. (2022). *Pseudomonas citronellolis* alleviates arsenic toxicity and maintains cellular homeostasis in chickpea (*Cicerarietinum* L.). *Plant Physiol. Biochem.*, **184**, 26-39.
- Ahlfen, S.V. and Schlumpberger, M. (2010). Effects of low A260/A230 ratios in RNA preparations on downstream applications. *QIAGEN Gene Expression Newsletter*. **15**: 6-7.
- Al-Ani, R.A.; Adhab, M.A.; Mahdi, M.H. and Abood, H.M. (2012). *Rhizobium japonicum* as a biocontrol agent of soybean root rot disease caused by *Fusarium solani* and *Macrophomina phaseolina*. *Plant Prot Sci.*, **48**:149-155.
- Ali, S.; Hameed, S.; Imran, A.; Iqbal, M. and Lazarovits, G. (2014). Genetic, physiological and biochemical characterization of *Bacillus* sp. strain RMB7 exhibiting plant growth promoting and broad spectrum antifungal activities. *Microb. Cell Factories*, **13**: 1-15.
- Andersen, E.J.; Ali, S.; Byamukama, E.; Yen, Y. and Nepal, M.P. (2018). Disease resistance mechanisms in plants. *Genes*, **9**(7): 339.
- Ashajyothia, M.; Kumara, A.; Sheorana, N.; Ganesana, P.; Gogoia, R.; Subbaiyanb, G.K. and Bhattacharya, R. (2020). Black pepper (*Piper nigrum* L.) associated endophytic *Pseudomonas putida* BP25 alters root phenotype and induces defense in rice (*Oryza sativa* L.) against blast disease incited by *Magnaporthe oryzae*. *Biol Control*. **143**:104181.
- Awad, H.; Khamis, M. M. and El-Aneed, A. (2015). Mass spectrometry, review of the basics: ionization. *Appl. Spectrosc. Rev.*, **50**(2): 158-175.
- Azmir, J.; Zaidul, I.S.M.; Rahman, M.M.; Sharif, K.M.; Mohamed, A.; Sahena, F.; Jahurul, M.H.A.; Ghafoor, K.; Norulaini, N.A.N. and Omar, A.K.M. (2013). Techniques for extraction of bioactive compounds from plant materials: A review. *J. Food Eng.*, **117**(4): 426-436.
- Azuddin, N.F.; Mohd, M.H.; Rosely, N.F.N.; Mansor, A. and Zakaria, L. (2021). Molecular Phylogeny of Endophytic Fungi from Rattan (*Calamus castaneus* Griff.) Spines and Their Antagonistic Activities against Plant Pathogenic Fungi. *J. Fungus.*, **7**(4): 301.
- Azwanida, N.N. (2015). A Review on the Extraction Methods Use in Medicinal Plants, Principle, Strength and Limitation. *Med.Aromat. Plants*, **4**(3): 3-8.
- Baard, V.; Bakare, O.O.; Daniel, A.I.; Nkomo, M.; Gokul, A.; Keyster, M. and Klein, A. (2023). Biocontrol potential of *Bacillus subtilis* and *Bacillus tequilensis* against four *Fusarium* sp. *Pathogens*, **12**(2): 254.

- Bai, Z.H.; Zhou, C.G.; Cao, J.X.; Xu, S.J.; Wu, S.H. and D.S. Li. (2014) Effects of *Bacillus amyloliquefaciens* biofertilizer on tea yield and quality *Agr. Sci. Tech.*, **15** (11): 1883-1887.
- Ball, A.; Ashby, A.; Daniels, M.; Ingram, D. and Johnstone, K. (1991). Evidence for the requirement of extracellular protease in the pathogenic interaction of *Pyrenopeziza brassicae* with oilseed rape. *Physiol. Mol. Plant Pathol.* **38**:147-161.
- Barnett, S.J.; Roget, D.K. and Ryder, M.H. (2006). Suppression of *Rhizoctonia solani* AG-8 induced disease on wheat by the interaction between *Pantoea*, *Exiguobacterium* and *Microbacteria*. *Soil Res.*, **44**:331-342.
- Bashan, Y.; De-Bashan, L.E.; Prabhu, S.R. and Hernandez, J.P. (2014). Advances in plant growth-promoting bacterial inoculant technology: formulations and practical perspectives (1998-2013) (a marschner review). *Plant Soil*. **378**:1-33.
- Bauer, J. and Gareis, M. (1987). Ochratoxin A in the food chain. *J. Vet. Med. B.*, **34**(1-10): 613-627.
- Begerow, D.; Nilsson, H.; Unterseher, M. and Maier, W. (2010). Current state and perspectives of fungal DNA barcoding and rapid identification procedures. *Appl. Microbiol. Biotechnol.*, **87**(1): 99-108.
- Bellemain, E.; Carlsen, T.; Brochmann, C.; Coissac, E.; Taberlet, P. and Kauserud, H. (2010). ITS as an environmental DNA barcode for fungi: an *in silico* approach reveals potential PCR biases. *BMC Microbiol.*, **10**(1): 1-9.
- Bessai, S.A.; Bensidhoum, L. and Nabti, E.H. (2022). Optimization of IAA production by telluric bacteria isolated from northern Algeria. *Biocatal. Agric. Biotechnol.*, **41**: 102319.
- Buszewski, B.; Rogowska, A.; Pomastowski, P.; Złoch, M. and Railean-Plugaru, V. (2017). Identification of Microorganisms by Modern Analytical Techniques. *J. AOAC Int.*, **100**(6): 1607-1623.
- Byrne, B.A. (2014). Laboratory Diagnosis of Fungal Diseases. In *Equine Infectious Diseases: Second Edition*. Elsevier Inc.
- Cazorla, F.M.; Romero, D.; Pérez-García, A.; Lugtenberg, B.J.J.; Vicente, A.D. and Bloemberg, G. (2007). Isolation and characterization of antagonistic *Bacillus subtilis* strains from the avocado rhizosphere displaying biocontrol activity *J. Appl. Microbiol.*, **103**(5): 1950-1959.
- Chandel, S.; Allan, E.J. and Woodward, S. (2010). Biological control of *Fusarium oxysporum* sp. *lycopersici* on tomato by *Brevibacillus brevis*. *J. Phytopathol.* **158**:470-478.
- Chaudhary, S.; Dhanker, R. and Goyal, S. (2017). Characterization and optimization of culture conditions for sulphur oxidizing bacteria after isolation from rhizospheric mustard soil, decomposing sites and pit house. *Int. J. Agric. Biol. Eng.*, **11**(6): 427-431.

- Chauhan, S.; Wadhwa, K.; Vasudeva, M. and Narula, N. (2012). Potential of *Azotobacter* spp. as biocontrol agents against *Rhizoctonia solani* and *Fusarium oxysporum* in cotton (*Gossypium hirsutum*), guar (*Cyamopsis tetragonoloba*) and tomato (*Lycopersicon esculentum*). *Arch Agron Soil Sci.* **58**:1365-1385.
- Chen, C.H.; Ferreira, J.C.B.; Gross, E.R. and Mochly-Rosen, D. (2014). Targeting aldehyde dehydrogenase 2: new therapeutic opportunities. *Physiol. Rev.*, **94**(1): 1-34.
- Chen, X.H.; Koumoutsis, A.; Scholz, R.; Eisenreich, A.; Schneider, K.; Heinemeyer, I. and Borriss, R. (2007). Comparative analysis of the complete genome sequence of the plant growth-promoting bacterium *Bacillus amyloliquefaciens* FZB42. *Nat. Biotechnol.*, **25**(9): 1007-1014.
- Chen, Y.P.; Rekha, P.D.; Arun, A.B.; Shen, F.T.; Lai, W.A. and Young, C.C. (2006). Phosphate solubilizing bacteria from subtropical soil and their tricalcium phosphate solubilizing abilities. *Appl. Soil Ecol.*, **34**(1): 33-41.
- Cheng, X.; Ji, X.; Li, J.; Qi, W.; Ge, Y. and Qiao, K. (2019). Characterization of antagonistic *Bacillus methylotrophicus* isolated from rhizosphere and its biocontrol effects on maize stalk rot. *Phyto. Pathology.* **109**:571-581.
- Cho, Y. (2015). How the necrotrophic fungus *Alternaria brassicicola* kills plant cells remains an enigma. *Eukaryot. Cell*, **14**(4): 335-344.
- Cho, Y.; Cramer, R.A.; Jr, Kim, K.H.; Davis, J.; Mitchell, T.K.; Figuli, P.; Pryor, B.M.; Lemasters, E. and Lawrence, C.B. (2007) The Fus3/Kss1 MAP kinase homolog Amk1 regulates the expression of genes encoding hydrolytic enzymes in *Alternaria brassicicola*. *Fungal Genet. Biol.*, **44**: 543-553.
- Cho, Y.; Kim, K.H.; La Rota, M.; Scott, D.; Santopietro, G.; Callihan, M. and Lawrence, C.B. (2009). Identification of virulence factors by high throughput targeted gene deletion of regulatory genes in *Alternaria brassicicola*. *Mol. Microbiol.* **72**: 1316-1333.
- Cho, Y.; Ohm, R.A.; Grigoriev, I.V. and Srivastava, A. (2013). Fungalspecific transcription factor AbPfl2 activates pathogenicity in *Alternaria brassicicola*. *The Plant Journal*, **75**(3): 498-514.
- Chomczynski, P. and Sacchi, N. (2006). The single-step method of RNA isolation by acid guanidiniumthiocyanate-phenol-chloroform extraction: twenty-something years on. *Nat. Protoc.*, **1**(2): 581-585.
- Chomzynski, P. and Sacchi, N. (1987). Single-Step Method of RNA Isolation by Acid Guanidinium Thiocyanate-Phenol-Chloroform Extraction. *Anal. Biochem.*, **162**(1): 156-159.
- Cicinnati, V.R.; Shen, Q.; Sotiropoulos, G.C.; Radtke, A.; Gerken, G. and Beckebaum, S. (2008). Validation of putative reference genes for gene expression studies in human hepatocellular carcinoma using real-time quantitative RT-PCR. *BMC Cancer*, **8**(1): 1-12.
- Cooks, R.G. and Yan, X. (2018). Mass spectrometry for synthesis and analysis. *Annu. Rev. Anal. Chem.*, **11**: 1-28.

- Deveau, A.; Bonito, G.; Uehling, J.; Paoletti, M.; Becker, M.; Bindschedler, S. and Wick, L.Y. (2018). Bacterial-fungal interactions: ecology, mechanisms and challenges. *FEMS Microbiol. Rev.*, **42**(3): 335-352.
- Dimopoulou, A.; Theologidis, I.; Benaki, D.; Koukounia, M.; Zervakou, A.; Tzima, A. and Skandalis, N. (2021). Direct antibiotic activity of bacillibactin broadens the biocontrol range of *Bacillus amyloliquefaciens* MBI600. *Mosphere*, **6**(4): 10-1128.
- Dixon, G.R. (1981). *Alternaria* spp. (dark leaf and pod spot). Vegetable Crop Diseases. London, UK: *Palgrave Macmillan*, pp. 119-23.
- Doehlemann, G.; Ökmen, B.; Zhu, W. and Sharon, A. (2017). Plant pathogenic fungi. *Microbiol. Spectr.*, **5**(1): 5-1.
- Dubey, A.; Saiyam, D.; Kumar, A.; Hashem, A.; Abd_Allah, E.F. and Khan, M.L. (2021). Bacterial root endophytes: Characterization of their competence and plant growth promotion in soybean (*Glycine max* (L.) Merr.) under drought stress. *Int. J. Environ. Res. Public Health*, **18**(3): 931.
- Dullah, S.; Hazarika, D.J.; Goswami, G.; Borgohain, T.; Ghosh, A.; Barooah, M.; Bhattacharyya, A. and Boro, R.C. (2021). Melanin production and laccase mediated oxidative stress alleviation during fungal-fungal interaction among basidiomycete fungi. *IMA Fungus*. **12**(1):33.
- Dyall, S.D.; Brown, M.T. and Johnson, P.J. (2004). Ancient invasions: from endosymbionts to organelles. *Science*, **304**(5668): 253-257.
- Dymock, D.; Weightman, A.J.; Scully, C. and Wade, W.G. (1996). Molecular analysis of microflora associated with dentoalveolar abscesses. *J. Clin. Microbiol.*, **34**(3): 537-542.
- El-Nahrawy, S.; Elhawat, N. and Alshaal, T. (2019). Biochemical traits of *Bacillus subtilis* MF497446: its implications on the development of cowpea under cadmium stress and ensuring food safety. *Ecotoxicol Environ Saf*, **180**:384-395.
- Farrar, K.; Bryant, D. and Cope, Selby, N. (2014). Understanding and engineering beneficial plant-microbe interactions: plant growth promotion in energy crops. *Plant Biotechnol. J.*, **12**(9): 1193-1206.
- Fiodor, A.; Ajijah, N.; Dziewit, L. and Pranaw, K. (2023). Biopriming of seed with plant growth-promoting bacteria for improved germination and seedling growth. *Front Microbiol*, **14**: 1142966.
- Fleige, S. and Pfaffl, M.W. (2006). RNA integrity and the effect on the real-time qRT-PCR performance. *Mol. Aspects Med.*, **27**(2-3): 126-139.
- Gamez, R.; Cardinale, M.; Montes, M.; Ramirez, S.; Schnell, S. and Rodriguez, F. (2019). Screening, plant growth promotion and root colonization pattern of two rhizobacteria (*Pseudomonas fluorescens* Ps006 and *Bacillus amyloliquefaciens* Bs006) on banana cv. Williams (*Musa acuminata* Colla). *Microbiol. Res.*, **220**: 12-20.

- Gardes, M. and Bruns, T.D. (1993). ITS primers with enhanced specificity for basidiomycetes-application to the identification of mycorrhizae and rusts. *Mol. Ecol.*, **2**(2): 113-118.
- Ghavami, N.; Alikhani, H.A.; Pourbabaee, A.A. and Besharati, H. (2016). Study the effects of siderophore-producing bacteria on zinc and phosphorous nutrition of canola and maize plants. *Commun Soil Sci. Plant Anal.* **47**(12):1517-1527.
- Ghazy, N. and El-Nahrawy, S. (2021) Siderophore production by *Bacillus subtilis* MF497446 and *Pseudomonas koreensis* MG209738 and their efficacy in controlling *Cephalosporium maydis* in maize plant. *Arch. Microbiol.* **203**: 1195-1209.
- Ghosh, R.; Barman, S.; Mukherjee, R. and Mandal, N.C. (2016). Role of phosphate solubilizing *Burkholderia* spp. for successful colonization and growth promotion of *Lycopodium cernuum* L. (Lycopodiaceae) in lateritic belt of Birbhum district of West Bengal, India. *Microbiol. Res.*, **183**: 80-91.
- Gkarmiri, K.; Finlay, R.D.; Alström, S.; Thomas, E.; Cubeta, M.A. and Högberg, N. (2015). Transcriptomic changes in the plant pathogenic fungus *Rhizoctonia solani* AG-3 in response to the antagonistic bacteria *Serratia proteamaculans* and *Serratia plymuthica*. *BMC Genomics*, **16**(1): 1-17.
- Glick, B.R. (2012). Plant growth-promoting bacteria: mechanisms and applications. Scientifica.
- Glick, W.H.; Miller, C.C. and Cardinal, L.B. (2007). Making a life in the field of organization science. *Journal of Organizational Behavior: The International Journal of Industrial, Occupational and Organizational Psychology and Behavior*, **28**(7): 817-835.
- Gordon, S.A. and Weber, R.P. (1951). Colorimetric estimation of indoleacetic acid. *Plant Physiol.*, **26**(1): 192.
- Grillo, M. and Margolis, F.L. (1990). Use of reverse transcriptase polymerase chain reaction to monitor expression of intronless genes. *BioTechniques*, **9**(3): 262-268.
- Grobelak, A. and Hiller, J. (2017). Bacterial siderophores promote plant growth: Screening of catechol and hydroxamate siderophores. *Int. J. Phytorem.* **19**(9): 825-833.
- Grover, M.; Ali, S.K., Z.; Sandhya, V. and Venkateswarlu, B. (2011). Role of microorganisms in adaptation of agricultural crops to abiotic stresses. *World J. Microbiol. Biotechnol.* **27**: 1231-1240.
- Gunasinghe, W.K.R.N. and Karunaratne, A.M. (2009). Interactions of *Colletotrichum musae* and *Lasiodiplodia theobromae* and their biocontrol by *Pantoea agglomerans* and *Flavobacterium* sp. in expression of crown rot of 'Embul' banana. *Biocontrol.* **54**:587-596.
- Gupta, A.; Meyer, J.M. and Goel, R. (2002). Development of heavy metal-resistant mutants of phosphate solubilizing *Pseudomonas* sp. NBRI 4014 and their characterization. *Curr. Microbiol.*, **45**: 323-327.

- Haas, D. and Défago, G. (2005). Biological control of soil-borne pathogens by *Fluorescent pseudomonads*. *Nat. Rev. Microbiol.*, **3**(4): 307.
- HaggagWafaa, M. (2008). Isolation of bioactive antibiotic peptides from *Bacillus brevis* and *Bacillus polymyxa* against *Botrytis grey* mould in strawberry. *Arch. J. Phytopathol Plant Prot.* **41**: 477-491.
- Hashem, A.; Tabassum, B. and Abd_Allah, E.F. (2019). *Bacillus subtilis*: A plant-growth promoting rhizobacterium that also impacts biotic stress. *Saudi J. Biol. Sci.*, **26**(6): 1291-1297.
- Hassett, D.J.; Schweizer, H.P. and Ohman, D.E. (1995). *Pseudomonas aeruginosa* sodA and sodB mutants defective in manganese- and iron-cofactored superoxide dismutase activity demonstrate the importance of the iron-cofactored form in aerobic metabolism. *J. Bacteriol.*, **177**(22): 6330-6337.
- Hayat, R.; Ali, S.; Amara, U.; Khalid, R. and Ahmed, I. (2010). Soil beneficial bacteria and their role in plant growth promotion: a review. *Ann Microbiol.* **60**: 579-598.
- Hazarika, D.J.; Gautom, T.; Parveen, A.; Goswami, G.; Barooah, M.; Modi, M.K. and Boro, R.C. (2020). Mechanism of interaction of an endofungal bacterium *Serratiamarcescens* D1 with its host and non-host fungi. *PLoS One*, **15**(4): 0224051.
- Hazarika, D.J.; Goswami, G.; Gautom, T.; Parveen, A.; Das, P.; Barooah, M. and Boro, R.C. (2019). Lipopeptide mediated biocontrol activity of endophytic *Bacillus subtilis* against fungal phytopathogens. *BMC Microbiol*, **19**(1): 1-13. 125
- Heimpel, G.E. and Mills, N.J. (2017). *Biological control*. Cambridge University Press.
- Howard, R.J. and Ferrari, M.A. (1989). Role of melanin in appressorium function. *Exp. Mycol.*, **13**:403-418.
- Hu, X.; Roberts, D.P.; Xie, L.; Maul, J.E.; Yu, C.; Li, Y.; Jiang, M.; Liao, X.; Che, Z. and Liao, X. (2014). Formulation of *Bacillus subtilis* by BY-2 suppresses *Sclerotinia sclerotiorum* oilseed rape in the field. *Biol Control.* **70**:54-64.
- Idris, E.E.; Iglesias, D.J.; Talon, M. and Borriss, R. (2007). Tryptophan-dependent production of indole-3-acetic acid (IAA) affects level of plant growth promotion by *Bacillus amyloliquefaciens* FZB42. *MPMI*, **20**(6): 619-626.
- Ji, C.; Zhang, M.; Kong, Z.; Chen, X.; Wang, X.; Ding, W. and Guo, Q. (2021). Genomic analysis reveals potential mechanisms underlying promotion of tomato plant growth and antagonism of soilborne pathogens by *Bacillus amyloliquefaciens* Ba13. *Microbiol. Spectr.*, **9**(3): 01615-21.
- Jiao, R.; Cai, Y.; He, P.; Munir, S.; Li, X.; Wu, Y. and He, Y. (2021). *Bacillus amyloliquefaciens* YN201732 produces lipopeptides with promising biocontrol activity against fungal pathogen *Erysiphe cichora cearum*. *Front. cell. infect. Microbiol.*, **11**: 598999.
- Joshi, R. and Gardener, B.M. (2006). Identification of genes associated with pathogen inhibition in different strains *B. subtilis*. *Phytopathology*, **96**: 145-154.

- Joubert, A.; Bataille, Simoneau, N.; Campion, C.; Guillemette, T.; Hudhomme, P.; Iacomì, Vasilescu, B. and Simoneau, P. (2011). Cell wall integrity and high osmolarity glycerol pathways are required for adaptation of *Alternaria brassicicola* to cell wall stress caused by brassicaceous indolic phytoalexins. *Cell. Microbiol.*, **13**(1): 62-80.
- Kakembo, D. and Lee, Y.H. (2019). Analysis of traits for biocontrol performance of *Pseudomonas parafulva* JBCS1880 against bacterial pustule in soybean plants. *Biol Control*. **134**:72-81.
- Kazerooni, E.A.; Maharachchikumbura, S.S.; Adhikari, A.; Al-Sadi, A.M.; Kang, S.M. Kim, L.R. and Lee, I.J. (2021). Rhizospheric *Bacillus amyloliquefaciens* protects *Capsicum annuum* cv. Geumsugangsan from multiple abiotic stresses via multifarious plant growth-promoting attributes. *Front. Plant Sci.*, **12**: 669693.
- Kenarova, A. and Boteva, S. (2023). Fungicides in agriculture and their side effects on soil enzyme activities: a review. *BJAS*, **29**(1).
- Khan, M.; Salman, M.; Jan, S.A. and Shinwari, Z.K. (2021). Biological control of fungal phytopathogens: A comprehensive review based on *Bacillus* species. *MOJ Biol. Med*, **6**: 90-92.
- 126 nahi, M.Y.; Ricciuti, P.; Allegretta, I.; Terzano, R. and Crecchio, C. (2018). Solubilization of insoluble zinc compounds by different microbial isolates in vitro condition. *Environ. Sci. Pollut. Res. Int*, **25**: 25862-25868.
- Khatun, A.; Farhana, T.; Sabir, A.A.; Smn, I.; West, H.M.; Rahman, M. and Islam T. (2018). *Pseudomonas* and *Burkholderia* inhibit growth and asexual development of *Phytophthora capsici*. *Z. Naturforsch.* **73**:123-135.
- Kim, K.; Jang, Y.J.; Lee, S.M.; Oh, B.T.; Chae, J.C. and Lee, K.J. (2014). Alleviation of salt stress by *Enterobacter* sp. EJ01 in tomato and *Arabidopsis* is accompanied by up-regulation of conserved salinity responsive factors in plants. *Mol. Cells*, **37**(2): 109.
- Kloepper, J.W.; Ryu, C.M. and Zhang S. (2004). Induced systemic resistance and promotion of plant growth by *Bacillus* spp. *Phytopathol*, **94**: 1259-1266.
- Kolte, S.J. (2002). Diseases and their management in oilseed crops-new paradigm. Rai, M. et al. (eds). Oilseeds and oils-research and development needs. *Indian Society of Oilseeds Research*, Hyderabad, India, pp. 244-253.
- Kuan, K.B.; Othman, R.; Abdul Rahim, K. and Shamsuddin, Z.H. (2016). Plant growth-promoting rhizobacteria inoculation to enhance vegetative growth, nitrogen fixation and nitrogen remobilisation of maize under greenhouse conditions. *PloS one*, **11**(3): 0152478.
- Kumar, S.; Stecher, G.; Li, M.; Nnyaz, C. and Tamura, K. (2018). MEGA X: molecular evolutionary genetics analysis across computing platforms. *Mol. Biol. Evol.*, **35**(6): 1547.
- Kumar, S.; Tamura, K. and Nei, M. (1994). MEGA: Molecular Evolutionary Genetics Analysis software for microcomputers. *CABIOS*, **10**(2): 189-191.

- Kupiec, T. (2004). Quality-control analytical methods: High-performance liquid chromatography. *Int. J. Pharm. Compd.*, **8**: 223-227.
- La, Y.; Feng, X.; Wang, X.; Zheng, L. and Liu, H. (2020). Inhibitory effects of *Bacillus licheniformis* BL06 on *Phytophthora capsici* in pepper by multiple modes of action. *Biol Control*. **144**:104210.
- Lafontaine, D.L.J. and Tollervey, D. (2001). The function and synthesis of ribosomes. *Nat. Rev. Mol. Cell Biol.*, **2**(7): 514-520.
- Landis, G.N. and Tower, J. (2005). Superoxide dismutase evolution and life span regulation. *Mech. Ageing Dev.*, **126**(3): 365-379.
- Lane, D.J. (1991). 16S/23S rRNA sequencing. In Nucleic acid techniques in bacterial systematics. pp. 125-175.
- Larena, I.; Salazar, O.; González, V.; Julián, M.C. and Rubio, V. (1999). Design of a primer for ribosomal DNA internal transcribed spacer with enhanced specificity for ascomycetes. *J. Biotechnol.*, **75**(2-3): 187-194.
- Lebeda, A.; Luhová, L.; Sedlářová, M. and Janc̣ová, D. (2001). The role of enz. plant-fungal pathogens interactions. *J. Plant Dis. Prot.* **108**:89-111.
- Levetin, E. and Dorsey, K. (2006). Contribution of leaf surface fungi to the air spora. *Aerobiologia*, **22**(1): 3-12.
- Lim, J.H. and Kim, S.D. (2013). Induction of drought stress resistance by multi-functional PGPR *Bacillus licheniformis* K11 in pepper. *Plant Pathol. J.*, **29**(2): 201.
- Liu, H.; Prajapati, V.; Prajapati, S.; Bais, H. and Lu, J. (2021). Comparative genome analysis of *Bacillus amyloliquefaciens* focusing on phylogenomics, functional Traits, and prevalence of antimicrobial and virulence genes. *Front. Genet*, **12**: 724217.
- Livak, K.J. and Schmittgen, T.D. (2001). Analysis of relative gene expression data using real-time quantitative PCR and the 2- $\Delta\Delta$ CT method. *Methods*, **25**(4): 402-408.
- Lodewyckx, C.; Vangronsveld, J.; Porteous, F.; Moore, E.R.; Taghavi, S.; Mezgeay, M. and der Lelie, D.V. (2002). Endophytic bacteria and their potential applications. *CRC Crit. Rev. Plant Sci.*, **21**(6): 583-606.
- Lu, P.; Jiang, K.; Hao, Y.Q.; Chu, W.Y.; Xu, Y.D.; Yang, J.Y. and Zhao, H.X. (2021). Profiles of bacillus spp. isolated from the rhizosphere of *Suaeda glauca* and their potential to promote plant growth and suppress fungal phytopathogens. pp. 1231-1240.
- Luo, L.; Zhao, C.; Wang, E.; Raza, A. and Yin, C. (2022). *Bacillus amyloliquefaciens* as an excellent agent for biofertilizer and biocontrol in agriculture: An overview for its mechanisms *Microbiol. Res.*, **259**: 127016.
- Luo, W.; D'Angelo, E.M. and Coyne, M.S. (2007). Plant secondary metabolites, biphenyl, and hydroxypropyl- β -cyclodextrin effects on aerobic polychlorinated biphenyl

- removal and microbial community structure in soils. *Soil Biol. Biochem.*, **39**(3): 735-743.
- Macioszek, V.K.; Gapińska, M.; Zmienko, A.; Sobczak, M.; Skoczowski, A.; Oliwa, J.; and Kononowicz, A.K. (2020). Complexity of *Brassica oleracea-Alternaria brassicicola* susceptible interaction reveals downregulation of photosynthesis at ultrastructural, transcriptional, and physiological levels. *Cells*, **9**(10): 2329.
- Macioszek, V.K.; Lawrence, C.B. and Kononowicz, A.K. (2018). Infection cycle of *Alternaria brassicicola* on *Brassica oleracea* leaves under growth room conditions. *Plant Pathol.*, **67**(5): 1088-1096.
- Maksimov, I.V.; Blagova, D.K.; Veselova, S.V.; Sorokan, A.V.; Burkhanova, G.F. and Cherepanova, E.A. (2020). Recombinant *Bacillus subtilis* 26DCryChS line with gene BtcryIIa encoding CryIIa toxin from *Bacillus thuringiensis* promotes integrated wheat defense against pathogen *Stagonosporanodorum* Berk and greenbug *Schizaphisgraminum* Rond. *Biol Control*. **144**:104242.
- Malinen, E.; Kassinen, A.; Rinttilä, T. and Palva, A. (2003). Comparison of real-time PCR with SYBR Green I or 5'-nuclease assays and dot-blot hybridization with rDNA-targeted oligonucleotide probes in quantification of selected faecal bacteria. *Microbiology*, **149**(1): 269-277.
- Matyjaszczyk, E. (2015). Products containing microorganisms as a tool in integrated pest management and the rules of their market placement in the European Union. *Pest Management Science*, **71**(9): 1201-1206.
- Meena, V.S.; Zaid, A.; Maurya, B.R.; Meena, S.K.; Bahadur, I.; Saha, M.; Kumar, A.; Verma, R. and Wani, S.H. (2018). Evaluation of potassium solubilizing rhizobacteria (KSR): enhancing K-bioavailability and optimizing K-fertilization of maize plants under Indo-Gangetic Plains of India. *Environ. Sci. Pollut. Res.*, **25**: 36412-36424.
- Mehta, P.; Walia, A.; Kulshrestha, S.; Chauhan, A. and Shirkot, C.K. (2015). Efficiency of plant growth promoting P. solubilizing *Bacillus circulans* CB7 for enhancement of tomato growth under net house conditions. *J. Basic Microbiol.*, **55**(1): 33-44.
- Merz, W.G. and Roberts, G.D. (2003). Algorithms for detection and identification of fungi. In *Manual of clinical microbiology*. Washington DC: American Society for Microbiology. p. 85.
- Mohammadi, P.; Tozlu, E.; Kotan, R. and Kotan, M.S. (2017). Potential of some bacteria for biological control of postharvest citrus green mold caused by *Penicillium digitatum*. *Plant Prot. Sci.*, **53**:1-14.
- Montesinos, E. and Bonaterra, A. (2017). Pesticides, microbial In Reference module in life sciences.
- Moreb, N.; Murphy, A.; Jaiswal, S. and Jaiswal, A.K. (2020). Cabbage. *Nutritional Composition and Antioxidant Properties of Fruits and Vegetables*, pp. 33-54.

- Morrison, T.B.; Weis, J.J. and Wittwer, C.T. (1998). Quantification of low-copy transcripts by continuous SYBR Green I monitoring during amplification. *Biotechniques*, **24**(6): 954-962.
- Nath, R.; Sharma, G.D. and Barooah, M. (2012). Efficiency of tricalcium phosphate solubilization by two different endophytic *Penicillium* sp. isolated from tea (*Camellia sinensis* L.). *Eur. J. Exp. Biol.*, **2**(4): 1354-1358.
- Navarro-Ródenas, A.; Berná, L.M.; Lozano-Carrillo, C.; Andrino, A. and Morte, A. (2016). Beneficial native bacteria improve survival and mycorrhization of desert truffle mycorrhizal plants in nursery conditions. *Mycorrhiza*, **26**: 769-779.
- Nikolin, B.; Imamović, B.; Medanhodžić-Vuk, S. and Sober, M. (2004). High performance liquid chromatography in pharmaceutical analyses. *Bosnian J. Basic Sci.*, **4**(2): 5-9.
- Nolan, T.; Hands, R.E. and Bustin, S.A. (2006). Quantification of mRNA using real-time RT-PCR. *Nat. Protoc.*, **1**(3): 1559-1582.
- Oh, I.S.; Park, A.R.; Bae, M.S.; Kwon, S.J.; Kim, Y.S.; Lee, J.E.; Kang, N.Y.; Lee, S.; Cheong, H. and Park, O.K. (2005). Secretome analysis reveals an Arabidopsis lipase involved in defense against *Alternaria brassicicola*. *Plant Cell*, **17**: 2832-2847.
- Ongena, M. and Jacques, P. (2008). *Bacillus* lipopeptides: versatile weapons for plant disease biocontrol. *Trends Microbiol.*, **16**(3): 115-125.
- Osbourn, A.E. (2001). Tox-boxes, fungal secondary metabolites and plant disease. *Proc Natl Acad Sci USA* **98**:14187–14188. <http://dx.doi.org/10.1073/pnas.261573598>.
- Oswald, A. (2010). Evaluating soil rhizobacteria for their ability to enhance plant growth and tuber yield in potato. *Ann. Appl. Biol.* **157**:259-271.
- Pal, K.K. and Gardener, B.M. (2006). Biological control of plant pathogens. The Plant Health Instructor DOI: 10.1094/PHI-A-2006-1117-02.
- Partida-Martinez, L.P.; Groth, I.; Schmitt, I.; Richter, W.; Roth, M. and Hertweck, C. (2007b). *Burkholderia rhizoxinica* sp. nov. and *Burkholderia endofungorum* sp. nov., bacterial endosymbionts of the plant-pathogenic fungus *Rhizopus microsporus*. *Int. J. Syst. Evol. Microbiol.*, **57**(11): 2583-2590.
- Peay, K.G.; Kennedy, P.G. and Bruns, T.D. (2008). Fungal Community Ecology: A Hybrid Beast with a Molecular Master. *Bio Science*, **58**(9): 799-810.
- Peruch, L.A.; Michereff, S.J. and Araújo, I.B. (2006). Survey of the intensity of *Alternaria* black spot and black rot on brassica species under organic farming systems in Pernambuco and Santa Catarina states, Brazil. *Hortic. Bras.*, **24**: 464-469.
- Peruch, L.A.M.; Michereff, S.J. and Araújo, I.B. (2006). Survey of the intensity of *Alternaria* black spot and black rot on brassica species under organic farming systems in Pernambuco and Santa Catarina states, *Hort. Bras.*, **24**(4): 464-469.

- Pikovskaya, R.I. (1948). Mobilization of phosphorus in soil in connection with the vital activity of some microbial species. *Microbiologiya*, **17**: 362-370.
- Prasanna K.S.P.; Gowtham, H.G.; Hariprasad, P.; Shivaprasad, K. and Niranjana, S. R. (2015). Delftiatsuruhatensis WGR-UOM-BT1, a novel rhizobacterium with PGPR properties from *Rauwolfia serpentina* (L.) Benth. ex Kurz also suppresses fungal phytopathogens by producing a new antibiotic AMTM. *Lett. Appl. Microbiol.*, **61**(5): 460-468.
- Qin, Y.; Han, Y.; Shang, Q. and Li, P. (2015). Complete genome sequence of *Bacillus amyloliquefaciens* L-H15, a plant growth promoting rhizobacteria isolated from cucumber seedling substrate. *J. Biotechnol.*, **200**: 59-60.
- Rahimi, F.; Katouli, M. and Karimi, S. (2016). Biofilm production among methicillin resistant *Staphylococcus aureus* strains isolated from catheterized patients with urinary tract infection. *Microb. Pathog.*, **98**: 69-76.
- Rahimloo, T. and Ghosta, Y. (2015). The occurrence of *Alternaria* species on cabbage in Iran. *Zemdirbyste- Agriculture*. **102**(3).
- Rai, M. and Agarkar, G. (2016). Plant-fungal interactions: what triggers the fungi to switch among lifestyles? *Crit. Rev. Microbiol.*, **42**(3): 428-438.
- Rajkumar, M.; Ae N.; Prasad, M.N.V. and Freitas, H. (2010). Potential of siderophore-producing bacteria for improving heavy metal phytoextraction. *Trends Biotechnol.* **28**(3): 142-149.
- Rani, S.; Chopra, G. and Wati, L. (2023). Deciphering the Potential of Sulphur-Oxidizing Bacteria for Sulphate Production Correlating with pH Change. *Microb. Ecol.*, pp. 1-11.
- Reis, A. And Boiteux, L.S. (2010). *Alternaria* species infecting *Brassicaceae* in the Brazilian neotropics: geographical distribution, host range and specificity. *JPPY*, **92**(3): 661-668.
- Reis, A. and Boiteux, L.S. (2010). *Alternaria* species infecting *Brassicaceae* in the Brazilian neotropics: geographical distribution, host range and specificity. *JPP*, **92**(3): 661-668.
- Rolph, H.J.; Lennon, A.; Riggio, M.P.; Saunders, W.P.; MacKenzie, D.; Coldero, L. and Bagg, J. (2001). Molecular Identification of Microorganisms from Endodontic Infections. *J. Clin. Microbiol.*, **39**(9): 3282-3289.
- Romero, D.; De Vicente, A.; Rakotoaly, R.H.; Dufour, S.E.; Veening, J.W.; Arrebola, E. and Pérez-García, A. (2007). The iturin and fengycin families of lipopeptides are key factors in antagonism of *Bacillus subtilis* toward *Podospaera fusca*. *MPMI*, **20**(4): 430-440.
- Rückert, C.; Blom, J.; Chen, X.; Reva, O. and Borriss, R. (2011). Genome sequence of *B. amyloliquefaciens* type strain DSM7T reveals differences to plant-associated *B. amyloliquefaciens* FZB42. *J. Biotechnol.*, **155**(1): 78-85.

- Saechow, S.; Thammasittirong, A.; Kittakoop, P.; Prachya, S. and Thammasittirong, S.N.R. (2018). Antagonistic activity against dirty panicle rice fungal pathogens and plant growth-promoting activity of *Bacillus amyloliquefaciens* BAS23. pp. 1527-1535.
- Saini, R.; Adhikary, A.; Juneja, S.; Kumar, R.; Singh, I.; Nayyar, H. and Kumar, S. (2023). Drought priming triggers diverse metabolic adjustments and induces chilling tolerance in chickpea (*Cicer arietinum* L.). *Plant Physiol. Biochem.*, **194**: 418-439.
- Saitou, N. and Nei, M. (1987). The neighbor-joining method: a new method for reconstructing phylogenetic trees. *Mol. Biol. Evol.*, **4**(4): 406-425.
- Samaras, A.; Efthimiou, K.; Roumeliotis, E. and Karaoglanidis, G.S. (2016). Biocontrol potential and plant-growth-promoting effects of *Bacillus amyloliquefaciens* MBI 600 against *Fusarium oxysporum* f. sp. radicis-lycopersici on tomato. In *V International Symposium on Tomato Diseases: Perspectives and Future Directions in Tomato Protection*. **1207**: 139-146.
- Saraf, M.; Pandya, U. and Thakkar, A. (2014). Role of allelochemicals in plant growth promoting rhizobacteria for biocontrol of phytopathogens. *Microbiol. Res.*, **169**(1): 18-29.
- Saravanan, V.S.; Madhaiyan, M. and Thangaraju, M. (2007). Solubilization of zinc compounds by the diazotrophic, plant growth promoting bacterium *Gluconacetobacter diazotrophicus*. *Chemosphere*, **66**(9): 1794-1798.
- Sattar, A.; Naveed, M.; Ali, M.; Zahir, Z.A.; Nadeem, S.M.; Yaseen, M. and Meena, H.N. (2019). Perspectives of potassium solubilizing microbes in sustainable food production system: A review. *Appl. Soil Ecol.*, **133**: 146-159.
- Savchuk, S. and Fernando, W.D.D. (2004). Effect of timing of application and population dynamics on the degree of biological control of *Sclerotinia sclerotiorum* by bacterial antagonists. *FEMS Microbiol Ecol.* **49**: 379-388.
- Schleifer, K.H. and Kandler, O. (1972). Peptidoglycan types of bacterial cell walls and their taxonomic implications. *Bacteriol. Rev.*, **36**(4): 407-477.
- Schoch, C.L.; Seifert, K.A.; Huhndorf, S.; Robert, V.; Spouge, J.L.; Levesque, C.A. and Chen, W. (2012). The internal transcribed spacer as a universal DNA barcode marker for Fungi. Fungal Barcoding Consortium. *Proc. Natl. Acad. Sci.*, **109**: 6241-6246.
- Schoina, C.; Stringlis, I.A.; Pantelides, I.S.; Tjamos, S.E. and Paplomatas, E.J. (2011). Evaluation of application methods and biocontrol efficacy of *Paenibacillus alvei* strain K-165, against the cotton black root rot pathogen *Thielaviopsis basicola*. *Biol. Control*, **58**(1): 68-73.
- Schwyn, B. and Neilands, J.B. (1987). Universal chemical assay for the detection and determination of siderophores. *Anal. Biochem.*, **160**(1): 47-56.
- Shahid, I.; Han, J.; Hanoq, S.; Malik, K.A.; Borchers, C.H. and Mehnaz, S. (2021). Profiling of metabolites of *Bacillus* spp. and their application in sustainable plant growth promotion and biocontrol. *Front. Sustain. Food Syst.* **5**: 605195.

- Sharifi, R. and Ryu, C.M. (2016). Are bacterial volatile compounds poisonous odors to a fungal pathogen *Botrytis cinerea*, alarm signals to *Arabidopsis* seedlings for eliciting induced resistance, or both. *Front Microbiol*, **7**: 196.
- Sharma, G. and Pandey, R.R. (2010). Influence of culture media on growth, colony character and sporulation of fungi isolated from decaying vegetable wastes. *J. Yeast Fungal Res.*, **1**(8): 157-164.
- Sherma, J. and Fried, B. (2003). Handbook of thin-layer chromatography. CRC Press. USA.
- Sheteiwiy, M.S.; AbdElgawad, H.; Xiong, Y.C.; Macovei, A.; Brestic, M.; Skalicky, M. and El, Sawah, A.M. (2021). Inoculation with *Bacillus amyloliquefaciens* and mycorrhiza confers tolerance to drought stress and improve seed yield and quality of soybean plant. *Physiol. Plant.*, **172**(4): 2153-2169.
- Singh, M.; Srivastava, P.K.; Verma, P.C.; Kharwar, R.N.; Singh, N. and Tripathi, R.D. (2015). Soil fungi for mycoremediation of arsenic pollution in agriculture soils. *J. Appl. Microbiol.*, **119**(5): 1278-1290.
- Sinha, A.K. and Parli, B.V. (2020). Siderophore production by bacteria isolated from mangrove sediments: a microcosm study. *J. Exp. Mar. Biol. Ecol.* **524**: 151290.
- Smit, E.; Leeftang, P.; Glandorf, B.; Dirk Van Elsas, J. and Wernars, K. (1999). Analysis of Fungal Diversity in the Wheat Rhizosphere by Sequencing of Cloned PCR-Amplified Genes Encoding 18S rRNA and Temperature Gradient Gel Electrophoresis. *Appl. Environ. Microbiol.*, **65**(6): 2614-2621.
- Soliman, S.A.; Al-Askar, A.A.; Sobhy, S.; Samy, M.A.; Hamdy, E.; Sharaf, O.A.; Su, Y.; Behiry, S.I. and Abdelkhalek, A. (2023). Differences in Pathogenesis-Related Protein Expression and Polyphenolic Compound Accumulation Reveal Insights into Tomato- *Pythium aphanidermatum* Interaction. *Sustainability*, **15**(8): 6551.
- Sowndhararajan, K.; Marimuthu, S. and Manian, S. (2013). Integrated control of blister blight disease in tea using the biocontrol agent *Ochrobactrum anthropi* strain BMO-111 with chemical fungicides. *J. Appl. Microbiol.* PMID. **114**.
- Stephenie, S.; Chang, Y.P.; Gnanasekaran, A.; Esa, N.M. and Gnanaraj, C. (2020). An insight on superoxide dismutase (SOD) from plants for mammalian health enhancement. *JFF*, **68**: 103917.
- Sundin, G.W.; Werner, N.A.; Yoder, K.S. and Aldwinckle, H.S. (2009). Field evaluation of biological control of fire blight in the eastern United States. *Plant Dis.*, **93**(4): 386-394.
- Suprapta, D.N. (2012). Potential of microbial antagonists as biocontrol agents against plant fungal pathogens. *J. ISSAAS*, **18**(2): 1-8.
- Szczecz, M. and Shoda, M. (2004). Biocontrol of *Rhizoctonia* damping-off of tomato by *Bacillus subtilis* combined with *Burkholderia cepacia*. *J. Phytopathol.* **152**: 549-556.
- Tamura, K.; Stecher, G.; Peterson, D.; Filipski, A. and Kumar, S. (2013). MEGA6: Molecular Evolutionary Genetics Analysis Version 6.0. *Mol. Biol. Evol.*, **30**(12): 2725-2729.

- Tariq, M.; Khan, A.; Asif, M.; Khan, F.; Ansari, T.; Shariq, M. and Siddiqui, M.A. (2020). Biological control: a sustainable and practical approach for plant disease management. *Acta Agric Scand B. Soil Plant Sci.*, **70**(6): 507-524.
- Tendulkar, S.R.; Saikumari, Y.K.; Patel, V.; Raghotama, S.; Munshi, T.K.; Balam, P.; and Chattoo, B.B. (2007). Isolation, purification and characterization of an antifungal molecule produced by *Bacillus licheniformis* BC98 and its effect on phytopathogen *Magnaporthe grisea*. *J. Appl. Microbiol.* **103**(6): 2331-2339.
- Thomma, B.P.; Nelissen, I.; Eggermont, K. and Broekaert, W.F. (1999). Deficiency in phytoalexin production causes enhanced susceptibility of *Arabidopsis thaliana* to the fungus *Alternaria brassicicola*. *Plant J.* (**19**): 163-171.
- Tian, J.; Ge, F.; Zhang, D.; Deng, S. and Liu, X. (2021). Roles of phosphate solubilizing microorganisms from managing soil phosphorus deficiency to mediating biogeochemical P cycle. *Biology*, **10**(2): 158.
- Tiwari, S.; Prasad, V.; Chauhan, P.S. and Lata, C. (2017). *Bacillus amyloliquefaciens* confers tolerance to various abiotic stresses and modulates plant response to phytohormones through osmoprotection and gene expression regulation in rice. *Front. Plant Sci.*, **8**: 1510.
- Tortora, M.L.; D'Áz-Ricci, J.C. and Pedraza, R.O. (2011). *Azospirillum brasilense* siderophores with antifungal activity against *Colletotrichum acutatum*. *Arch Microbiol.* **193**:275-286.
- Tsukanova, K.A.; Meyer, J.J.M. and Bibikova, T.N. (2017). Effect of plant growth-promoting *Rhizobacteria* on plant hormone homeostasis. *S. Afr. J. Bot.*, **113**: 91-102.
- Turner, N.W.; Subrahmanyam, S. and Piletsky, S.A. (2009). Analytical methods for determination of mycotoxins: A review. *Anal. Chim. Acta*, **632**(2): 168-180.
- van de Mortel, J.E.; de Vos, R.C.; Dekkers, E.; Pineda, A.; Guillod, L.; Bouwmeester, K. and Raaijmakers, J.M. (2012). Metabolic and transcriptomic changes induced in *Arabidopsis* by the rhizobacterium *Pseudomonas fluorescens* SS101. *Plant Physiol.*, **160**(4): 2173-2188.
- Van Scoy, A.R. and Tjeerdema, R.S. (2014). Environmental fate and toxicology of chlorothalonil. *Rev Environ Contam Toxicol.* **232**: 89-105.
- Vansuyt, G.; Robin, A.; Briat, J.F.; Curie, C. and Lemanceau, P. (2007). Iron acquisition from Fe-pyoverdine by *Arabidopsis thaliana*. *MPMI*, **20**(4): 441-447.
- Vidhyasekaran P. (2008). Fungal pathogenesis in plant crops: molecular biology and host defense mechanisms, 2nd ed. CRC Press, New York, NY.
- Voigt, C.A.; Schafer, W. Salomon, S. (2005). A secreted lipase of *Fusarium graminearum* is a virulence factor required for infection of cereals. *Plant J.* **42**:364-375.
- Wallace, R.L.; Hirkala, D.L. and Nelson, L.M. (2018). Efficacy of *Pseudomonas fluorescens* for control of Mucor rot of apple during commercial storage and potential modes of action. *Can. J. Microbiol.* **64**:420-431.

- Wang, M.; Geng, L.; Sun, X.; Shu, C.; Song, F. and Zhang, J. (2020). Screening of *Bacillus thuringiensis* strains to identify new potential biocontrol agents against *Sclerotinia sclerotiorum* and *Plutella xylostella* in *Brassica campestris* L. *Biol. Control*, **145**:1-9.
- Warwick, S.I. and Francis, A. (1994). Guide to the wild germplasm of Brassica and allied crops. Part 5. Life history and geographical data for wild species in the tribe Brassiceae (Cruciferae). *Agric. Can Res. Branch Tech. Bull.* **2**.
- Weisburg, W.G.; Barns, S.M.; Pelletier, D.A. and Lane, D.J. (1991). 16S ribosomal DNA amplification for phylogenetic study. *J. Bacteriol.*, **173**(2): 697-703.
- White, T.J.; Bruns, T.; Lee, S.J.W.T. and Taylor, J. (1990). Amplification and direct sequencing of fungal ribosomal RNA genes for phylogenetics. PCR protocols: a guide to methods and applications, **18**(1): 315-322.
- Wilson, K. (2001). Preparation of genomic DNA from bacteria. *Curr. Protoc. Mol. Biol.*, **56**(1): 2-4.
- Wipf, D.; Fribourg, A.; Munch, J.C.; Botton, B. and Buscot, F. (1999). Diversity of the internal transcribed spacer of rDNA in morels. *Canad. J. Microbiol.*, **45**(9): 769-778.
- Woese, C.R. and Fox, G.E. (1977). Phylogenetic structure of the prokaryotic domain: the primary kingdoms. *Proc. Natl. Acad. Sci.*, **74**(11): 5088-5090.
- Wu, Y.; Zhou, J.; Li, C. and Ma, Y. (2019). Antifungal and plant growth promotion activity of volatile organic compounds produced by *Bacillus amyloliquefaciens*. *Microbiology Open*, **8**(8): 00813.
- Xue, L.; Sun, B.; Yang, Y.; Jin, B.; Zhuang, G.; Bai, Z. and Zhuang, X. (2021). Efficiency and mechanism of reducing ammonia volatilization in alkaline farmland soil using *Bacillus amyloliquefaciens* biofertilizer. *Environ. Res.*, **202**: 111672.
- You, M.; Fang, S.; MacDonald, J.; Xu, J. and Yuan, Z.C. (2020). Isolation and characterization of *Burkholderia cenocepacia* CR318, a phosphate solubilizing bacterium promoting corn growth. *Microbiol. Res.*, **233**: 126395.
- Yu, S.M.; Oh, B.T. and Lee, Y.H. (2012). Biocontrol of green and blue molds in postharvest satsuma mandarin using *Bacillus amyloliquefaciens* JBC36. *Biocontrol Sci. Technol.*, **22**(10): 1181-1197.
- Zambino, P.J. and Szabo, L.J. (1993). Phylogenetic Relationships of Selected Cereal and Grass Rusts Based on rDNA Sequence Analysis. *Mycologia*, **85**(3): 401.
- Zhang, D.; Yu, S.; Yang, Y.; Zhang, J.; Zhao, D.; Pan, Y.; Fan, S.; Yang, Z. and Zhu, J. (2020). Antifungal effects of volatiles produced by *Bacillus subtilis* against *Alternaria solani* in potato. *Front Microbiol.*, **11**: 1196.
- Zhou, C.; Guo, J.; Zhu, L.; Xiao, X.; Xie, Y.; Zhu, J. and Wang, J. (2016). *Paenibacillus polymyxa* BFKC01 enhances plant iron absorption via improved root systems and activated iron acquisition mechanisms. *Plant Physiol. Biochem.*, **105**: 162-173.

- Zhou, K.; Yamagishi, M. and Osaki, M. (2008). Biocontrol of brown stem rot disease in soybean *Paenibacillus* BRF-1 has biocontrol ability against *Phialophora gregata* disease and promotes soybean growth. *Soil Sci. Plant Nutr.* **54**:870-875.
- Zhu, D.; Ouyang, L.; Xu, Z. and Zhang, L. (2015). Rhizobacteria of *Populus euphratica* promoting plant growth against heavy metals. *Int. J. Phytoremediation*, **17**(10): 973-980.
- Zuo, H.L.; Yang, F.Q.; Huang, W.H. and Xia, Z.N. (2013). Preparative gas chromatography and its applications. *J. Chromatogr. Sci.*, **51**(7): 704-715.

APPENDIX I

MEDIA COMPOSITIONS

Half Strength NA and PDA Medium

Ingredients	Quantity (g/l)
Nutrient Agar (Himedia; India)	14
Potato Dextrose Agar (Himedia; India)	19.5
Agar	10

APPENDIX II

BUFFER COMPOSITIONS

TAE buffer

Components	50X TAE buffer		1X TAE buffer	
	Concentration (M)	Quantity (g/l)	Concentration (mM)	Quantity (g/l)
Tris	2	242.2	40	4.844
Acetic acid	1	60.5	20	1.21
EDTA disodium salt	0.05	18.612	1	0.372

1X TE buffer (pH 8.0)

Components	Concentration(mM)	Quantity(g/l)
Tris	10	1.214
EDTA disodium salt	1	0.372

Trypan Blue Solution

Components	Quantity
Trypan Blue	40 mg
Lactic Acid (85 % w/w)	10 ml
Phenol (pH 7.5-8)	10 ml
Glycerol	10 ml
H ₂ O	10 ml